

INVESTIGATION OF LIGHT ATTENUATION IN LAKE EYMIR

A THESIS SUBMITTED TO  
THE GRADUATE SCHOOL OF NATURAL AND APPLIED SCIENCES  
OF  
MIDDLE EAST TECHNICAL UNIVERSITY

BY

SELEN ATIKER

IN PARTIAL FULFILLMENT OF THE REQUIREMENTS  
FOR  
THE DEGREE OF MASTER OF SCIENCE  
IN  
ENVIRONMENTAL ENGINEERING

JANUARY 2012

Approval of the thesis:

**INVESTIGATION OF LIGHT ATTENUATION IN LAKE EYMIR**

submitted by **SELEN ATIKER** in the partial fulfillment of the requirement for the degree of **Master of Science in Environmental Engineering Department, Middle East Technical University** by,

Prof. Dr. Canan ÖZGEN  
Dean, Graduate School of **Natural and Applied Sciences**

\_\_\_\_\_

Prof. Dr. Göksel N. DEMİRER  
Head of Department, **Environmental Engineering**

\_\_\_\_\_

Assoc. Prof. Dr. Ayşegül AKSOY  
Supervisor, **Environmental Engineering Dept., METU**

\_\_\_\_\_

Assoc. Prof. Dr. Selim SANİN  
Co-Supervisor, **Environmental Engineering Dept., Hacettepe Univ.**

\_\_\_\_\_

**Examining Committee Members:**

Prof. Dr. Cemal SAYDAM  
Environmental Engineering Department, Hacettepe Univ.

\_\_\_\_\_

Assoc. Prof. Dr. Ayşegül AKSOY  
Environmental Engineering Department, METU

\_\_\_\_\_

Assoc. Prof. Dr. Selim SANİN  
Environmental Engineering Department, Hacettepe Univ.

\_\_\_\_\_

Assist. Prof. Dr. Tuba ERGÜDER  
Environmental Engineering Department, METU

\_\_\_\_\_

Assist. Prof. Dr. Barış KAYMAK  
Environmental Engineering Department, METU

\_\_\_\_\_

**Date:** January 20, 2012

**I hereby declare that all information in this document has been obtained and presented in accordance with academic rules and ethical conduct. I also declare that, as required by these rules and conduct, I have fully cited and referenced all material and results that are not original to this work.**

Name, Last Name: Selen ATIKER

Signature:

## **ABSTRACT**

### **INVESTIGATION OF LIGHT ATTENUATION IN LAKE EYMR**

Selen ATIKER

M.Sc, Department of Environmental Engineering

Supervisor: Assoc. Prof. Dr. Ayşegül Aksoy

Co-Supervisor: Assoc. Prof. Dr. Selim Sanin

January 2012, 164 pages.

Light penetration and attenuation has significant impact on the water quality of lakes. Algal activity, which is important for the levels of several water quality parameters, is dependent on light penetration besides availability of nutrients. In this study, change in light penetration and attenuation in Lake Eymir was studied. The relationships of extinction coefficient ( $k_e$ ), and water quality parameters were investigated. The effect of  $k_e$  on Chl-a over nutrients were investigated. The water quality parameters measured were; total suspended solid (TSS), phosphate, ammonium, nitrate, photosynthetically active radiation (PAR), chlorophyll-a (Chl-a), Secchi disk depth and lake Depth. The measurements were conducted at five different stations in Lake Eymir. Secchi disk, PAR and

lake depth measurements were done on site, while TSS, Chl-a and phosphate analyses were done in laboratory, using standard methods. Nitrate and ammonium analyses were conducted through laboratory kits. Linear and non-linear regression models of  $k_e$  and Chl-a were developed to understand their relationships with the the measured parameters, using XLSTAT software. Analyses of the data at sampling stations revealed that Station 2 and 3 were the most representative stations in general. The model results indicated that  $k_e$  is as important as nutrients for Chl-a abundance. Secchi disk and Chl-a are the most correlated parameters with  $k_e$ . Moreover Secchi disk depth is nonlinearly correlated with  $k_e$ , while linearly correlation is present between Chl-a and  $k_e$ .

Keywords: Lake Eymir, PAR, Secchi disk, Chlorophyll-a, light attenuation, light extinction coefficient, regression modeling.

## ÖZ

### EYMİR GÖLÜ'NDE IŞIK SOĞURMASININ İNCELENMESİ

Selen ATİKER

Yüksek Lisans, Çevre Mühendisliği Bölümü

Tez Danışmanı: Doç.Dr.Ayşegül Aksoy

Ortak Tez Yöneticisi: Doç. Dr. Selim Sanin.

Ocak 2012, 164 sayfa

Işık geçirgenliği ve ışık şiddetinin düşmesinin göllerdeki su kalitesinde önemli bir etkisi vardır. Pek çok su kalitesi parametresi açısından önemi olan alg aktivitesi, ışık geçirgenliği ve besin maddelerinin uygunluğuna bağlıdır. Bu çalışmada Eymir Gölündeki ışık geçirgenliği ve ışık şiddetinin düşmesi çalışılmıştır. Işık sönmeme katsayısı ( $k_e$ ), ve su kalitesi parametreleri incelenmiştir. Besin maddelerinin yanı sıra Chl-a üzerinde  $k_e$  etkisi araştırılmıştır. Ölçülen parametreler, askıda katı madde (AKM), fosfat, amonyum, nitrat, fotosentetik aktif radyasyon (FAR), Klorofil-a, Secchi disk derinliği ve göl derinliğidir. Ölçümler Eymir Gölü'nde beş ayrı istasyondan yapılmıştır. Secchi disk, FAR ve göl derinliği ölçümleri sahada gerçekleştirilirken, AKM, Klorofil-a, fosfat analizleri standart metodu kullanarak laboratuarda gerçekleştirilmiştir. Nitrat ve amonyum analizleri ise analiz kitleri ile laboratuarda gerçekleştirilmiştir. Ölçülen parametrelerin birbirleriyle ilişkilerini anlamak için XLSTAT'ı kullanarak klorofil-a ve  $k_e$ 'nin

lineer ve non-lineer modelleri geliştirilmiştir. İstasyonlardan elde edilen data analizleri 2. ve 3. ölçüm istasyonlarının Eymir Gölü'nü en iyi temsil eden istasyonlar olduğu göstermiştir. Model sonuçları  $k_e$ 'nin Klorofil-a üzerinde en az besi maddeleri kadar etkili olduğunu göstermiştir. Secchi disk ve Klorofil-a,  $k_e$  ile en yüksek korelasyon gösteren parametrelerdir. Buna ek olarak, Secchi disk,  $k_e$  ile non-lineer olarak ilişkili iken Klorofil-a ile  $k_e$  arasında lineer bir ilişkilidir gözlenmiştir.

Anahtarsözcük: Eymir gölü, FAR, Secchi disk, klorofil-a, ışık soğurması, ışık sönümlene katsayısı, modellenmesi.

*To my beloved family*



## ACKNOWLEDGMENTS

I would like to express my sincere gratitude to everyone who contributed this study. Especially my thesis supervisor Assoc. Prof. Dr. Ayşegül Aksoy, for her endless understanding, patience and tolerance throughout my study, I would like to thank her also for her valuable guidance and encouragement and support, whenever I needed. And I would like to express my thanks to my co-supervisor Assoc. Prof. Dr. Selim Sanin for his valuable inputs. I am also pleased to acknowledge *TUBITAK* for the financial support. This thesis was financed by TUBITAK, project no: 108Y116.

I would like to express my deepest appreciation to all my friends who helped me, gave wise advices and encouraged me about my thesis study and cheered me up whenever I'm down. I would like to thank F. Mehmet Dumanogullari, Gizem Uğurlu Turan, Devrim Kaya, Elif Küçük, Tolga Pilevneli and Onur Yüzügüllü for helping me in my laboratory studies, in my modeling studies and for sharing their wide knowledge and experience with me throughout my thesis study. I would like to thank also Nihat Ersin, Özge Can, Hande Bozkurt, Müge Erkan, Selcen Sönmez, Ebru Sarıkaya, Murat Varol and Güray Doğan and for their support in every way. And I would like to especially thank my closest friends, Buse Kütükçüoğlu, Gaye Şahin, Çağla Giray and Yasemin Binici Şen who were there for me in my good and bad times.

Finally I would like to thank my parents, Aysin and A. Demir Atiker, for believing in me, being very understanding and for supporting me in every way through all my life but especially when I most needed; through my thesis process. And I am thankful to my sister Evren Atiker Huş, for providing me her help whenever I needed, especially for reaching to papers that are impossible to find. I wouldn't be able to accomplish my thesis study if it weren't for them.

## TABLE OF CONTENTS

ABSTRACT.....	iv
ÖZ.....	vi
ACKNOWLEDGMENTS .....	ix
TABLE OF CONTENTS.....	x
LIST OF TABLES.....	xiii
LIST OF FIGURES .....	xiv
ABBREVIATIONS .....	xvii
CHAPTERS	
1. INTRODUCTION .....	1
2. LITERATURE REVIEW & THEORETICAL BACKGROUND.....	5
2.1 Study Area and History of Lake Eymir .....	5
2.2 Eutrophication.....	10
2.3 Light Attenuation.....	13
2.4 Previous Studies on PAR.....	18
3. METHODOLOGY.....	28
3.1. Field Study.....	29
3.1.1. Locations of Sampling Stations .....	29
3.1.2. In-Situ Measurements .....	31

3.1.2.1.	PAR Analysis .....	31
3.1.2.2.	Secchi Disk Analysis .....	32
3.1.3.	Water Sampling.....	33
3.2.	Laboratory Studies.....	34
3.2.1.	TSS Analysis .....	34
3.2.2.	Chl-a Analysis .....	35
3.2.3.	Nitrate (NO <sub>3</sub> -N) and Ammonium (NH <sub>4</sub> -N).....	36
3.2.4.	Phosphorus (PO <sub>4</sub> -P).....	36
3.3.	Calculation of Light Extinction Coefficient.....	37
3.4.	Data Analysis and Modeling of k <sub>e</sub> .....	38
4.	RESULTS and DISCUSSIONS .....	40
4.1.	Analysis of the Study Data.....	40
4.1.1	Data Analysis With Respect to Time.....	40
4.1.2	Data Analysis With Respect to Sampling Stations.....	46
4.2	Evaluation of Light Extinction Coefficient in Lake Eymir .....	52
4.3	Modeling of k <sub>e</sub> .....	56
5.	CONCLUSIONS & RECCOMENDATIONS FOR FUTURE STUDIES	95
	REFERENCES .....	98

APPENDIX

$k_e$  CALCULATIONS ..... 110

## LIST OF TABLES

### TABLE

Table 2-1: Annual Average biomass of algal species in percentages, in Lake Eymir.....	17
Table 2-2. The constants representing $SD \times k_e$ according to different scientists.....	20
Table 4-1. Correlation matrix of linear regression model of $k_e$ , with one-year data.....	58
Table 4-2. Correlation matrix of linear regression model of $k_e$ , with data obtained before gate broke.....	63
Table 4-3. Correlation matrix of linear regression model of $k_e$ , with data obtained after gate broke.....	69
Table 4-4. The goodness of fit statistics.....	74
Table 4-5. Correlation matrix of linear regression model of Chl-a, With one-year data.....	82
Table 4-6. Defining Limiting Nutrient by Dissolved N:P Ratio. ....	90
Table 4-7. The Summary of the Models Studied .....	91

## LIST OF FIGURES

### FIGURE

Figure 2-1: Location of Lake Eymir.....	6
Figure 2-2: The path of photons passing through a water column, by the scattering and absorption processes .....	22
Figure 3-1: Sampling stations in Lake Eymir.....	30
Figure 3-2: PAR Sensor Device .....	31
Figure 3-3: Secchi Disk.....	32
Figure 3-4: Van dorn sampler .....	33
Figure 3-5: TSS analysis procedure.....	34
Figure 4-1 Mean SD value of 5 stations vs. Time .....	41
Figure 4-2. Mean Depth value of 5 stations vs. Time.....	42
Figure 4-3. Mean TSS value of 5 stations vs. Time .....	42
Figure 4-4. Mean Chl-a value of 5 stations vs. Time.....	43
Figure 4-5. Mean NO <sub>3</sub> -N value of 5 stations vs. Time.....	44
Figure 4-6. Mean NH <sub>4</sub> -N value of 5 stations vs. Time .....	45
Figure 4-7. Mean PO <sub>4</sub> -P value of 5 stations vs. Time .....	45
Figure 4-8. Mean depth values of each sampling station.....	47
Figure 4-9. Mean Secchi Depth values of each sampling station. ....	48

Figure 4-10. Mean Extinction Coefficient values of each sampling station. .....	48
Figure 4-11. Mean TSS values of each sampling station.....	49
Figure 4-12. Mean Chl-a values of each sampling station. ....	50
Figure 4-13. Mean NO <sub>3</sub> values of each sampling station. ....	50
Figure 4-14. Mean NH <sub>4</sub> values of each sampling station. ....	51
Figure 4-15. Mean PO <sub>4</sub> values of each sampling station. ....	51
Figure 4-16. In PAR values versus Depth.....	53
Figure 4-17. Extinction Coefficient vs. Time.....	55
Figure 4-18. Mean Extinction Coefficient Value of 5 Stations vs. Time ...	56
Figure 4-19. Standardized Coefficients vs. variables of k <sub>e</sub> M1 model....	60
Figure 4-20. Predicted k <sub>e</sub> versus measured k <sub>e</sub> for k <sub>e</sub> M1 model.....	60
Figure 4-21. Standardized Coefficients vs. variables of k <sub>e</sub> M2 model.....	61
Figure 4-22. Predicted k <sub>e</sub> versus measured k <sub>e</sub> for k <sub>e</sub> M2 model .....	62
Figure 4-23. Standardized Coefficients vs. variables of k <sub>e</sub> M3 model.....	65
Figure 4-24. Predicted k <sub>e</sub> versus measured k <sub>e</sub> for k <sub>e</sub> M3 model.....	66
Figure 4-25. Standardized Coefficients vs. variables of k <sub>e</sub> M4 model.....	67
Figure 4-26. Predicted k <sub>e</sub> versus measured k <sub>e</sub> for k <sub>e</sub> M4 model .....	67
Figure 4-27. Predicted k <sub>e</sub> versus measured k <sub>e</sub> for k <sub>e</sub> M5 model .....	70
Figure 4-28. Standardized Coefficients vs. variables of k <sub>e</sub> M5 model.....	71
Figure 4-29. Predicted k <sub>e</sub> versus measured k <sub>e</sub> for k <sub>e</sub> M6 model .....	72

Figure 4-30. Standardized Coefficients vs. variables of keM6 model....	72
Figure 4-31. Predicted $k_e$ versus measured $k_e$ for keM7 model .....	75
Figure 4-32. Standardized Coefficients vs. variables of keM7 model.....	76
Figure 4-33: $k_e$ vs. SD.....	77
Figure 4-34: $k_e$ vs. Chl-a.....	77
Figure 4-35. Predicted $k_e$ versus measured $k_e$ for $k_e^*$ <i>all time</i> model.....	79
Figure 4-36. Predicted $k_e$ versus measured $k_e$ for $k_e^*$ <i>before gate broke</i> model.....	80
Figure 4-37. Predicted $k_e$ versus measured $k_e$ for $k_e^*$ <i>after gate broke</i> model.....	81
Figure 4-38. Standardized Coefficients vs. variables of CM1 model.....	84
Figure 4-39. Predicted Chl-a versus measured Chl-a for CM1 model.....	84
Figure 4-40. Standardized Coefficients vs. variables of CM2 model.....	85
Figure 4-41. Predicted Chl-a versus measured Chl-a for CM2 model.....	86
Figure 4-42. Standardized Coefficients vs. variables of CM3 model.....	87
Figure 4-43. Predicted Chl-a versus measured Chl-a for CM3 model.....	88
Figure 4-44. N:P Ratio of Lake Eymir.....	89
Figure 4-45. Normalized Chl-a and R square values versus time.....	92



## LIST OF ABBREVIATIONS

PAR	: Photosynthetically Active Radiation
Chl-a	: Chlorophyll-a
NO <sub>3</sub> -N	: Nitrate
NH <sub>4</sub> -N	: Ammonium
k <sub>e</sub>	: Extinction Coefficient
TSS	: Total Suspended Solid
SD	: Secchi Disk Depth
TP	: Total Phosphorus
N	: Nitrogen
P	: Phosphorus
RMSE	: Root Mean Square Error

## **CHAPTER 1**

### **INTRODUCTION**

Lakes are valuable resources that are very important for the living and used for many purposes such as transport, industry, fishing, agriculture, recreation and tourism. Unfortunately today, water quality of most of the lakes around the world is so low that it is impossible to be recovered by natural means (Brivio et al. 2001). In general, in inland waters eutrophication is a process that occurs in a water body when the concentration of the nutrients such as nitrogen and phosphorus, which promote the reproduction of primary producers such as phytoplankton, increase.

One of the parameters that induce the lake to be classified as eutrophic is turbidity. Turbidity might result due to inorganic suspended material, high chlorophyll-a (Chl-a) concentrations or detritus material (Christian & Sheng 2003). In aquatic systems, phytoplankton and Chl-a abundance are among the major indicators of eutrophication. Chl-a is a parameter that helps in classifying the lake as eutrophic. In other words it provides us to determine eutrophication levels (Danilov & Ekelund 1999; Hasegawa et al. 2010).

Turbidity causes attenuation of light in a water body, thus affects the productivity of phytoplanktons. The penetration of sun light in to a lake depends on backscattering and absorption of light by particles, which are mostly composed of phytoplankton. Light attenuation occurs when the

quality of the water is deteriorated, it is directly related to algal growth and it depends on turbidity and the nutrient content of the lake (Fisher et al. 1999)

In turbid environments sub-surface light conditions have a significant effect on growth of aquatic plants especially phytoplanktons. Particularly in nearshore environments there is a considerable amount of suspended particulate material, and this suspended material can highly restrict the transition of light. The light availability also alters algal competition and phytoplankton community structure. The level of photosynthetically active radiation (PAR) in natural waters is necessarily important in determining the growth of phytoplankton and macrophytes (Devlin et al. 2008).

Comprehending the contributions of different parameters responsible for attenuation of light is important. It is possible to estimate the conditions of light in the water at different depths, from the concentrations of those parameters. The major parameter that cause attenuation of light, in near-shore water bodies, may vary from dissolved organic matter to phytoplankton, to suspended solids or some combination of these components (Devlin et al. 2008). Briefly, light attenuation, Chl-a concentration and nutrients such as nitrogen (N) and phosphorus (P) are parameters that are dependent to each other and in most cases have significant effects on eutrophication (Fisher et al. 1999).

Lake Eymir is an eutrophic, shallow lake which is located at 20km south of the capital city of Turkey; Ankara. Until 1990, it served as the primary drinking water supply for the Middle East Technical University campus. In the last 30 years the water quality of Lake Eymir has deteriorated due to the waste loads, uncontrolled settlements around the area and drought conditions. Since 1990, Lake Eymir was taken under environmental protection, due to its importance with its rich ecosystem and being one of the few recreational places in Ankara (Yenilmez et al. 2010).

In 1995, a diversion line was in operation to bypass the load from Gölbaşı district. It was observed that the total phosphorus (TP) reduced by half, while high turbidity and low submerged plants persisted in Lake Eymir (Atınbilek et. al, 1995). Beklioğlu suggested that this poor clarity was due to the domination of specific kinds of fish. Therefore they started a biomanipulation project in 1998 (Beklioğlu et al. 2002). In 2001, a large drop ( $100\pm 10\text{cm}$ ) occurred in lake water levels, due to extreme drought conditions. This triggered an increase in submerged macrophytes by around 90%. But the water level restored back in 2002 to its average level (Tan & Beklioğlu 2005).

Investigation of previous studies shows that turbidity and nutrient concentrations are spatially and temporarily variable in lakes. However, most of the studies in literature focus on nutrient levels in evaluating the growth of algae (Schindler, 1978; Smith et. al, 1999; Scheffer et. al, 2007). It is a fact that light limitation may be as important as nutrient concentrations for growth of algal species (Chapra, 1997; Underwood et. al, 1999), especially in turbid lakes such as Lake Eymir.

This study aims investigating the seasonal changes of the light attenuation in Lake Eymir. Moreover, its importance for algal growth relative to nutrient concentrations is examined. In order to conduct the study, measurements were done both at site and at laboratory. Field work was conducted from June 2009 to June 2010. Secchi disk depth, PAR, and lake depth measurements were conducted on site, while nitrate, phosphate, ammonium, Chl-a, total suspended solid (TSS) analyses were made in the laboratory. Light attenuation and the parameters that affect light attenuation were studied. In addition to this, the relationships of the measured parameters with each other were examined. Moreover, dependence of chlorophyll-a on limiting factors such as nitrate, ammonium, phosphate, and light extinction coefficient ( $k_e$ ) was investigated. Statistical analysis of data was performed using XLSTAT. Linear regression models were developed using this software. The

regression analyses helped understanding the effects of the measured parameters on  $k_e$  and the limiting effect of  $k_e$  on Chl-a concentrations over nutrients.

## CHAPTER 2

### LITERATURE REVIEW & THEORETHICAL BACKGROUND

#### 2.1 Study Area and History of Lake Eymir

Lake Eymir is located 20 km south of Ankara. It is located at the coordinates of 39.28 N and 32.30 E, at an altitude of 969 m (Tan, 2002). Lake Eymir's location is given in Figure 2-1. Lake Eymir is a significant recreational area and especially used for rowing activities since 1962 for Middle East Technical University (METU) and Ankara. Lake was confiscated by METU in 1957 and used as a drinking water resource, until 1990's. With verdict of Turkish Cabinet of Ministers, Lake Eymir got under environmental protection and become a "Specially Protected Area" (SPA) in 1990 (Altınbilek et al., 1995).

The lake's dimensions are approximately 3000 m x 500 m x 5.5 m with a corresponding area of 1.25 km<sup>2</sup> (Camur et al., 1997). It has a shoreline of 13 km (Tan et al., 2005). The approximate volume of the water in the lake is 3.88x10<sup>6</sup> m<sup>3</sup> (Karakoc et al., 2003). Tan (2002) stated that the water depth in the lake was between 4.3 to 6.0 m in 2002.

Lake Eymir and Mogan are two hydrologically interconnected lakes with an inflow from Mogan Lake (South) to Lake Eymir (North). The level of water in Lake Mogan is 3 m higher than the water level in Lake Eymir. The water levels in both lakes vary seasonally. Lake Eymir's water level changes by 0.5 – 1.0 m (Yagbasan & Yazicigil, 2009).



Figure 2-1 Location of Lake Eymir (URL3)

The major inflow to Lake Eymir is generated by Lake Mogan. Precipitation, which is approximately  $390 \pm 76$  mm/year, should also be considered as a contribution to the water budget of Lake Eymir (Ozaydin et al., 2001). Lake Eymir drains into Imrahor Creek at south of the lake. The outflows from the lake are groundwater discharge and evaporation. The approximate evaporation amount is 1092.2 mm/year. In 1995, Altınbilek reported that there was a discharge of 2L/s to groundwater. At northern part, a groundwater inflow feeds Lake Eymir with a flowrate of 17 L/s (Altınbilek et al., 1995). Diker (1992) also reported that the catchment basin of the lake

encompasses a part of the region in the Elma Dag Mountain which is another water source for the lake.

Once the lake was in clear state and Secchi disk depth was above 4 m (Geldiay, 1949). In June 1947, he even observed 6 m of Secchi depth. Within last 25 years Lake Eymir began to be contaminated due to discharges and uncontrolled settlements (Yenilmez et al. 2010). Today Lake Eymir is a eutrophic lake.

Since 1970, Lake Eymir, especially the southern part of the lake, became a discharge area for the wastewaters of Gölbaşı Municipality. Gölbaşı District is the largest and the main residential area, with an approximate population of 86,749 capita (URL2). The discharges are the main reason of the eutrophication problem in the lake. Moreover, the land that the lakes are located in is mainly used for agricultural purposes, and besides Station sources, nonpoint discharges from these agricultural activities contribute to the pollution of both lakes (Karakoç et al. 2003).

There was a natural channel connecting the two lakes. It was modified to control the flow from Lake Mogan to Lake Eymir by constructing a gated concrete channel. At the inlet, a wetland was formed which received the input from Lake Mogan, rich with nutrients (Yagbasan et al., 2009).

Between July 1993 and June 1994, the waste water of the area was discharged into the canal that connected Lake Mogan and Eymir since the bypass line for the Gölbaşı sewage system was not in operation. Therefore, there was a direct discharge to Lake Eymir. In spite of commissioning of the sewage system, Lake Eymir continued to receive pollutant loads because of illegal Station discharges and the bypass line not being operated continuously (Altınbilek et al., 1995). The major contamination sources of the lake included the waste water discharges from TEK residential area and Police College facilities as well as perennial Kışlakçı Stream (Yagbasan et al., 2009). Another pollutant source was the



slaughter house which discharged its waste to an area near by Eymir, which was closed in 1994 (Altınbilek et al., 1995).

In 1995 Lake Eymir was in highly eutrophic state with high concentrations of Chl-a, TP and TSS. The lake was phosphorus limited. The recorded Secchi disk depths were quite low (37-75 cm).

There were several studies conducted in Lake Eymir. For example Beklioğlu and others claimed that some specific kind of fish was responsible of low water quality. They studied on biomanipulation project between August 1998 and December 1999 in Eymir. Tench and carp fish were removed 45% and 83% respectively and as a result the Secchi depth increased, inorganic suspended solid and Chl-a concentration decreased therefore an improvement in water quality was attained (Beklioğlu et al. 2002).

Impacts of pollutant sources and water quality of Lake Eymir, was investigated by Karakoç et al (2003). According to their study chemical oxygen demand (COD), total phosphorus (TP), and total Kjeldahl Nitrogen (TKN) concentrations were close to or slightly lower than the levels recorded in 1995 by ASKİ. This improved water quality conditions were attributed to the construction of the sewage system and the starting of its operation.

In March 20<sup>th</sup>, 2010, the gate was broken due to the pressure caused by the large quantity of water in Lake Mogan. As a result, the water depth in Lake Eymir suddenly increased by 1 m in a couple of days in March 20<sup>th</sup> 2010 due to the inflow from Lake Mogan to Lake Eymir. Further with high precipitation, the rise in the water level of Lake Eymir approached to 1.5 – 1.7 m. Right after the incident, Gölbaşı Municipality rehabilitated the channel and reinstalled the gate again in May 2010 (URL3).

After biomanipulation, in 2001 drought conditions occurred and the water level reduced by 90 to 110 cm. Due to the drought and decreased water

level and disappeared thermal stratification, concentrations of TP increased. The water level didn't restore back to its original level until 2002. TP concentrations slightly decreased and Chl-a concentrations increased (Tan & Beklioğlu, 2005).

According to the results of Ozen's study (2005), biomanipulation tended to give favorable results at start in general. After 4 or 5 years of implementation, he saw that during biomanipulation, concentrations of some parameters like Chl-a and TP decreased, and some parameters like ammonium, remained the same. After a while they all increased to levels higher than their clear state concentrations. Secchi disk increased during the biomanipulation but then decreased drastically. TSS was the only parameter that significantly decreased due to the project but it also began to increase in 2005 (Ozen, 2006).

Changes in the Secchi depth values can be caused by variations in concentrations of TSS. TSS concentrations reduced similar to Secchi depth until the first biomanipulation and were stable until 2005. But unlike the Secchi depth, TSS concentrations increased after year 2005. Increase in Chl-a concentrations resulted in decreasing of Secchi disk depths with increasing TSS concentrations. The reduction in nutrient content during biomanipulation can be associated with the diversion of the waste water loads which used to be discharged into Lake Eymir until 1994, besides the biomanipulation project (Tan, 2002).

Ozen also conducted a long term study on Lake Eymir between 1997 and 2007 (Ozen et al. 2010) and revealed that the lake reversed back to its pre-biomanipulated state in 5 years. In 2006-2007 second biomanipulation was carried out in Eymir. The fish manipulation actions resulted in positive outcomes in cold temperate lakes but in Lake Eymir it did not work well since it is a warm tempered lake. The study revealed that a reduction in the capacity of nutrient retention in warm tempered shallow lakes led to rapidly progressing eutrophication (Ozen et al., 2010).

When the nutrient rich inputs discharged to Lake Eymir are considered, it is not hard to estimate the high potential of algal growth. Besides this high nutrient load, the feature of Lake Eymir being shallow provides optimum conditions for eutrophication. In almost all studies done after 2000, the lake was reported as highly eutrophic (Karul et al., 2000; Yenilmez et al., 2010) with an abundance of surface and submerged plants (Tan & Beklioğlu., 2005).

## **2.2 Eutrophication**

Eutrophication is a combination of two words; “eu” means well and “trophe” means feeding or nutrition. It is a natural aging process. It can be defined as the outrageous increase of phytoplanktons, and the sum of its consequences. Eutrophication generally caused from nutrient loads, excessive use of fertilizers near by a water body and waste water discharges. Water eutrophication is widespread throughout the world. It is observed in reservoirs, lakes, rivers and estuaries (Yang et al., 2008).

Naumann, in 1919, was the first scientist who defined eutrophication of a lake as the increasing of nutrients, especially nitrogen and phosphorus (Hutchinson, 1967). This definition was made for lake ecosystems, but when it came to marine systems, the definition of eutrophication changed. Steele (1974) related eutrophication to the growth rate of algal biomass, rise in nutrient amount and their impacts. Vollenweider (1992), combined these two definitions and defined eutrophication for both marine and fresh systems. According to his definition, eutrophication is enrichment of the water body with nutrients, especially with phosphorus and nitrogen that stimulates the primary production, and their extreme growth which leads to algal scums and blooms, and the advanced benthic algal growth of both floating and submerged macrophytes (Kitsiou & Karydis, 2011).

Studies show that 53% of the lakes in Europe, 28% in Africa, 41% in South America, 48% in North America and 54% in Asia are in eutrophic state. As stated before, unless it is caused by an anthropogenic activity, eutrophication is a process that takes thousands of years and occurs naturally. Artificial eutrophication, which is originated from human activities, has become a major concern in developing and also in developed countries. Countries with high population such as, India, China, Pakistan, Indonesia, Bangladesh, and industrialized countries in Europe, USA and Canada, are directly under threat of eutrophication (Ansari et al., 2004).

Vitousek et al (1997) stated that the production of fertilizers in the world was below 10 million metric tons of nitrogen in 1950's, this amount increased to 80 million metric tons of nitrogen in 1990, and it is estimated that it will be above 130 million metric tons by 2030. When fertilizers is used in agriculture, the amount of nitrogen might be more than the plant need for growth, so this surplus nitrogen would either accumulate in the soil, or move to surface and ground waters, or it would go to the atmosphere via chemical processes. Phosphorus is also generating from fertilizers and accumulating in soils. For example in Ireland, over the past 50 years, phosphorus reserves accumulated at a rate of 1000 kg phosphorus per km<sup>2</sup> year. This rate would become significant over decades or more (Foy et al., 1995).

Most of the studies done on Chl-a abundance; which is directly related to phytoplankton biomass, is based on nutrient limitation. One of the earliest studies done on nutrient load and its relationship with plant growth, was conducted by an agricultural chemist Justus von Liebig in 1855. He discovered that aquatic plants including phytoplanktons show the same response to nutrient loads with the terrestrial plants. He also found that plant growth can be limited by the nutrient presented, if it's relatively less compared to demand. And in further studies scientists explored that the nutrient which limit the plant growth are Nitrogen (N) and Phosphorus (P).

The N and P loads might be derived from fluvial, groundwater and atmospheric inputs through agricultural activities and wastewater discharges. Sources might be Station or non-Station sources depending on the local population density and land use (Smith et al., 1999).

Li and others (2011) also found out that Chl-a shows a parallel pattern with N and P concentrations so it can be said that excessive nutrient loads to a water system triggers Chl-a concentrations to increase. Shallow lakes differ from deeper lakes with their lack of long term stratification, internal nutrient loadings and easily mixing structure in water column. In shallow lakes, water conditions such as total phosphorus (TP), Chl-a, turbidity and algal blooms may give complex responds to nutrient loads from outside. With the conditions of shallow and eutrophic lakes, light extinction can be a more important factor compared to nutrient availability (Havens et al., 2001).

Larger and deeper lakes are less affected by the eutrophication causing conditions, where shallower and smaller lakes are affected rapidly. Shallow lakes give response to conditions that cause eutrophication immediately. In a shallow lake, consequences of eutrophication are observed more dramatically. With a high nutrient load a shallow lake reacts expeditious and tend to become dominated by phytoplankton therefore become more turbid (Hein L., 2006).

Hootsman is another scientist who studied eutrophication in shallow lakes (1994). He reported that eutrophication in shallow lakes is often due to domination of phytoplanktons and as a result increase in turbidity thus light limitation (Hootsmans et al., 1994). Based on this conclusion, Asaeda and others developed a model which incorporates nutrient dynamics, phytoplanktons abundances. As a result they found that with high nutrient loads, phytoplankton blooms occur therefore attenuation in light is observed. In shallow lakes, with continuous load of nutrients, existing phytoplankton amount increases drastically (Asaeda et al., 2001).

Another study which focused on the relationship of Chl-a and nutrients was done on Barton Broad Lake, according to results Chl-a concentrations were dependent on N, P. Recovery of eutrophication was tested by reducing P load in to lake but they observed that the in-lake P concentration was maintained for years in spite of the P load reduction for 90%, which proves that solely nutrient load reduction is insufficient (Lau and Lane 2001). This is because in most water ecosystems Chl-a concentrations are limited by light availability, rather than available nutrient concentrations (Loiselle et al., 2007)

### **2.3 Light Attenuation**

Light attenuation and turbidity in a water body is mainly due to anthropogenic activities such as mining or erosion resulting with particle input (Davies-Colley et al., 1993). In 1978 Jewson and Tylor reported that these changes would lead to a reduction in primary production due to the limitation of light and low reduced visibility, resulting with an affected prey-predator interaction (Jaun et al., 2007).

Light, temperature and wind are parameters that affect the lake ecosystem most. Among these parameters light has the biggest role in water bodies. First of all temperature is directly correlated with it. The temperature of a lake, especially the surface water, increases with sunlight especially during summer. In the deeper parts of a lake, the water is less affected by the sun light, thus less warmed. Sometimes layers occur due to this temperature difference, and it is called thermal stratification. In shallow lakes stratification doesn't occur in summer. In winter, the water under the ice cover is 0°C and deeper water is (4°C) slightly warmer. Since the wind cannot reach under the coverage of ice and mix the water below it, winter stratification continues until the ice melts. Winter stratification doesn't occur in subtropical or tropical lakes, in temperate-zone large lakes, or in salty lakes. In spring and autumn the lakes that stratify in winter and

summer mix from top to bottom and this is called turnover. Lakes which don't stratify both in summer and winter, mix continuously throughout those seasons. Due to the angle of the sunlight the lakes in tropical zones may stratify every day and they may mix every night. Lakes are divided in to two layers due to the summer stratification, a warm and illuminated part; epilimnion where photosynthesis is carried out by phytoplankton such as algae and photosynthetic cyanobacteria, and a cool and dark zone; hypolimnion where the production of photosynthesis is decomposed and anoxic conditions occur when the decomposing organic matter is in excessive amounts (Hairston & Fussman, 2002).

Light has a big role even on the ice algae which live in the ice covered water bodies and are adjusted to low light conditions (Kudoh et al., 1997). In a study done in 1952 by Sorokin and Krauss, 5 different types of green algae were tested under different light conditions, with light intensities up to 10.000 lm/ft<sup>2</sup> and revealed that among other parameters (temperature, CO<sub>2</sub>, nutrients supply) light intensity has a major effect on algal growth but still, all these parameters should be considered together.

According to the most of the studies done on algal behaviour, growth of algae depends on nutrients (N and P), light and temperature. When excessive growth is considered, the consequences are not favorable. Increased concentrations of algae, impacts turbidity and dissolved oxygen concentrations. Light is an important parameter for algal growth. Available light leads to an increase in algal population and higher algal concentrations cause turbidity which is one of the main reasons of light attenuation. So besides nutrients and temperature, light has a very important role in algal growth in a water body. This is why monitoring of these parameters is very important for the control of water quality (Elahdab, 2006).

In their study Hairston and Fussman (2002) confirmed that light is consumed and taken up by algae and promotes algal growth. Light is an

important parameter for phytoplankton because it is required for photosynthesis. Especially for the algae which lives in the deeper parts of a water body, light can be more limiting compared to nutrients. Algal bloom is observed when algae population increase excessively. It causes light limitation, in other words; the algal biomass close to the surface of water shades the algae living in deeper parts. As a result, both phytoplankton and macrophyte growth in the water can be affected (Hairston & Fussman, 2002).

Most of the sunlight falling on the surface of a water body is refracted before proceeding into the lake. A part of the light is lost at the surface and the rest of the light is absorbed and scattered by water and, organic and inorganic particles in the water. The rate of light attenuation with depth is a property of a water body which is different in every lake. Light attenuation can be an important property to define the trophic status of a lake, but other parameters such as oxygen concentration, nutrient availability, should be considered all together in order to obtain more accurate results (Schanz, 1985).

Light availability influences the benthic algae biomass accumulation in streams and lakes shaded by wide forests (Gregory, 1980). Increased concentrations of inorganic suspended solids restrict light penetration into the water column, and this leads to potential limitation of the growth of both suspended and benthic algae in fresh waters. In turbid reservoirs, it can also restrict phytoplankton biomass (Hoyer & Jones, 1983). The water body nutrient enrichment studies done on Pacific Northwest streams by Gregory (1980) suggested that nitrogen was the limiting nutrient, but the responses of algae to nutrient enrichment were strongly abated by low light availability.

Phytoplankton tend to live in mediums with high light availability because photosynthetic pigments can only absorb a part of the light passing through water, and use it for photosynthesis. Light absorption by algae



rises with biomass and reduces with increased non-algal turbidity. However, raised interception of light by algae underwater causes the light gradient to steepen and thus decrease in euphotic zone in the vertical extent (Tilzer, 1983). Rodhe (1965) showed that the vertical distribution of phytoplankton which is mainly controlled by the intensity of light is affected by self-shading. Megard's (1972) study revealed that there is an optimum light availability for algae to use in photosynthesis and growth.

De Jonge (1997) investigated Dutch Wadden Sea and found out that there was a serious increase in primary production between years 1960 – 1986 and associated this increase to high phosphorus loads to the sea. But in 1980, despite the reduction in phosphorus loads, production still increased and this was mainly due to light availability. As De Jonge (1997), Cloern (1999) also concluded that although primary production and algal biomass is dependent on nutrient load, it also changes according to light conditions. Solar radiation is needed as an energy source in photosynthesis for algae to utilize nutrients. Light becomes a more limiting factor in turbid systems for algal growth rate.

Different types of algae responded in dissimilar ways to varied light intensions and temperature was another factor affecting the response of algae to light attenuation (Sorokin and Krauss, 1952). Since different types of algae gives different responses to light attenuation, the effects of PAR should be considered by investigating the specific type of algae that exists in Lake Eymir. Study of Beklioğlu (2006) revealed that algae distribution in Lake Eymir is dominated with green algae. The percentage distribution is given below in Table 2-1

Table 2-1: Annual Average biomass of algal species in percentages, in Lake Eymir (Bekliöglu, 2002)

Algae	Annual Average Biomass %
Green Algae	76
Cryptophyta (Various Colors)	15
Cyanobacteria (Blue-Greens)	3.6
Dinoflagellates (Red Brown)	2.5
Diatoms (Golden Brown)	2.5

Green algae, which is the type of algae dominated in Lake Eymir, is all photoautotrophic; in other words they produce their own food from inorganic material by using light, so their growth may depend on light availability under the water and nutrient amount. Growth of other algae is also linked to light availability as well as to parameters such as temperature, conductivity and transparency (Hansson & Brönmark 2009). Green algae, is a type of algae that requires environments with higher light conditions compared to other algal groups such as cyanobacteria and diatoms (Pillsbury et al., 2002).

Blue-green algae, which is another algae kind that lives in Lake Eymir, is an algae type that can fix nitrogen from atmosphere. That is why, while phosphate is consumed as soon as it becomes available, nitrate is not consumed immediately in the lake (Elahdab, 2006)

## **2.4 Previous Studies on PAR**

Fine suspended particles lead to a foggy appearance in a water body. This is due to the light scattering effect of these particles. This incident is called as turbidity (Kirk, 1994). Water bodies with high amounts of suspended particles are reported as turbid. Nephelometer is a device which measures turbidity in nephelometric turbidity unit (NTU). Turbidity changes the spectral quality of the sunlight and the ratio of depth at which light is sufficient for algae and submerged plants to grow, in other words the euphotic depth. It causes rapid light attenuation. Turbidity also affects the composition of phytoplankton. Their variety reduces with the increasing turbidity. While most of the phytoplankton species vanishes in highly turbid water bodies, cyanobacteria generally become dominant, because they can regulate themselves to turbid conditions (Grobbelaar, 2009).

The simplest procedure to measure the light attenuation is done by using Secchi disk, a black & white disk that is lowered in water until it just disappears from sight. The depth the disk disappears is called as the Secchi depth (*SD*). It is an indication of the light transmitting potential of a water body. This is a slightly uncertain method which depends on the person's ophthalmic senses (Otto, 1966).

There are two other more objective methods for measuring light attenuation, which involve photoelectric cells. One of them is called irradiance meter which measures the fraction of sunlight that penetrates at particular depths. The other type is called the beam transmittance meter and works with a collimated light source. This collimated light beam

traverses a particular distance in water and a photo-electric cell measures the transmitted light. The data measured with both of instruments are given in extinction or attenuation coefficients. But the attenuation coefficients obtained with these two instruments are significantly different. The data obtained with latter instrument have more clear physical meaning. Unlikely, the irradiance meters measurements depend on sunlight that penetrates into the lake (Otto, 1966).

There is a relationship between Secchi depth and light attenuation coefficient ( $k_e$ ). Scientists studied some theories relating the light transmission to Secchi depth measurements, and determined light attenuation based on Secchi depth. Joseph (1952), Clarke (1941), Tibby and Barnard (1963) derived formulas and each of them found different constants obtained by the multiplication of extinction coefficient and Secchi disk depth. Examples for these constants found by different researchers are provided in Table 2-2.

Hanoka and others (1956) found a more different relationship between Secchi depth (SD) and extinction coefficient ( $k_e$ ) given as below;

$$SD^{0.3} \times k_e = \text{constant}$$

(Eq- 1)

Hanoka suggested a different equation due to the low depth conditions of the lake they studied, which was below 30 cm. It is a known fact that at shallow lakes with low Secchi depth values, the relationship between SD and  $k_e$  is more complicated.

Table 2-2. The constants representing  $SD \times k_e$  according to different scientists (Otto, 1966)

<b>Scientists</b>	<b>Constant <math>SD \times k_e</math> Value</b>
Atkins and Poole (1931)	0.74
Le Grand (1939)	0.65 (for turbid water)
Le Grand (1939)	1.74 (for clear water)
Clarke (1941)	0.74
Joseph (1952)	0.95
Tibby and Barnard (1963)	0.61

TSS is another water quality parameter that cause light attenuation. It is a ubiquitous pollutant that leads to a significant economic cost and environmental damage (Clark et al., 1985). Suspended sediment has an important potential of causing environmental impact including transportation of toxic organics and other pollutants (Tessier, 1992). Among all other effects of suspended solids, the most obvious and certain impact is the decreased light transmission, in other words, light attenuation (Davies-Colley & Smith, 2001).

Light attenuation that is caused by suspended solids has two main biotic effects; decreased visual range of visible living organisms (Vogel & Beauchamp, 1999) and decreased light penetration into water for photosynthesis (Kirk, 1994). Besides effecting the primary production in a water body, reduction in visual range also has an effect on perception of human for use of the water body for recreational purposes and fishing activities (Smith et al. 1995a). Light attenuation in water bodies is ecologically very important (Kirk, 1994). The parameters that cause light attenuation, limit the light used by submerged plants and algae. The reduced optical clarity in water not only affects the recreational activities but also the aquatic birds and fish (Davies-Colley & Smith, 2001).

Kirk (1994) examined water as a light transmitting medium. He investigated the basic parameters that are responsible of light attenuation in water. It was reported that some of the photons disappeared by scattering and while others by absorption. The disappeared photon energy was transferred to another form, mostly heat, by absorption process. Other photons changed direction due to scattering process. If absorption coefficient is “ $a$ ”, and scattering coefficient is “ $s$ ”, then the sum of them gives the beam attenuation coefficient,  $k_b$ . These quantities; beam attenuation, absorption and scattering coefficients, are inherent optical properties that do not depend on any parameters other than water itself. They may also be considered as conservative parameters (Kirk, 1994). In Figure 2-2, the path of photons passing through a water column is given.

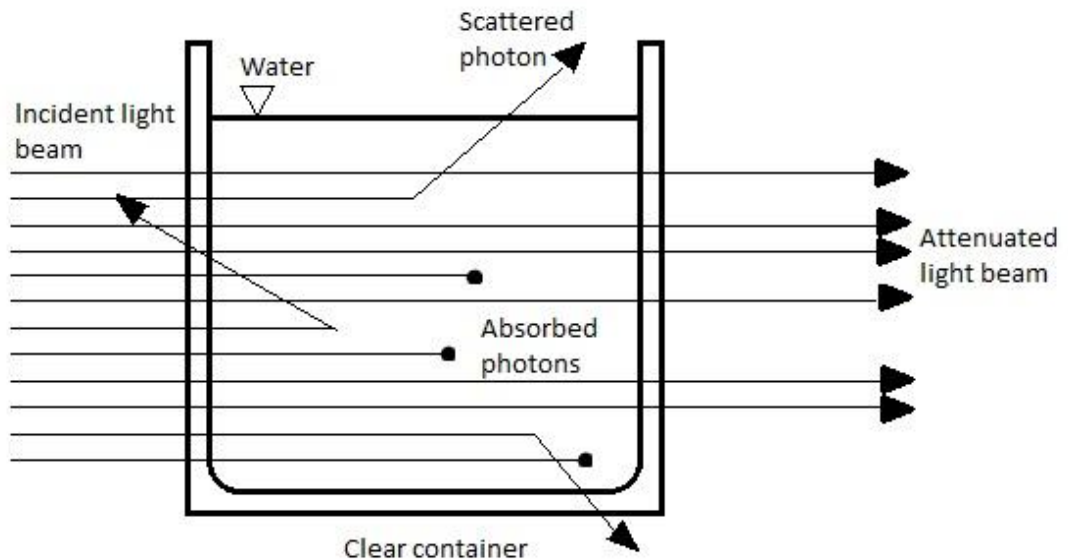


Figure 2-2. The path of photons passing through a water column by scattering and absorption processes (Davies-Colley et al., 1993).

Light and beam attenuation governs Secchi disk depth, therefore it can be said that it is based on the reduction of irradiance with depth. Oppositely beam attenuation is defined as the weakening of a ray of light sent through a water sample. The responsible of light attenuation, as mentioned before, is scattering and absorption (Kirk, 1994). Different from eutrophic lakes, in oligotrophic lakes the attenuation of light is due to organic particles. Phytoplankton is very low and scattering is mainly due to inorganic particles. Scattering may lead to beam attenuation, while light attenuation is less affected. The scattering type that affects light attenuation is backscattering, whereas forward-scattering increases absorption by prolonging the light path (Kirk, 1985).

Light penetration into a water body with depth is evaluated by light attenuation or  $k_e$ . It may be defined as a proportional decrease in light, in other words in irradiance, per unit depth interval. It is also called diffuse attenuation coefficient. The depth at which light is sufficient for algae and submerged plants to grow is called as the euphotic depth, as mentioned before. This is also the depth where PAR is reduced to 1% of its initial

value. It should be noted that even though the names of beam attenuation coefficient and light attenuation coefficient is very similar, these two parameters are indeed presenting very different units (Davies-Colley & Smith, 2001).

In year 1984, Effler and others worked on a hypereutrophic Lake Onondaga in New York for seven months. They derived an applicable model to distribute the partition of light extinction between the scattering and absorption processes. According to them, 40% of the light attenuation during the study was due to the scattering of light. Light attenuation coefficient for whole PAR wave-band is given as  $k_e(\text{PAR})$ . It is inversely proportional with euphotic depth.

In 1980 Walmsley et al. examined Rudt der Winter Reservoir in South Africa which had high TSS concentrations. They observed a linear increase in  $k_e$  with turbidity. Lloyd and others (1987) also found a linear relationship between TSS and  $k_e(\text{PAR})$  in Alaskan rivers which are impacted by gold-mining activities nearby in 1987. Studies done on optical modeling showed that  $k_e(\text{PAR})$  is more or less equaled to the square root of the scattering in water and it was directly proportional with absorption (Kirk, 1985).

The light attenuation coefficient,  $k_e$ , is directly correlated with total suspended solids (TSS) or in other words nephelometric turbidity and Secchi depth. In general, a nonlinear relationship may be expected between light attenuation and Secchi depth and suspended particles concentration depending on the characteristic properties of the particles. Even though light attenuation coefficient  $k_e$ , seems to be increasing linearly with suspended solids concentration, because of its contribution to both absorption and scattering, there is no existing universal relationship between light penetration and suspended solids concentration, or turbidity. So the relationship between these two parameters should be investigated case specifically in a given water body (Kirk 1994).



Unlike inherent parameters light attenuation coefficient is an apparent property of a water body which means that it depends on inherent optical parameters and also on light conditions, notably cloud cover and solar altitude. Reflectance is another apparent parameter, defined as the ratio of upwards to downwards directed irradiance in water. PAR sensor is a device that measures the irradiance in water. It is a submersible light sensor with a convenient spatial and spectral response and it may also be used to estimate the light attenuation coefficient,  $k_e$  (Kirk, 1994). But most of the investigators who do not possess appropriate light sensors tried to estimate  $k_e$  from Secchi disk depths using the simple equation;

$$k_e = K/SD \quad (\text{Eq-2})$$

where K is a constant. Using this equation along with empirical values for  $k_e$  from the literature would mean that PAR at the Secchi depth is constant and equal to a proportion of PAR at the surface. But Davies Colley and Vant (1988) stated that the assumed constant K, in other words  $SDk_e$ , varies spatially mainly due to reflectance,  $R$ . Thus they concluded that estimating light attenuation from Secchi depth measurements may have errors.

Tyler (1968) found another formula that relates Secchi depth and light attenuation coefficient.

$$SD = G / (k_b + k_e) \quad (\text{Eq-3})$$

where G is a coefficient, usually in range of 6-9, depending on the reflectance of water. In this equation the Secchi depth is inversely proportional with the sum of both light extinction and beam attenuation coefficient, while in the previous equation it is only inversely proportional with light attenuation coefficient.

Lee and Rust (1997) worked on a shallow and turbid lake; Lake Hudson in Texas. They collected water samples from surface and did light

measurements between years 1989-90 at six sites. They revealed that light attenuation in Lake Hudson depended on more than one parameter. The factors affecting attenuation of light in the lake were TSS, color; dissolved organic matter and chlorophyll-a. They also concluded that the primary production was limited by light, not by nutrients. Due to high variability, the light attenuation coefficient in Lake Hudson did not correlate well with measured parameters that generally would contribute to light extinction.

Another study was on the light level variation in Lake Tutira, by Johnstone and Robinson (1987). In 1987 heavy rainfalls caused landslides and high amounts of sediment entered into the lake. As a result, a 5 m reduction was observed in the water depth at which PAR was 5% of the surface PAR value. Suspended sediment led to increased turbidity and caused a reduction in light levels in the lake. The light level reduction was measured and monitored with the vertical attenuation coefficient and this reduction was observed for three months after the rainfalls.

Brock, 1969, studied the effect of light on photosynthesis of algae in Yellowstone. They observed that the rate of photosynthesis dropped increasingly with decreasing light. The light intensity over the algae was reduced and changes in chlorophyll concentration were investigated. The chlorophyll content of the algae decreased with the reduced light. Brock's study is one of the earliest studies done on Chl-a and light relationships. Another study based on light topic was done by Schwarz in 1999. He aimed to determine the potential effects of benthic production on changing spectral quality of light and attenuation in the water column. They also concluded that with the increase in the turbidity of water,  $k_e$  also increased.

In 2009 Karlsson and others conducted a study based on light limitation on algal growth. Water samples were collected and analyzed for, total phosphorus and total nitrogen. The attenuation coefficient ( $k_e$ ) was calculated from the slope of the linear regression of the natural logarithm

of PAR versus depth. He concluded that small and unproductive lakes with natural nutrient content are not nutrient limited, but light limited. In other words light attenuation controls the primary production in small and nutrient-poor lakes.

Another study concluding that light availability controls the primary production instead of nutrients was done by Loiselle and others (2007). They studied on temporal and spatial variations in algal concentrations. They claimed that algal concentrations were mainly controlled by the availability of light in many water ecosystems rather than nutrients. When such light limiting conditions occur, changes in the optical characteristics of the water column would directly impact biomass concentrations. They used the Lambert–Beer law in his study. According to this law, in a homogenous medium, the irradiance of a single wavelength would be attenuated exponentially, depending on the quality and quantity of the decreasing components within the path-length. They revealed that it was not sufficient to study only nutrients in order to understand the pattern of algal growth. Light attenuation was a very critical parameter for the primary production.

Armengol and others, (2003) also used Lambert-Beer equation for  $k_e$  calculations. They studied on the relationship between Secchi disk and  $k_e$ . Considered variables were Chl-a, detritus particulate matter and phytoplankton. The results revealed that detritus particulate matter was the most important factor that affected water clarity. Secchi depth was a good indicator of the  $k_e$ . They also revealed that Chl-a was correlated with Secchi depth. As expected, the results showed that as Chl-a decreased Secchi depth increased.

It is safe to say that Lambert-Beer law is an appropriate method to calculate  $k_e$  (Armengol et al, 2003;Loiselle et. al, 2007; Karlsson et. al, 2009). But there are some cases that this law is not applicable. Gallegos (2001), studied on a procedure for calculating Chl-a and TSS

concentrations, assuming  $k_e$  conforms to the Lambert-Beer law. The validity of applying Lambert-Beer law to  $k_e$  in water ecosystems was tested. The testing was done by comparing the data simulated using a simple spectrally integrated algebraic summary (SIAS) model of light attenuation with performance of a linear model of  $k_e$ . The linear regression model failed. It underestimated  $k_e$  at high light attenuation. So he concluded that for Case 2 waters it might not be appropriate to apply the Lambert-Beer law. Where the classification of waters into “Case 1” and “Case 2” was as, Case 1 is that of a concentration of phytoplankton high compared to other particles. In contrast, the inorganic particles are dominant in case 2 waters according to Morel and Prieur (1977). Gallegos also concluded that at constant  $k_e$ , the correlated variation of Chl-a and TSS was almost linear (2001).

## CHAPTER 3

### METHODOLOGY

The aim of this study is to investigate the spatial and temporal changes in the attenuation of light in Lake Eymir. In addition to this,  $k_e$ 's importance on Chl-a abundance over nutrient concentrations is examined. In order to perform the study, in-situ and laboratory measurements were conducted. Samples were collected from the lake from June 2009 to June 2010. Secchi disk depth, PAR, and lake depth measurements were done on site, while nitrate, phosphate, ammonium, Chl-a and TSS analyses were done at the laboratory. Light attenuation and the parameters that affect light attenuation were studied. Their relationships with each other were examined.

Correlations between light limitation on measured parameters (nitrate, ammonium, phosphate, TSS and Chl-a) were also investigated using statistical analysis. For this purpose a statistical analysis software, XL STAT was used. Linear and non-linear regression models of  $k_e$  were developed using this software. The analyses helped to understand the limiting effect of light and its consequences in Lake Eymir.

With XL-STAT,  $k_e$  was modeled with respect to alternative parameters and also at different time periods representing different hydrological conditions. In order to understand the effect of flooding of the lake resulting from the breakage of the gate that connected Lake Eymir and Lake Mogan on March 20<sup>th</sup> 2010, data was parsed into before and after groups.

The field studies and laboratory measurements were performed with the help of Onur Yuzugullu and Tolga Pilevneli. The study was supported by a TUBITAK project (108Y116). Measurement of parameters other than

ammonia, TSS, Secchi depth and PAR were realized by the mentioned researchers.

### **3.1. Field Study**

In field, PAR, water depth, and Secchi disk depths were measured. The laboratory analyses were conducted with the water samples collected at three different depths at each sampling station. These analyses included nitrate, ammonium, TSS, Chl-a, and phosphate. These parameters were chosen due their wide usage in literature in evaluation of light attenuation. For instance, Secchi disk is a commonly used measurement device to indicate turbidity, which is generally highly correlated to light attenuation in water bodies (Jamu et al. 1999). In most cases Chl-a is the source of TSS and therefore turbidity, so Chl- a is correlated with Secchi depth (Giardino et al. 2001).

#### **3.1.1. Locations of Sampling Stations**

Throughout the study, the samples were taken from 4 different Stations until November 10<sup>th</sup>, 2009. After that date, a 5<sup>th</sup> Station was added to the study in order to obtain more representative results. The Stations were determined to match the sampling stations used in previous studies (i.e. Elahdab, 1996). These Stations are shown with numbers 1, 2, 3, 4 and 5 in Figure 3-1.



Figure 3-1 Sampling stations in Lake Eymir(URL1).

At each sampling station, water samples were taken at approximately 25 cm above the bottom of the lake, which is referred to as “deep sample”, 25 cm below the water surface which is referred to as “surface sample” and at the mean depth of each sampling station, which is referred to as “mean depth sample”. Since vertical variations can be observed in water quality parameters in a lake in certain seasons (MacIntyre & Cullen 1995, Antonopoulos & Gianniou et al. 2003), it is common to take at least three samples at different depths. A motorboat was used for sampling. Samples were stored and brought to the laboratory in coolers, and analyzed immediately.

### 3.1.2. In-Situ Measurements

In-situ measurements were conducted using a standard Secchi disk and PAR sensor. The Secchi disk was used to indicate the Secchi depth. The PAR sensor was used to record PAR values at different depths.

#### 3.1.2.1. PAR Analysis

PAR analysis was done in-situ using a PAR sensor device. The device used was a LI-COR LI-193SA PAR sensor. This device (shown in Figure 3-2) contains a bulb which senses the sunlight and an electronic part that reports data. The PAR sensor was plunged into the water column, and data were noted in 25 cm intervals. PAR readings depend on weather conditions.



Figure 3-2 PAR Sensor Device (URL4,5,6)



### 3.1.2.2. Secchi Disk Depth Analyses

Secchi depth measurements were conducted on site with a 20 cm diameter standard Secchi disk which had black and white quadrants (Figure 3-3). It was lowered into the water until the white and black segments were no longer spottable. In other words and the sight of the disk was lost. Then Secchi disk depth was determined measuring the length of the rope the disk is attached.

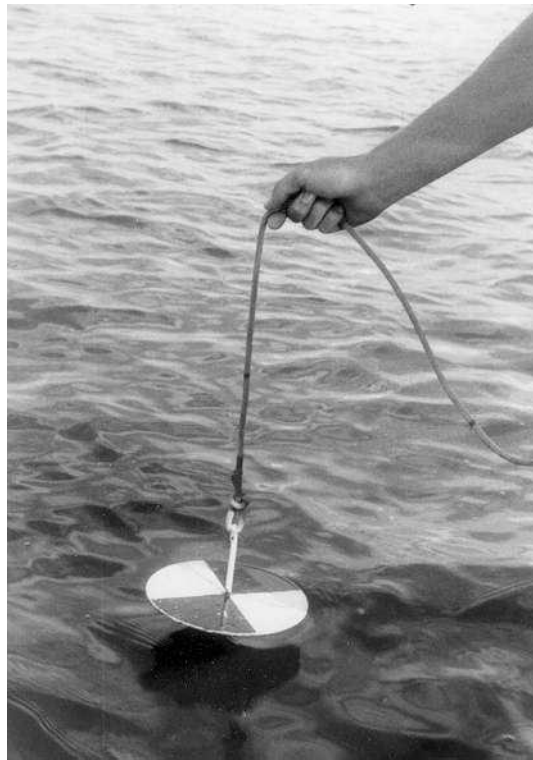


Figure 3-3 The Secchi Disk (URL7)

The water depth was also determined with the Secchi disk. The disk was lowered through the water column until it touched the bottom. That depth was recorded as the water depth of that sampling station.

### 3.1.3. Water Sampling

Samples were taken with a Van-Dorn horizontal water column sampler. This sampler consists of a cylinder that can be closed at both ends by rubber lids. Before the device is plunged into the water the lids were pulled out and restrained by a releasing mechanism. With both ends open, the sampler was lowered into the depth desired. Then a messenger, a heavy item attached to the rope, was released. When the messenger hit the assembly which held the lids, the lids close and the water sample is captured in the sampler. In Figure 3-4, examples for Van Dorn samplers are provided.

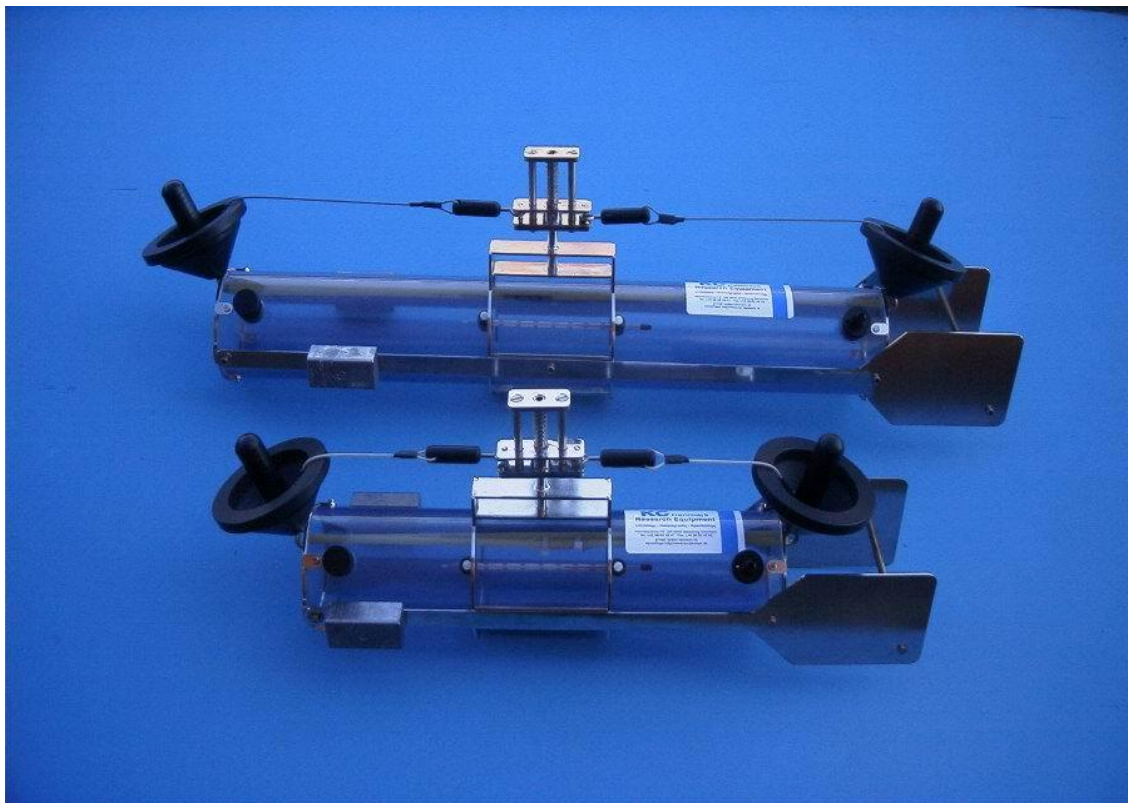


Figure 3-4 Van Dorn samplers (URL8).

### 3.2. Laboratory Analyses

TSS, Chl-a, ammonium, nitrate, and phosphate analyses were done in the laboratory. Water samples were kept in a cooler, brought to the laboratory and analyzed at same day.

#### 3.2.1. TSS Analysis

Standard Methods 2540D was used in this study, for TSS analyses. In general, both methods require drying and weighing glass fiber filters until a constant weight is achieved. In Figure 3-5, TSS analysis procedure is summarized.

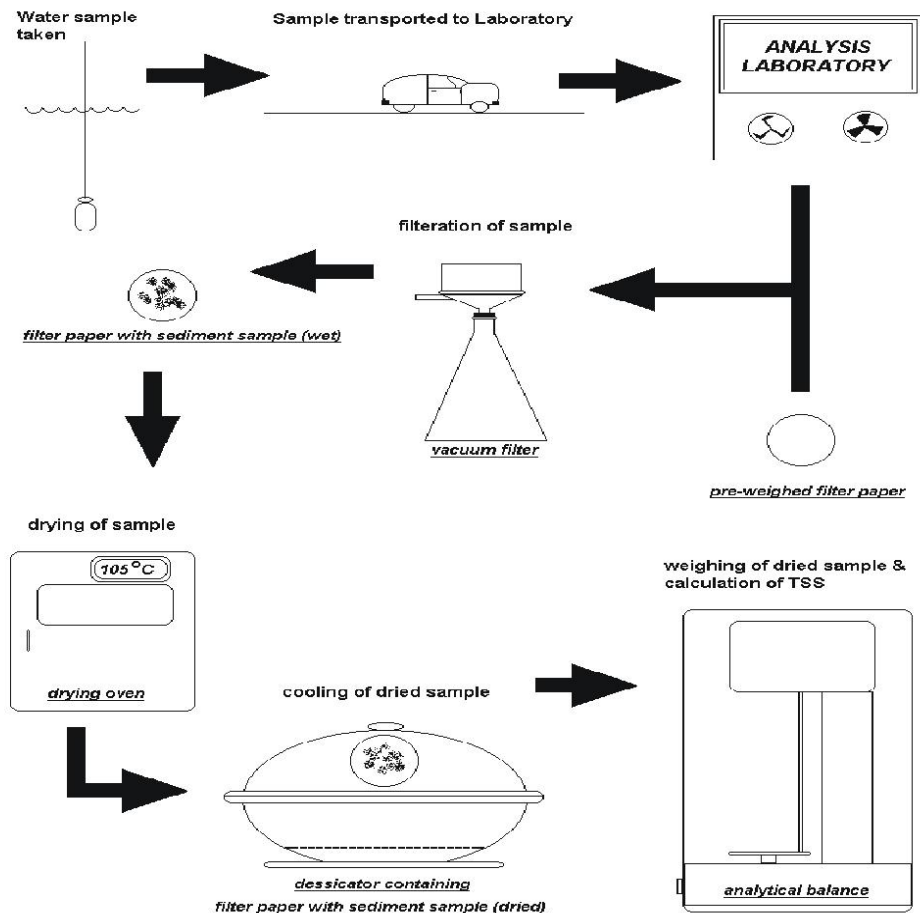


Figure 3-5 TSS analysis procedure (URL9).

First 0.45 µm Whatman filters were dried in the drying oven at 105°C for 1 hour. Then they are kept in desiccator to avoid deliquescence until it cools to room temperature. After cooling, filters were weighted in a precision balance and their initial weights were recorded.

The sample bottle was well mixed in order to obtain more accurate results, after mixing, depending on the diluteness of water 2.5 to 200mL water sample was taken and filtered through the filter. The filters used in filtration was taken gently and dried in drying oven in 105°C for 24 hour, and cooled in desiccator. These filters which contain residue, was weighted and the weight was recorded.

The formula for TSS is given below;

$$\text{Total Suspended Solid Concentration (mg/L)} = (A - B) \times 1000 / V$$

(Eq-4)

Where A is final, B is initial weight of the filter in milligrams and V is used sample volume in mL.

### **3.2.2. Chlorophyll-a Analysis**

Chl-a analysis were done according to the ISO 10260, 1992 Standard Ethanol Extraction Method. From the well mixed sample, 250 mL water was taken, and filtered through a glass fiber filter. The filter was put in the chlorophyll-a jar, 20 mL pure ethanol was added on it. The jar was heated in a water bath then cooled to room temperature. The sample in the jar was taken in to a spectrophotometer glass cuvette for determination of absorbance. It was analyzed in DR/2400 Hach Lange Spectrophotometer. Then 0.1 mL of 0.1 N HCl acid was added to the sample and kept for reaction. After that it was again analyzed in the spectrophotometer. The

absorbance values in both readings, was recorded at 665 and 750 nm against ethanol blank.

Chlorophyll-a concentration was calculated with the given formula;

$$\text{Chl-a } (\mu\text{g/L}) = (A - A_a) \times 29.6 \times V_e / (V_n \times 1) \quad (\text{Eq-5})$$

Here A is absorption difference between 665 and 750 nm before acid addition, and  $A_a$  is after acid addition. Since these two parameters are difference in absorption, they are unitless.  $V_e$  and  $V_n$  are ethanol and sample volume respectively.

### **3.2.3. Nitrate ( $\text{NO}_3\text{-N}$ ) and Ammonium ( $\text{NH}_4\text{-N}$ )**

Ammonium and ammonia concentrations were analyzed with the Hach analysis kits and samples were read with a spectrophotometer. In this study DR/2400 Hach large spectrophotometer was used.

### **3.2.4. Phosphorus ( $\text{PO}_4\text{-P}$ )**

Ascorbic acid method in the standard methods was used in determination of phosphorus concentration in this project. First sample is treated with phenolphthalein indicator and mixed reagent containing sulfuric acid, ascorbic acid, potassium antimonyl tartrate and ammonium molybdate solution. Absorbance of samples were measured with a blank solution at 880 nm. Then correction for turbidity is carried out by subtracting the blank samples absorbance value from absorbance of other samples.

Absorbance vs. phosphate concentration is plotted is calculated by the following equation;

$$\text{mg P/L} = (\text{mg P} \times 1000) / \text{mL sample} \quad (\text{Eq-6})$$

### 3.3 Calculation of Light Extinction Coefficients

In order to examine the light effect, light extinction coefficient,  $k_e$  were calculated through the PAR data obtained from the study. It was assumed that  $k_e$  conformed to the Lambert-Beer law. Thus for the calculation of  $k_e$ , the Lambert Beer equation given below was used;

$$I_z = I_0 \exp [-k_e z] \quad (\text{Eq-7})$$

Where  $I_0$  and  $I_z$  are PAR values measured at the surface and at depth  $z$  respectively. Rearrangement of this equation gives;

$$k_e = (\ln I_z/I_0) 1/z \quad (\text{Eq-8})$$

In this study instead of using a single PAR value at a specific depth  $z$ , PAR values measured at each 25 cm were used in determination of overall  $k_e$ . In other words instead of using the ratio of surface PAR and PAR at depth  $z$ , the whole PAR values through a water column was used and the overall attenuation with depth was considered. Depth versus  $\ln(\text{PAR})$  graphics were plotted for each sampling station and each sampling date. The slope of the linear line gave the  $k_e$ .

The  $k_e$  was calculated for each Station and date. Then at each Station yearly average  $k_e$  was calculated to examine whether variations in  $k_e$  at different Stations were similar. Moreover, the seasonal changes in  $k_e$  values were examined based on the overall average of five sampling stations.

### **3.4. Data Analysis and Modeling of $k_e$**

The data obtained from the laboratory analyses and in-situ measurements were analyzed with respect to variations in time and location. By this means, the yearly pattern of the measured parameters is investigated. The changes in the concentrations were determined at each sampling station.

Data analysis was conducted using XLSTAT program. In total, 8 parameters were analyzed on this statistical software. XLSTAT is an add-in feature of Microsoft Excel which provides linear and non-linear regression. This statistical analysis software was used to determine the limiting effect of light on Chl-a growth. In literature, most of the studies done on Chl-a is based on nutrient limitation but not on  $k_e$  (Hoyer & Jones, 1983; Chong, 2005), In this study, importance of  $k_e$  on Chl-a is shown in the modeling stage as well.

The problem with using a large set of functions to describe a system is that estimating the parameters becomes very difficult when the number of parameters, and types of functions increases (Altunbilek, 2005).

The data were analyzed with linear regression models. The limiting effect of light was tested through XL-STAT. The parameters that effect  $k_e$  were also examined through the model.

For the development of linear regression  $k_e$  model, the goodness of fit was determined based on adjusted coefficient of determination ( $R^2$ ),  $R^2$ , root

mean square error (RMSE), mean square error and p value for the equation of the regression models.

$R^2$  square is calculated with the equation given below.

$$r^2 = 1 - \frac{\sum_{i=1}^n (Y_i - \hat{Y}_i)^2}{\sum_{i=1}^n (Y_i - \bar{Y})^2} \quad (\text{Eq-9})$$

Here,  $\sum_{i=1}^n (Y_i - \hat{Y}_i)^2$  is the sum of squared prediction errors, and  $\sum_{i=1}^n (Y_i - \bar{Y})^2$  is sum of squared deviations about the mean. p value is also considered in order to decide whether the model is correct or not. p value is the probability of null hypothesis being true. Null hypothesis is the hypothesis that claims the actual hypothesis studied is wrong. So the lower the p value, the better the model is (Smith, 2012)

RMSE is calculated as given below.

$$RMSE = \sqrt{\frac{1}{k} \sum_{i=1}^k \varepsilon_i^2} \quad (\text{Eq-10})$$

Where k is number of data sets, and  $\varepsilon$  is error at each evaluated data (Yang et al., 2005)



## CHAPTER 4

### RESULTS and DISCUSSIONS

#### 4.1. Analysis of the Data

Data obtained from the study was investigated through graphics plotted with respect to time and sampling stations.

##### 4.1.1. Data Analysis With Respect To Time

The results obtained, were investigated with respect to time. The seasonal pattern for each parameter was examined. Parameters studied were; Secchi disk depth, lake depth, TSS,  $k_e$ , Chl-a,  $\text{NH}_4\text{-N}$ ,  $\text{NO}_3\text{-N}$ , and  $\text{PO}_4\text{-P}$ . Secchi disk depth, lake depth, TSS,  $k_e$ , Chl-a were measured and analyzed throughout the study period.  $\text{NH}_4\text{-N}$ ,  $\text{NO}_3\text{-N}$  analyses were conducted after September 29<sup>th</sup> and 14<sup>th</sup>, 2009 respectively. And  $\text{PO}_4\text{-P}$  was measured after August 3<sup>rd</sup>, 2009.

Figure 4-1 depicts the change in average Secchi depths in the lake. Throughout the study period, Secchi depths varied between 0.25 m to 3.20 m. When Figure 4-1 is examined, it can be seen that Secchi depth increased through the winter seasons and slightly decreased in summer seasons.

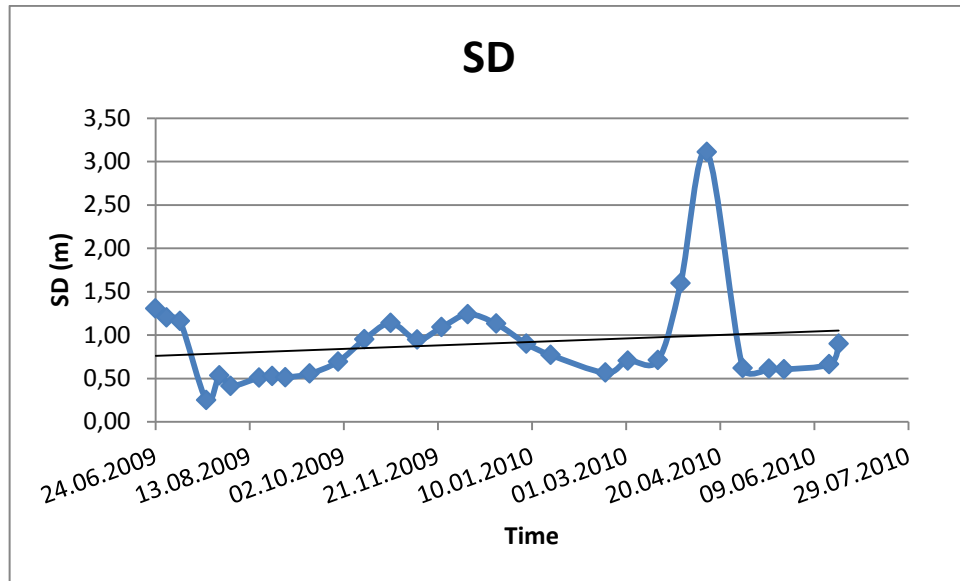


Figure 4-1: Mean Secchi Disk value of 5 Stations vs. Time

As mentioned before, the gate that connected Lake Eymir and Lake Mogan was broken in March 20<sup>th</sup> 2010. In Figure 4-1, it is seen that there is a significant increase in Secchi depth after this date, regardless of the seasonal change. In addition to the increase in water depth due to broken gate, flocculation of suspended matter may be the cause of this sudden increase in Secchi depth in April 2010. Although the exact reason cannot be speculated, flocs were observed during the field study. Since distributed flocs do not completely block light penetration, higher Secchi disk depths could be measured. In the study period an increasing pattern was observed in Secchi depths.

Lake depth and TSS versus time plots are depicted in Figures 4-2 and 4-3, respectively. In Figure 4-2 it can be seen that there was a significant increase in the depth of the lake following the rainy season and flooding due to the broken gate in April 2010. In proceed, TSS decreased (Figure 4-3) and Secchi depth increased (Figure 4-1). It is possible that due to the excessive water coming from Lake Mogan, dilution was established and TSS concentrations decreased. However, as the gate was repaired and inflow from Lake Mogan diminished, TSS concentrations may restore

back. Shallow lakes tend to be more turbid. Whereas, deeper lakes would be expected to be more clear (Hein, 2006). In general it can be said increase in water depth positively impacted turbidity problem such that TSS had a decreasing pattern in the study period.

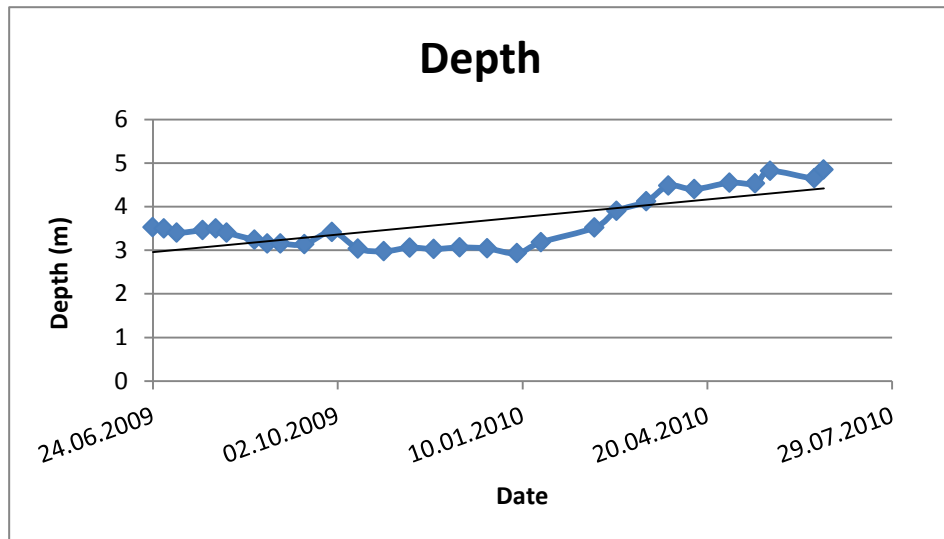


Figure 4-2: Mean Depth value of 5 Stations vs. Time

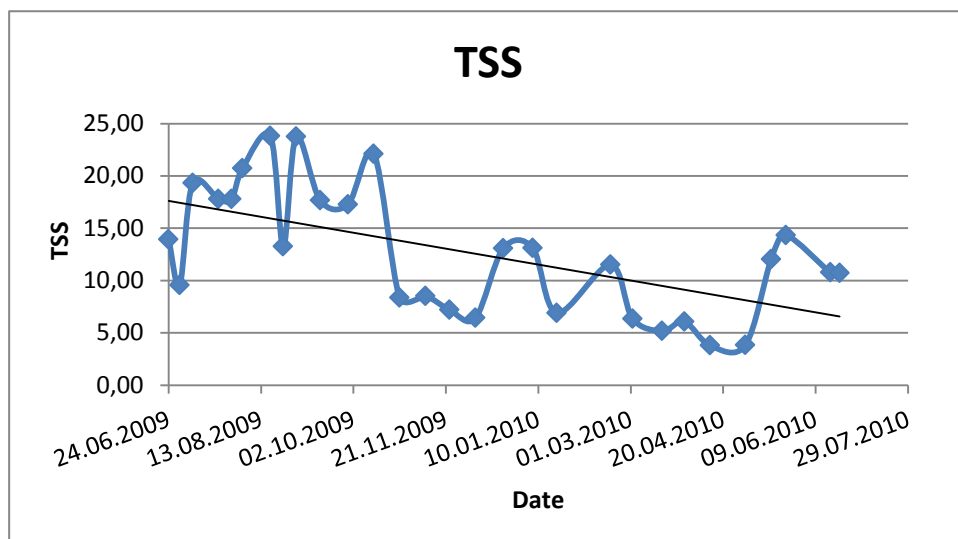


Figure 4-3: Mean TSS value of 5 Stations vs. Time

It must also be noted that problems were observed during TSS analysis. In order to keep filters from clogging during TSS analysis, sampled with high TSS were diluted. This might have caused some of the fluctuations observed in Figure 4-3. Nonetheless, decrease in TSS concentrations with the increase in water depth is an expected result.

Figure 4-4 depicts the temporal variation in Chl-a concentrations. It is seen that before the time the gate was broken, Chl-a concentrations were high in warmer months and low in winter of 2010. However, there was a sharp drop in Chl-a concentrations following the flooding of Lake Eymir. The minimum TSS concentrations were observed in this period as well (Figure 4-3).

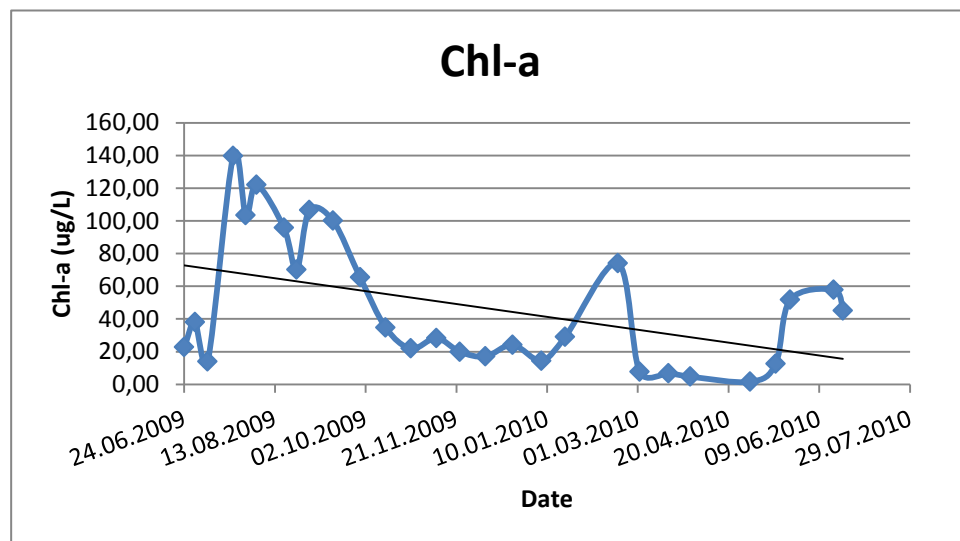


Figure 4-4 Mean Chl-a value of 5 Stations vs. Time

In Figure 4-4, Chl-a concentrations exhibit a decreasing pattern throughout 2009 to 2010 which was the case for TSS as well. In previous studies it was shown that Chl-a was strongly correlated with TSS (Elahdab, 2006). Chl-a was a major factor contributing to turbidity. It is expected TSS values change with Chl-a (Christian & Sheng 2003).

NH<sub>4</sub>-N and NO<sub>3</sub>-N analyses were conducted after October 2009. Concentrations are provided in Figures 4-5 and 4-6, respectively. It can be seen that NH<sub>4</sub>-N is increasing while NO<sub>3</sub>-N is decreasing. Nitrification is a process where NH<sub>4</sub>-N is converted to NO<sub>3</sub>-N, and mineralization is a process where organic nitrogen is mineralized to NH<sub>4</sub>-N (Yang et. al, 2007). With this respect, according to the Figure 4-5 and 4-6, it may be possible that nitrification process was slower than nitrogen mineralization process in Lake Eymir. This might be the reason of the condition observed in this study, which is, NO<sub>3</sub>-N is decreasing while NH<sub>4</sub>-N is increasing. Aquatic plants, phytoplankton and macrophytes may utilize N mostly in the form of NO<sub>3</sub>-N, rather than NH<sub>4</sub>-N (Harrison et. al, 2004). This might be the reason of decreasing NO<sub>3</sub>-N or vice versa since the lake was N limited throughout the study period. As Chl-a concentrations were decreasing, NH<sub>4</sub>-N was increasing since it was not used for algal growth.

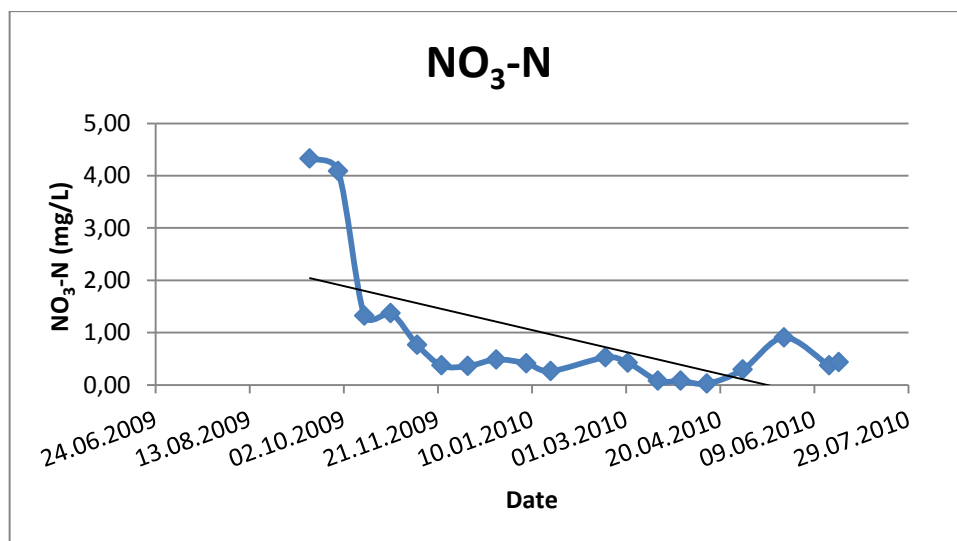


Figure 4-5: Mean NO<sub>3</sub>-N value of 5 Stations versus time

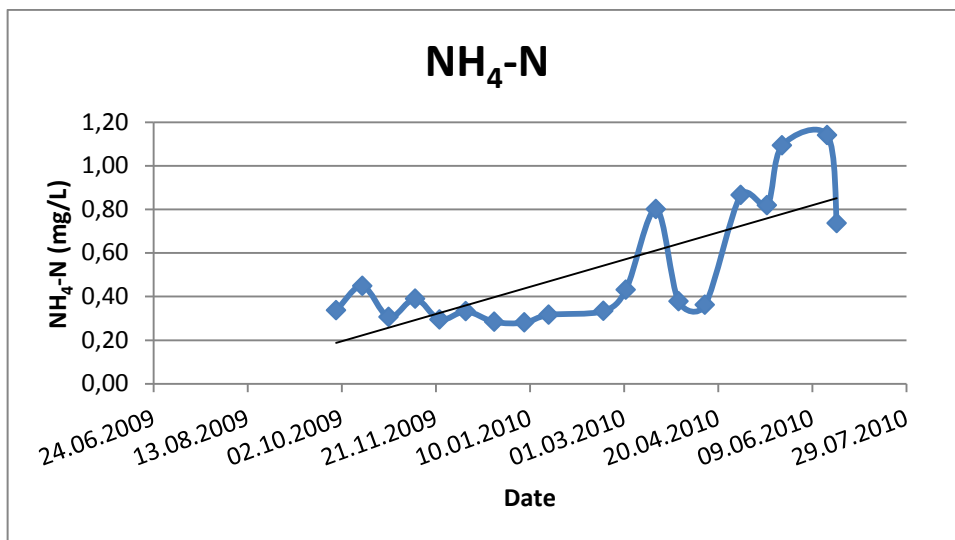


Figure 4-6: Mean NH<sub>4</sub>-N value of 5 Stations vs. Time

In Figure 4-7, the PO<sub>4</sub>-P concentrations can be seen. PO<sub>4</sub>-P analyses were done after August 2009. The concentrations are fluctuating.

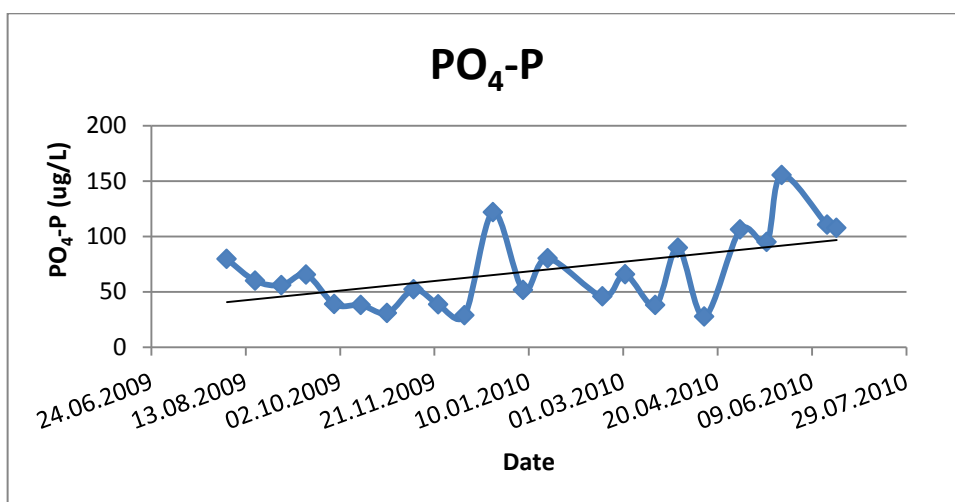


Figure 4-7: Mean PO<sub>4</sub>-P value of 5 Stations vs. Time

On some sampling days the water samples taken from the deep part of Station 3 contained very high amounts of P and also N. Since the values in Figure 4-7 represents average values, these high quantities may lead to elevated mean concentrations which may lead to fluctuations in mean concentrations.

#### **4.1.2 Data Analysis With Respect to Sampling stations**

Variations in concentrations or values were also examined for different sampling stations. Variations were examined based on minimum and maximum observations at a sampling station within the study period. It was aimed to analyze if variations at different sampling stations were comparable or not.

Figure 4-8 depicts the minimum, maximum and average depths at sampling stations. Stations closer to the inlet and outlet of Lake Eymir, which are Station 1 and Station 5, are the shallowest sampling stations. The lake gets deeper at the sampling stations which are in the middle part of the lake. Station 2 and 3 had the same depth value along the study period. Station 4 is slightly shallower than Station 2 and 3. All the sampling stations follow the same pattern during year 2009-2010. During the study period the difference between the minimum and the maximum depths at a given Station changed by almost up to 100%.

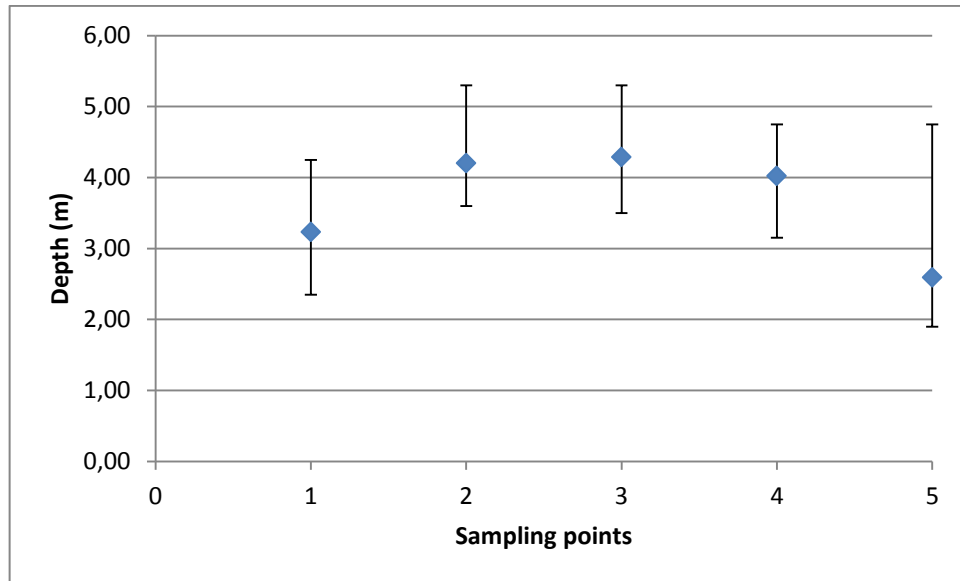


Figure 4-8: Mean depth values of each sampling station.

Figure 4-9 represents the variation in Secchi depths at observation Stations. The average Secchi depth was around 1 m throughout the study period. Each sampling station follow the same pattern in terms of Secchi disk depths. Along the sampling period Secchi depth reached over 3 m and dropped down to 0.5 m. This is a significant variation considering the average depth of the lake. The maximum Secchi depth was observed at 4<sup>th</sup> Station with a depth of 3.75 m, in April 13<sup>th</sup> 2010. This is the date when the gate was broken following a rainy period. On average, the maximum Secchi depth was observed at Station 4. As expected when Station based graphic of variations in  $k_e$  was examined (Fig. 4-10), it can be seen that the lowest average  $k_e$  was observed at 4<sup>th</sup> Station.



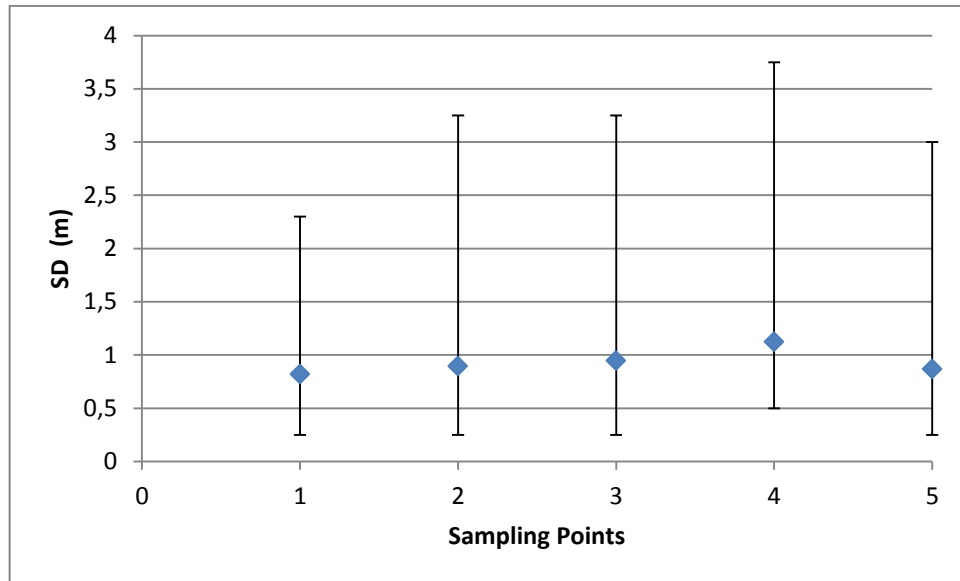


Figure 4-9. Mean Secchi depth values at each sampling station.

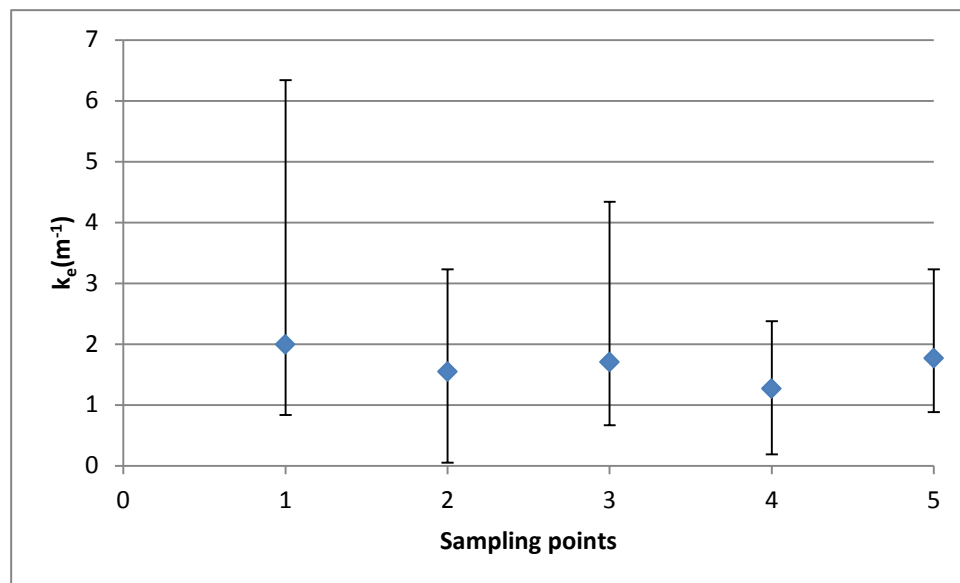


Figure 4-10: Mean Extinction Coefficient values of each sampling station.

As seen in the Figure 4-10, mean  $k_e$  was higher at Stations 1 and 5 which were the shallowest and more turbid sampling stations. Mean TSS values followed the same pattern with  $k_e$ .  $k_e$  reached its maximum value at 1<sup>st</sup>

Station with  $6.3 \text{ m}^{-1}$ . In general mean  $k_e$  values ranged approximately between 1 and  $2 \text{ m}^{-1}$ .  $k_e$  reached its maximum value at Station 1 with a value of  $1.99 \text{ m}^{-1}$  on yearly average and its minimum at Station 2 with a value of  $1.27 \text{ m}^{-1}$ .

Figure 4-11 and 4-12 depicts the variations in TSS and Chl-a concentrations at different sampling stations in the study period, respectively. The maximum TSS concentration ( $34 \text{ mg/L}$ ) was observed at Station 1, which is close to the inlet of the lake. The minimum observed TSS was  $3 \text{ mg/L}$  (Figure 4-11). The average TSS values at different sampling stations varied between  $7\text{-}14 \text{ mg/L}$  during the sampling period. Since Chl-a is correlated with turbidity, the extend of variations in Chl-a concentrations were similar to that for TSS at given sampling stations. The average Chl-a concentrations were approximately  $50 \text{ }\mu\text{g/L}$  at Stations 1, 2, 3, and 5. The lowest average Chl-a concentration was at Station 4. This is the Station where the average TSS concentration and  $k_e$  are the highest.

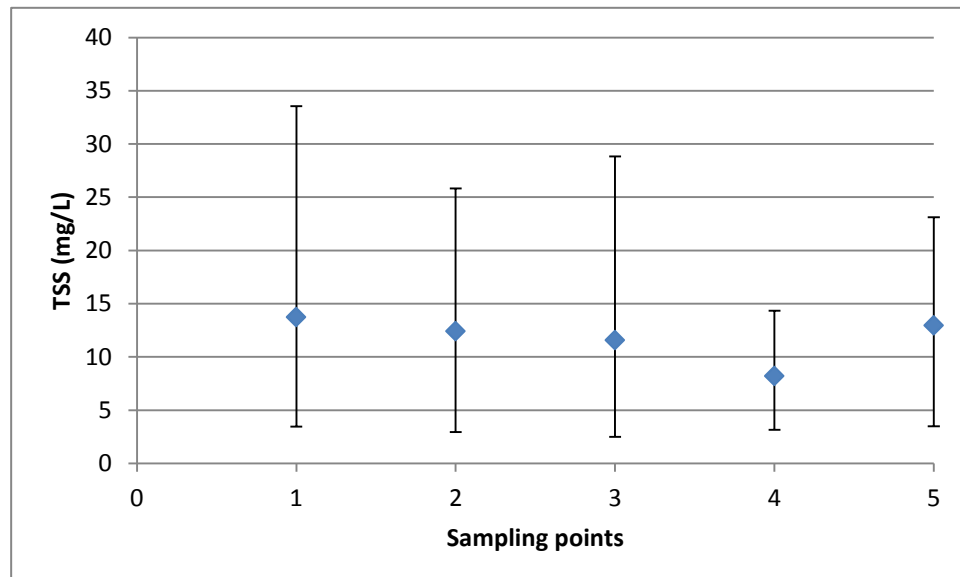


Figure 4-11: Mean TSS values of each sampling station.

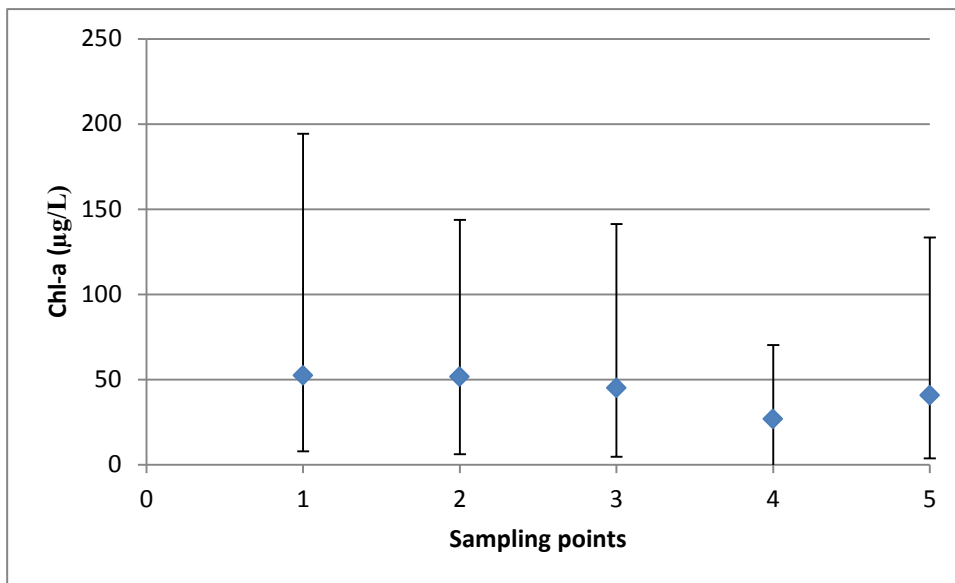


Figure 4-12. Mean Chl-a values of each sampling station.

Figures 4-13, 4-14, and 4-15 show the minimum, average, and maximum concentrations of  $\text{NO}_3\text{-N}$ ,  $\text{NH}_4\text{-N}$ , and  $\text{PO}_4\text{-P}$  at different sampling stations, respectively. It is seen that the average  $\text{NO}_3\text{-N}$  concentrations have similar spatial pattern as Chl-a concentrations.

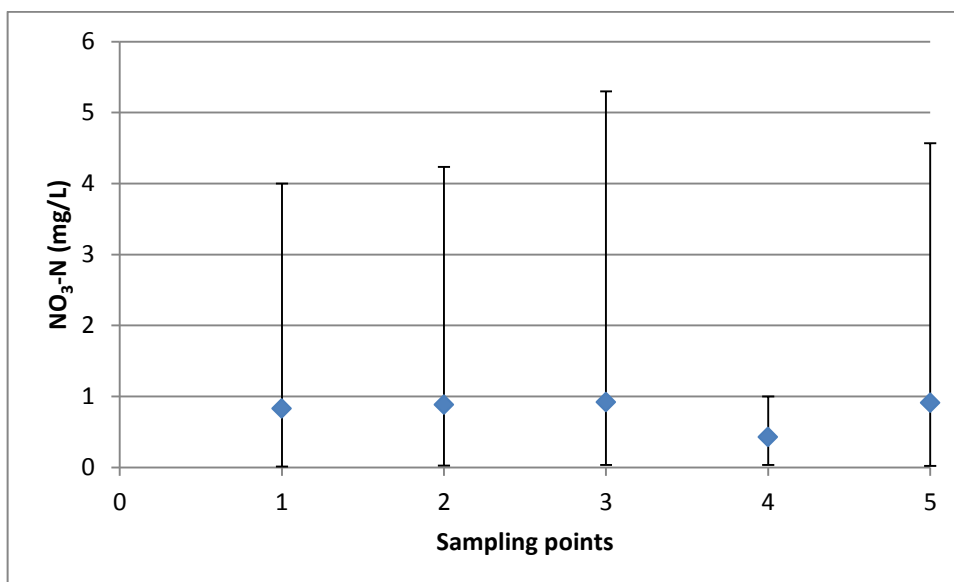


Figure 4-13 Mean  $\text{NO}_3\text{-N}$  values of each sampling station.

The average  $\text{NO}_3\text{-N}$  values varied between 0.5-1 mg/L during years 2009-2010 (Fig.4-13). Station 4 was the most conservative part of the lake with respect to the range of observed  $\text{NO}_3\text{-N}$  concentrations. This was in line with Chl-a and TSS concentration ranges as well.

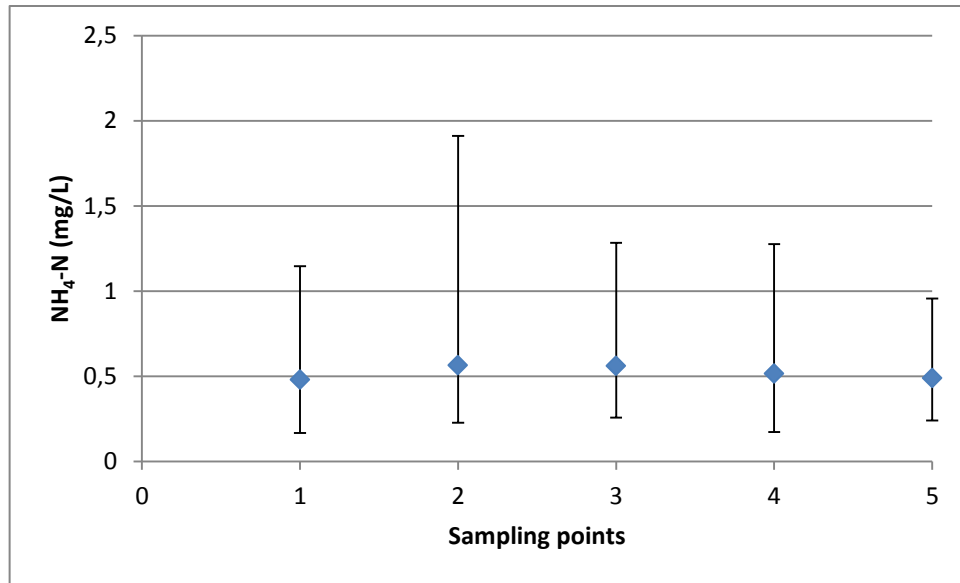


Figure 4-14. Mean  $\text{NH}_4\text{-N}$  values of each sampling station.

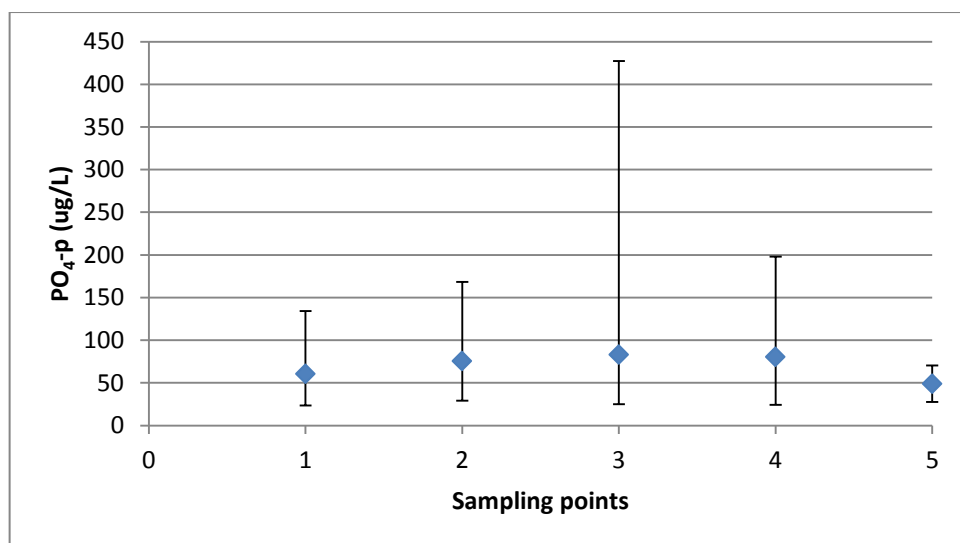


Figure 4-15: Mean  $\text{PO}_4\text{-P}$  values of each sampling station.

The maximum  $\text{NH}_4\text{-N}$  value was 1.9 mg/L at sampling station 2 (Figure 4-14). At all Stations, the average concentration was around 0.5 mg/L. For all the parameters except  $\text{PO}_4\text{-P}$ ,  $\text{NH}_4\text{-N}$ , Station 4 showed the least fluctuation through the study period. So it can be said that Station 4 is the least effected part of the lake from seasonal changes. But it should also be considered that Station 4 was added to the study after November 10<sup>th</sup>, 2009. And since the fluctuations in data were generally observed at the first few months of the study, it would be wrong to say that Station 4 is the sampling station at which least fluctuation is observed.

When these graphics of mean values of the measured parameters are investigated, in general, the 2<sup>nd</sup> and 3<sup>rd</sup> stations are most representative in the lake. According to the Fig 4-10, for  $k_e$ , the most representative stations are 3<sup>rd</sup>, 2<sup>nd</sup> and the 5<sup>th</sup> stations respectively.

#### **4.2 Evaluation of Light Extinction Coefficients in Lake Eymir**

$k_e$  values at sampling stations were determined by plotting  $\ln(\text{PAR})$  values measured with an increment of 25 cm versus depth.  $k_e$  values were calculated for each Station and each sampling date. In Figure 4-16, an example of a  $\ln(\text{PAR})$  versus depth graph is given.

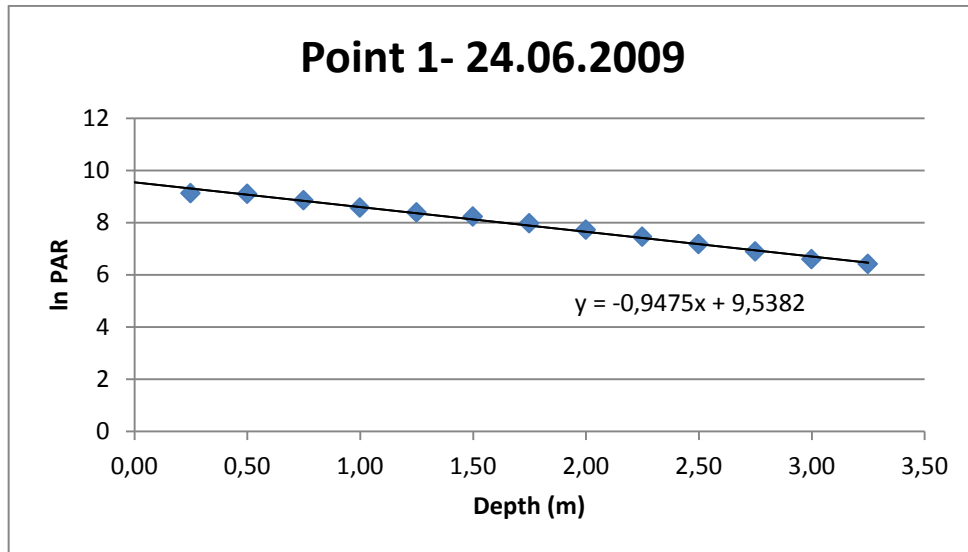


Figure 4-16: ln PAR values versus Depth

The rest of the calculation graphics are given in the Appendices. Values of  $k_e$  for each sampling station and each date were calculated. As mentioned before, in the calculation of  $k_e$  Lambert Beer equation was used. The linearity in ln(PAR) versus depth graphs indicate that  $k_e$  conforms to the Lambert Beer law. Only the attenuation rate in the water column was considered. The Slope of the line in the ln(PAR) versus depth graph gives the  $k_e$  of that Station in the given sampling date. For example, in Figure 4-16,  $k_e$  is calculated as  $0.95 \text{ m}^{-1}$ . Higher slope indicated higher  $k_e$ , and therefore, higher light attenuation. Temporal variation in  $k_e$  values at different Stations can be seen in Figure 4-17. In general, the temporal variations in  $k_e$  are similar at different Stations. Time of peak values are consistent with the Chl-a values. For instance, a peak value of  $k_e$  is observed on July 21<sup>st</sup>, 2009 at Station 1. On the same date and sampling station, the Chl-a concentration was at peak as well. This is an expected result since Chl-a is a parameter that contributes TSS, and TSS is correlated with  $k_e$  (Walmsley et al, 1980). As light attenuation increases, Chl-a concentrations decrease. The average  $k_e$  values with respect to time are plotted in Figure 4-18. As mentioned above  $k_e$  values were calculated

through PAR data which was taken at each 25 cm. In general, a slightly decreasing pattern was observed temporarily. Therefore, it can be said that light was less attenuated with decreasing Chl-a concentrations.

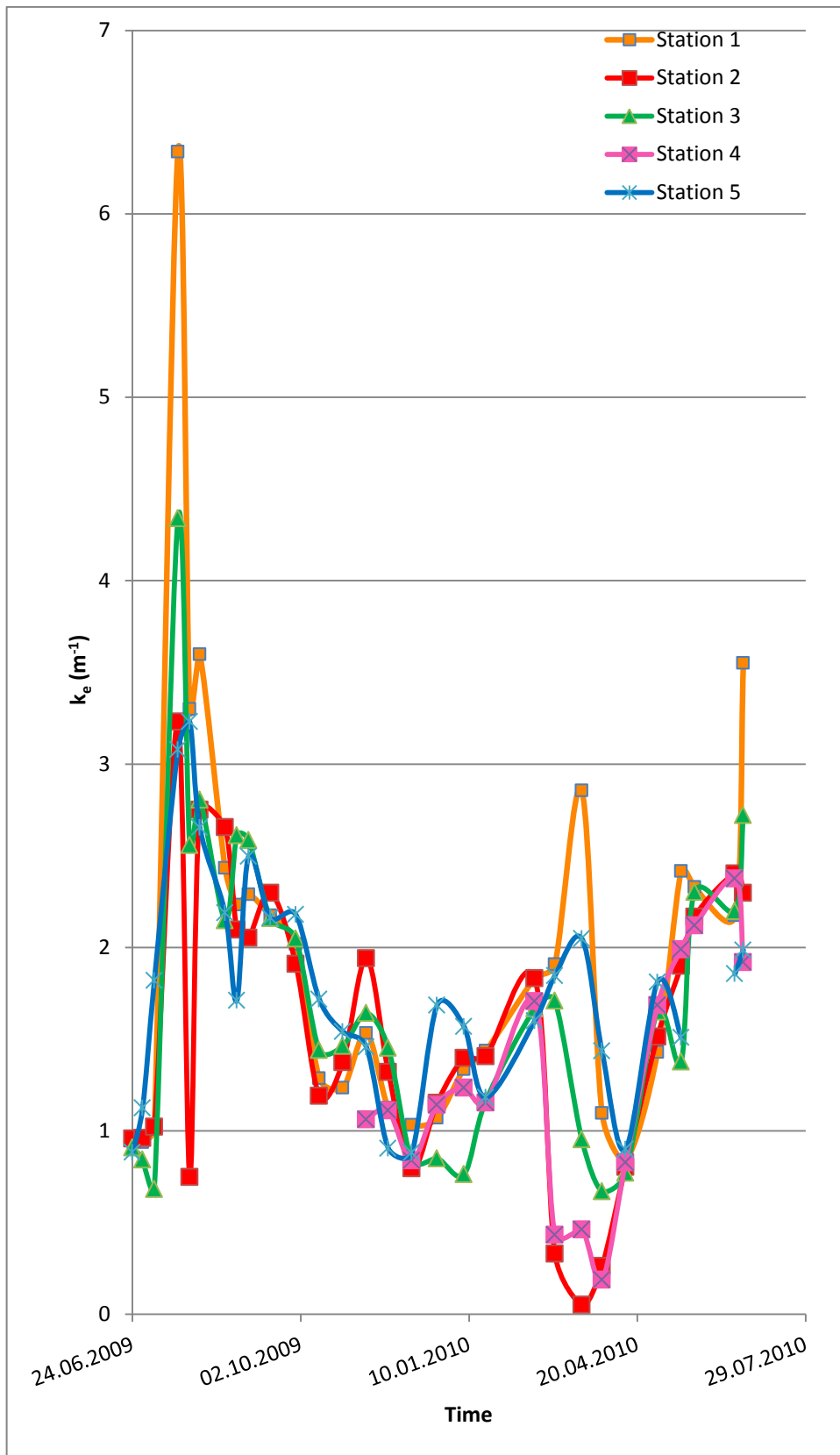


Figure 4-17: Extinction Coefficient of 5 Stations vs. Time



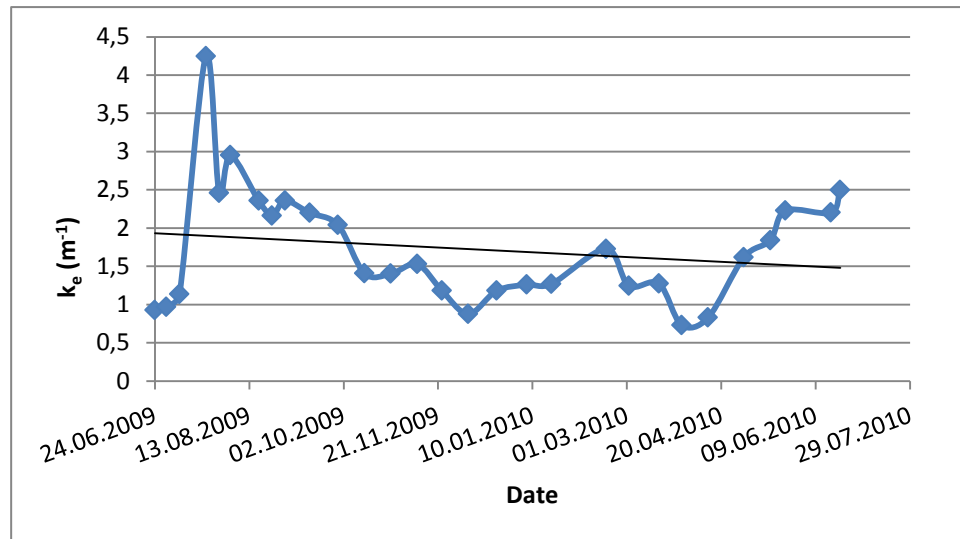


Figure 4-18: Mean Extinction Coefficient Value of 5 Stations vs. Time

### 4.3 Modeling of $k_e$

Linear regression models of  $k_e$  were developed using XLSTAT. To understand the effect of the broken gate and increased water depth, models were developed using different groups of data sets. The modeling study was done with the overall data, the data obtained before time the gate was broken and with the data after the gate was broken. Correlation matrixes were generated for these data sets. The goodness of fit statistics were examined and given in Table 4-4. A summary of this study is given in Table 4-7.

Chl-a and  $k_e$  models were studied. First, the correlation matrix of these linear regression models, were investigated. Then the decision of which parameters to involve to the model was considered. The parameter elimination was done according to the collinearity effect. The best solution for eliminating collinearity is to remove the correlated parameters. Collinearity occurs when two or more variables are related or they measure the same thing. If one of the variables in the model doesn't seem essential to the model, removing it would reduce collinearity. Examining

the correlation coefficients between variables and taking into account the importance of the variables is the procedure of deciding about what variables to drop from the model (Graham, 2003).

R values higher than 0.6 were accepted to indicate acceptable correlation. In regression model development, independent variables should not exhibit collinearity. Using correlated explanatory variables in the model would affect the results negatively. So in order to eliminate this situation one of the two parameters that have high correlation ( $R^2 > 0.6$ ) was removed from model development.

First the parameters to be used in the models were selected according to their effect and correlation coefficients. Then two  $k_e$  models were derived with each data set. First model contained all parameters, except one of the both parameters which have a correlation coefficient higher than 0.6. The second model derived, contained lesser parameters compared to the first model, it contained only the ones that have the highest correlation coefficients. Using more number of parameters would lead to a high  $R^2$ , but the model derived with lesser parameters could give more accurate result with a higher adjusted  $R^2$ , regardless of the number of parameters used. This model derivation approach was applied on the all time data, data obtained before the gate broke and the data obtained after the gate broke.

First the all time data was studied. On table 4-1 the correlation matrix of the linear regression model of  $k_e$  is given. The correlation coefficients higher than 0.6, was given in italic and underlined. When we look at Table 4-1., it is seen that depth and  $\text{NH}_4\text{-N}$ ,  $\text{PO}_4\text{-P}$  and  $\text{NH}_4\text{-N}$ , and  $\text{PO}_4\text{-P}$  and depth are correlated with a correlation coefficient of 0.840, 0.636 and 0.688 respectively.

Decision of removing one of the two correlated parameters was done based on background knowledge and the analyze method of the parameter. In addition to this, for making the decision, the correlation

coefficient of the parameters with the modeled parameter,  $k_e$ , was checked.

Table 4-1. Correlation matrix of linear regression model of  $k_e$ , with one-year data.

Variables	SD	Chl-a	TSS	NH <sub>4</sub> -N	NO <sub>3</sub> -N	Depth	PO <sub>4</sub> -P	$k_e$
SD	<b>1,000</b>	-0,398	-0,176	-0,529	-0,126	-0,329	-0,211	-0,656
Chl-a	-0,398	<b>1,000</b>	0,563	0,131	0,509	0,050	0,096	0,669
TSS	-0,176	0,563	<b>1,000</b>	-0,017	0,553	-0,169	0,030	0,387
NH <sub>4</sub> -N	-0,529	0,131	-0,017	<b>1,000</b>	-0,216	<u>0,840</u>	<u>0,636</u>	0,641
NO <sub>3</sub> -N	-0,126	0,509	0,553	-0,216	<b>1,000</b>	-0,253	-0,277	0,302
Depth	-0,329	0,050	-0,169	0,840	-0,253	<b>1,000</b>	<u>0,688</u>	0,546
PO <sub>4</sub> -P	-0,211	0,096	0,030	0,636	-0,277	0,688	<b>1,000</b>	0,452
$k_e$	-0,656	0,669	0,387	0,641	0,302	0,546	0,452	<b>1,000</b>

In this case, NH<sub>4</sub>-N and PO<sub>4</sub>-P were removed from the model. When we check the correlation coefficients of depth and PO<sub>4</sub>-P with  $k_e$ , depth has a higher correlation coefficient which is 0.654, compared to PO<sub>4</sub>-P which is

0.452. So among depth and PO<sub>4</sub>-P, PO<sub>4</sub>-P was the parameter removed. And when depth and NH<sub>4</sub>-N is considered, even though NH<sub>4</sub>-N has a higher correlation coefficient compared to depth, NH<sub>4</sub>-N is removed from the model, because depth is a parameter that is much easier to measure.

Two linear regression models were considered for k<sub>e</sub> with all time data. One was named k<sub>e</sub>M1 and involved Secchi depth, Chl-a, TSS, NO<sub>3</sub>-N and depth. The other was named k<sub>e</sub>M2 and involved lesser parameters which had higher correlation coefficients compared to other parameters; Secchi depth, Chl-a and depth. k<sub>e</sub>M1 model gave the following equation;

$$k_eM1 = 0.42 - 0.53 * SD + 8.65 * 10^{-03} * Chl-a + 1.34 * 10^{-02} * TSS + 5.73 * 10^{-02} * NO_3-N + 0.31 * Depth \quad (Eq-11)$$

The goodness of fit statistics of each model ran in this study is given in Table 4-4. As seen in the Table 4-4. the R square of the k<sub>e</sub>M1 model is 0.808, adjusted R square is 0.728, RMSE is 0.250 and p value is 0.001. With these statistics it can be said that the k<sub>e</sub>M1 model is a convenient model. In Figure 4-19 standardized coefficients is seen.

When Table 4-1 is investigated, the negative sign of the correlation coefficient of k<sub>e</sub> and Secchi disk indicates that k<sub>e</sub> is negatively proportional with Secchi disk depth, which is an expected result (Tyler, 1968). The same result is observed in the graphics of standardized coefficients of k<sub>e</sub>M1 and k<sub>e</sub>M2 model (Figure 4-19,21).

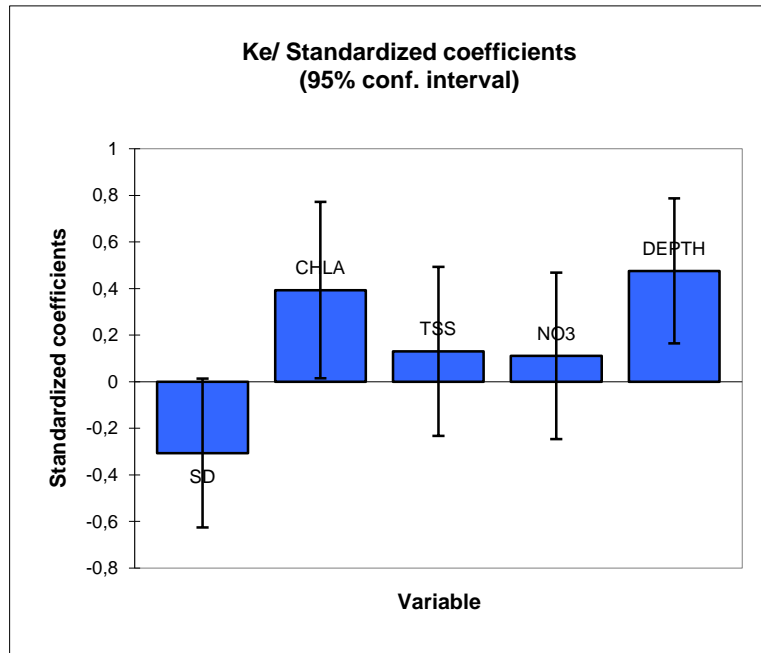


Figure 4-19. Standardized Coefficients vs. variables of  $k_e$ M1 model.

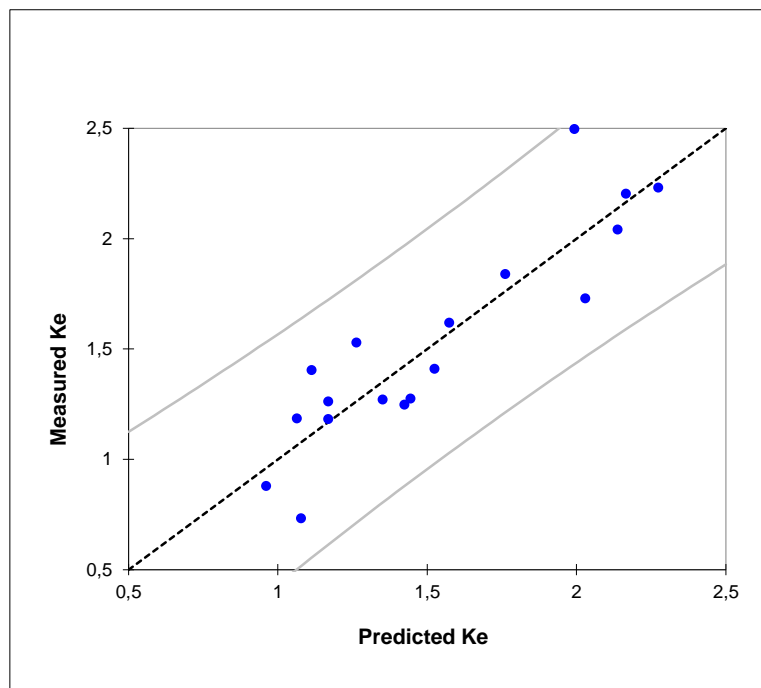


Figure 4-20. Predicted  $k_e$  versus measured  $k_e$  for  $k_e$ M1 model

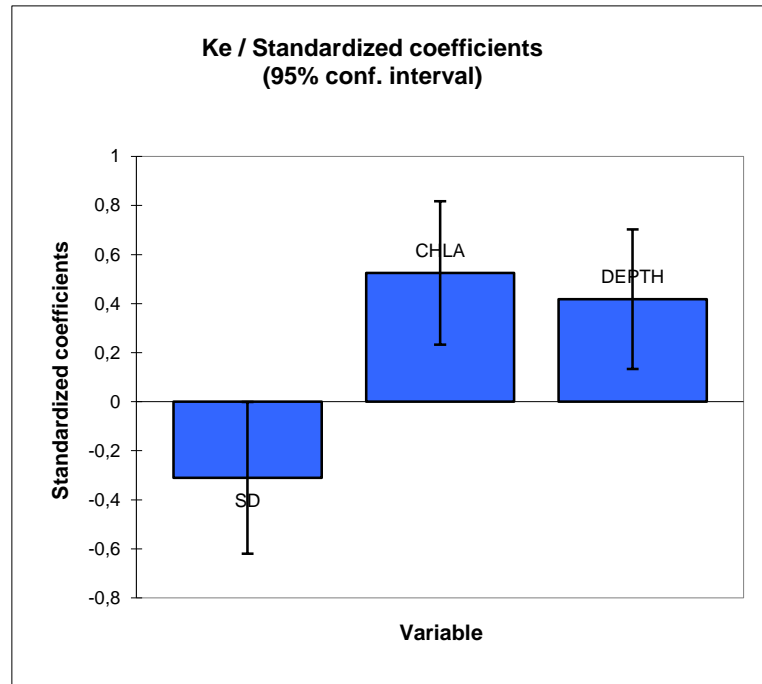


Figure 4-21. Standardized Coefficients vs. variables of  $k_e$ M2 model.

$k_e$ M2 model gave the following equation as a result;

$$k_eM2 = 0.66 - 0.54 * SD + 1.15 * 10^{-02} * Chl-a + 0.27 * Depth$$

(Eq-12)

The goodness of fit statistics of  $k_e$ M2 model is given in Table 4-4. The R square is 0.782, adjusted R square is 0.736, RMSE is 0.246 and p value is smaller than 0.0001. As another indicator of the goodness of the model, predicted  $k_e$  versus measured  $k_e$  graphics were examined (Figure 4-18,22). The closer the dots are to the centered line, the better the model is. So by looking at Figure 4-18 and 4-22 it can be said that  $k_e$ M1 and  $k_e$ M2 models are both convenient.

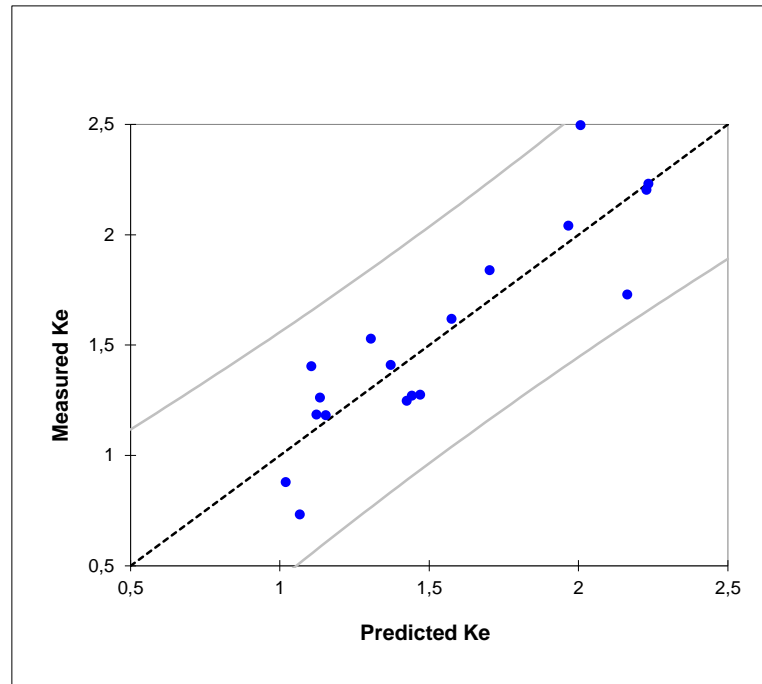


Figure 4-22. Predicted  $k_e$  versus measured  $k_e$  for  $k_eM2$  model

When the two models,  $k_eM1$  and  $k_eM2$  are compared, it is seen that R square of  $k_eM1$  is higher than R square of  $k_eM2$ . Since R square is an indicator of how well the parameters represent the model, as the number of parameters increase, R square is also expected to be higher. In this case to compare these two models regardless of the parameter number, adjusted R squares is needed to be compared. Even though  $k_eM2$  has a smaller R square value, the adjusted R square of  $k_eM2$  model is higher than  $k_eM1$  model, which means that  $k_eM2$  model is a more representative model for  $k_e$ .

After the gate broke, the water entered to the lake from Lake Mogan changed the water quality in Lake Eymir. To investigate this change besides using a one year data, model was also run with the data before and after the gate broke, separately.

The linear regression model of  $k_e$  data obtained before the gate broke gave the correlation matrix given in table 4-2.

Table 4-2. Correlation matrix of linear regression model of  $k_e$ , with data obtained before gate broke.

Variable	s	SD	Chl-a	TSS	NH <sub>4</sub> -N	NO <sub>3</sub> -N	Depth	PO <sub>4</sub> -P	$k_e$
SD		<b>1,000</b>	-0,528	-0,216	-0,273	-0,267	0,073	0,270	-0,742
Chl-a		-0,528	<b>1,000</b>	0,550	-0,284	<u>0,608</u>	-0,240	-0,204	0,817
TSS		-0,216	0,550	<b>1,000</b>	-0,198	<u>0,601</u>	-0,393	-0,078	0,532
NH <sub>4</sub> -N		-0,273	-0,284	-0,198	<b>1,000</b>	-0,169	0,563	-0,223	-0,026
NO <sub>3</sub> -N		-0,267	0,608	0,601	-0,169	<b>1,000</b>	-0,180	-0,301	0,745
Depth		0,073	-0,240	-0,393	0,563	-0,180	<b>1,000</b>	0,206	-0,246
PO <sub>4</sub> -P		0,270	-0,204	-0,078	-0,223	-0,301	0,206	<b>1,000</b>	-0,335
$k_e$		-0,742	0,817	0,532	-0,026	0,745	-0,246	-0,335	<b>1,000</b>

The same procedure was followed with this model. One of the two parameter having a correlation coefficient higher than 0.6, was removed. When Table 4-2. is investigated, it's seen that NO<sub>3</sub>-N is correlated with



TSS and Chl-a with a correlation coefficient of 0.601 and 0.608 respectively.

Chl-a is an important parameter in this study. When Table 4-2 is examined it I seen that Chl-a has the highest correlation coefficient with  $k_e$  which is 0.817. So it is important to keep Chl-a in the model, and in order to do this,  $\text{NO}_3\text{-N}$  was removed from the model. Since  $\text{NO}_3\text{-N}$  and TSS is correlated and  $\text{NO}_3\text{-N}$  is removed from the model, TSS was kept in the model. Two models were derived resulting from this linear regression model ran with the data obtained before the gate broke. One was named  $k_e\text{M3}$ , and involved the parameters that are not removed from the model; SD, Chl-a, TSS, depth,  $\text{PO}_4\text{-P}$ . The other was named  $k_e\text{M4}$  and involved parameters that have slightly higher correlation coefficients with  $k_e$ , which are; SD, Chl-a and TSS.

Eventhough  $\text{NO}_3\text{-N}$  has a higher correlation coefficient with  $k_e$ , which is 0.745, compared to TSS which is 0.532, it was not involved to the model, because it was removed from the model at the beginning, due to its correlation coefficient higher than 0.6 with two other parameters; Chl-a and TSS.

$k_e\text{M3}$  model gave the following equation as a result;

$$k_e\text{M3} = 1.6 - 0.5 \cdot \text{SD} + 7.53 \cdot 10^{-03} \cdot \text{Chl-a} + 1.08 \cdot 10^{-02} \cdot \text{TSS} \\ - 9.3 \cdot 10^{-03} \cdot \text{Depth} - 1.3 \cdot 10^{-03} \cdot \text{PO}_4\text{-P}$$

(Eq-13)

The goodness of the fit statistics is given in Table 4-4. The R square of model  $k_e\text{M3}$  is 0.831, the adjusted R square is 0.711, the RMSE is 0.179 and the p value is 0.012.

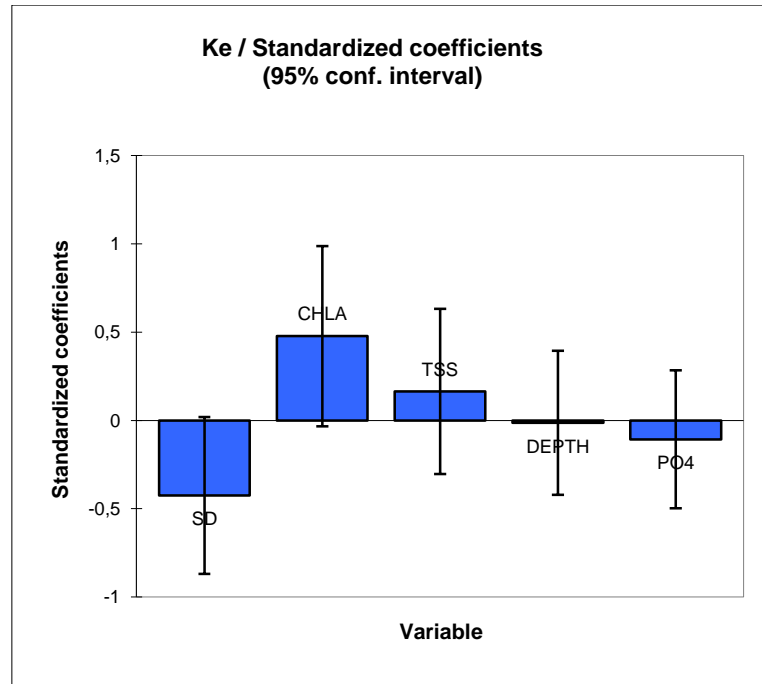


Figure 4-23. Standardized Coefficients vs. variables of  $k_e$ M3 model.

In Figure 4-23 it is seen that SD was again negatively proportional with  $k_e$  before the gate was broken. And Chl-a is the most correlated parameter with  $k_e$ . The comparison of the measured  $k_e$  to the predicted  $k_e$  resulting from  $k_e$ M3 is given in Figure 4-24. As it is seen, the dots are very close to the centered line.

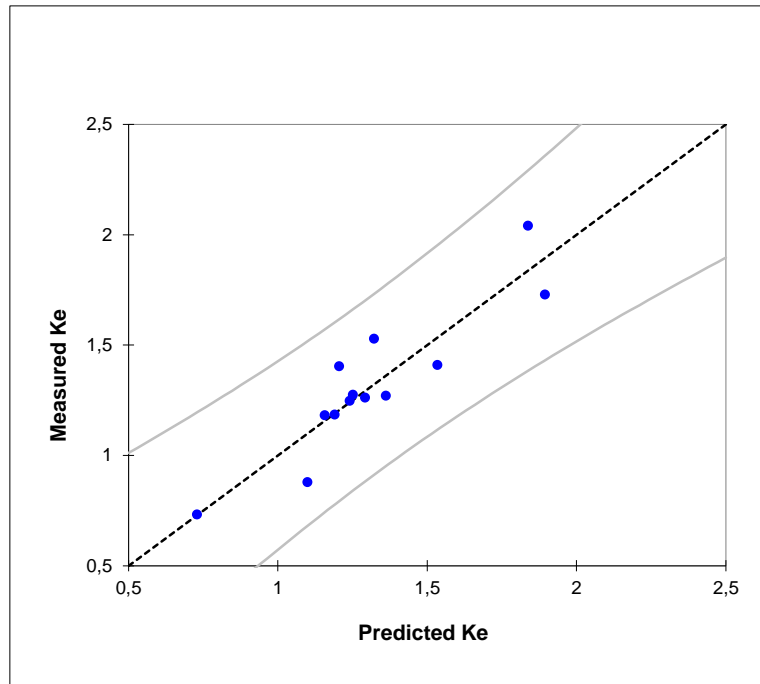


Figure 4-24. Predicted  $k_e$  versus measured  $k_e$  for  $k_e$ M3 model

$k_e$ M4 model gave the following equation as a result;

$$k_eM4 = 1.51 - 0.53 * SD + 7.71 * 10^{-03} * Chl-a + 0.011 * TSS$$

(Eq-14)

The R square of model  $k_e$ M4 is 0.820, the adjusted R square is 0.760, the RMSE is 0.163 and the p value is 0.001.

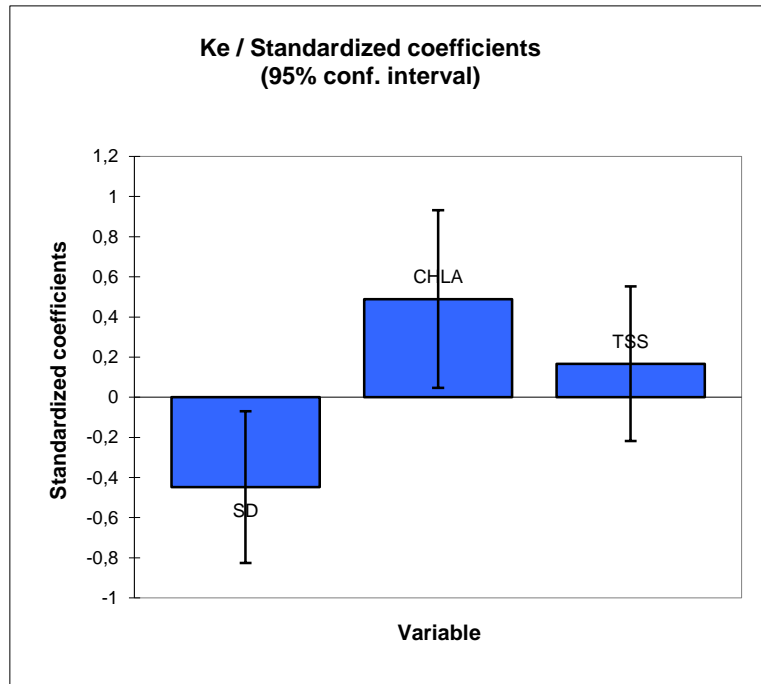


Figure 4-25 Standardized Coefficients vs. variables of  $k_e$ M4 model.

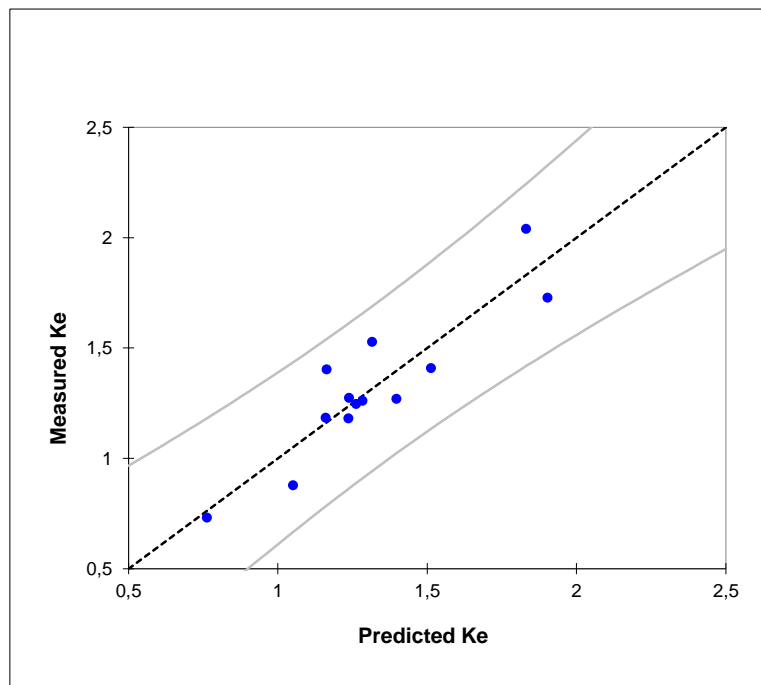


Figure 4-26 Predicted  $k_e$  versus measured  $k_e$  for  $k_e$ M4 model

When the models ran with the data obtained after the gate broke, in other words after 20<sup>th</sup> March, 2010, which are the models  $k_e$ M3 and  $k_e$ M4, are compared, it is seen that  $k_e$ M3 has a higher R square and  $k_e$ M4 has a higher adjusted R square. Since model  $k_e$ M4 has less parameters than  $k_e$ M3, the higher adjusted R square suggests that  $k_e$ M4 model is a more representative model. So it can be said that with the conditions before the gate broke, SD, Chl-a and TSS are the parameters that contribute to  $k_e$  most.

The Figures of (Fig. 4-26 and 4-24) suggests that the models gave better results when ran with the data before the gate broke, compared to the model ran with the all time data. This indicates that the entered water to Lake Eymir altered the water quality. Therefore the data obtained after the gate broke was investigated separately.

The linear regression model of  $k_e$  data obtained after the gate broke gave the correlation matrix given in Table 4-3.

Table 4-3. Correlation matrix of linear regression model of  $k_e$ , with data obtained after gate broke.

Variable	s	SD	Chl-a	TSS	NH <sub>4</sub> -N	NO <sub>3</sub> -N	Depth	PO <sub>4</sub> -P	$k_e$
SD	<b>1,000</b>	0,331	0,025	-0,526	0,024	<u>0,617</u>	-0,225	0,706	
Chl-a	0,331	<b>1,000</b>	<u>0,661</u>	0,578	<u>0,630</u>	<u>0,741</u>	0,531	0,871	
TSS	0,025	0,661	<b>1,000</b>	0,324	0,397	0,511	0,489	0,625	
NH <sub>4</sub> -N	-0,526	0,578	0,324	<b>1,000</b>	0,526	0,078	0,596	0,107	
NO <sub>3</sub> -N	0,024	0,630	0,397	0,526	<b>1,000</b>	<u>0,770</u>	<u>0,957</u>	0,510	
Depth	0,617	0,741	0,511	0,078	0,770	<b>1,000</b>	<u>0,620</u>	0,892	
PO <sub>4</sub> -P	-0,225	0,531	0,489	0,596	0,957	0,620	<b>1,000</b>	0,351	
$k_e$	0,706	0,871	0,625	0,107	0,510	0,892	0,351	<b>1,000</b>	

The correlation coefficients higher than 0.6, is given in italic and underlined text. When we consider Table 4-3, it is seen that Chl-a is highly correlated with TSS, NO<sub>3</sub>-N and depth. Since Chl-a is a parameter that we

specifically aim to investigate, it was kept in the model, while the other three parameters are removed. By this means, while depth is removed, the two parameters that are correlated with depth, which are SD and PO<sub>4</sub>-P, were kept in the model.

By checking this matrix we derived two models. One was named k<sub>e</sub>M5 and contained SD, Chl-a NH<sub>4</sub>-N and PO<sub>4</sub>-P. The other was named k<sub>e</sub>M6 and it was run with lesser parameters; SD and Chl-a only. The k<sub>e</sub>M5 model gave the following equation;

$$k_eM5 = -1.5 + 1.76 * SD - 1.67 * 10^{-03} * Chl-a + 0.56 * NH_4-N + 1.71 * 10^{-02} * PO_4-P$$

(Eq-15)

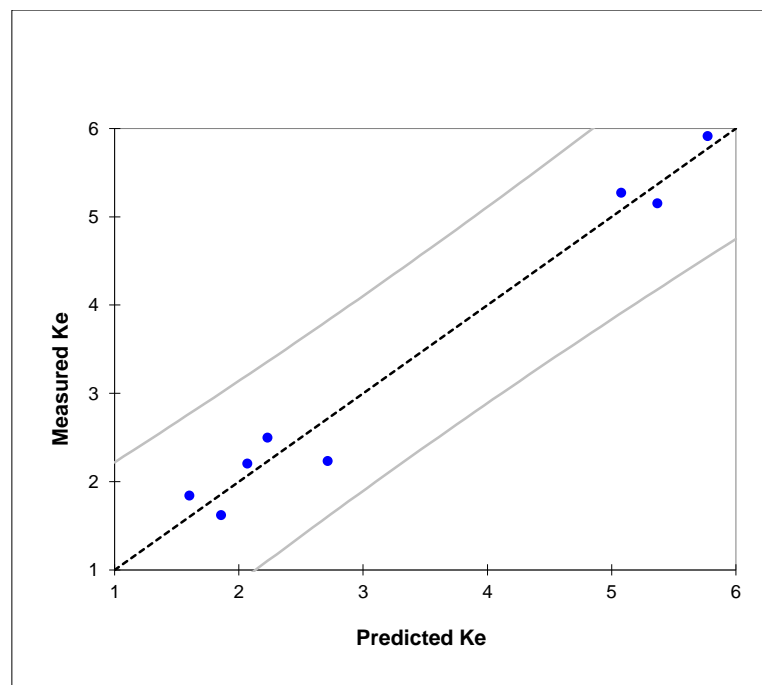


Figure 4-27. Predicted k<sub>e</sub> versus measured k<sub>e</sub> for k<sub>e</sub>M5 model

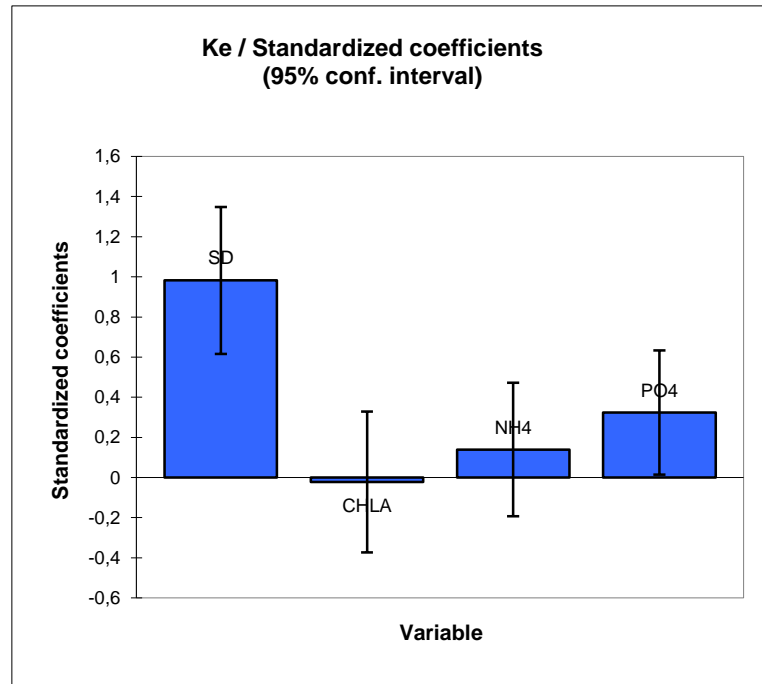


Figure 4-28. Standardized Coefficients vs. variables of  $k_e$ M5 model.

The R square of model  $k_e$ M5 is 0.976, the adjusted R square is 0.943, the RMSE is 0.424 and the p value is 0.009.

The  $k_e$ M6 model gave the following equation;

$$k_eM6 = 0.91 + 1.70 * SD + 5.04 * 10^{-03} * Chl-a$$

(Eq-16)

The R square of model  $k_e$ M6 is 0.834, the adjusted R square is 0.768, the RMSE is 0.856 and the p value is 0.011. With these statistics, it is seen that after the gate broke  $k_e$ M5 is a much better model for  $k_e$ , than  $k_e$ M6.



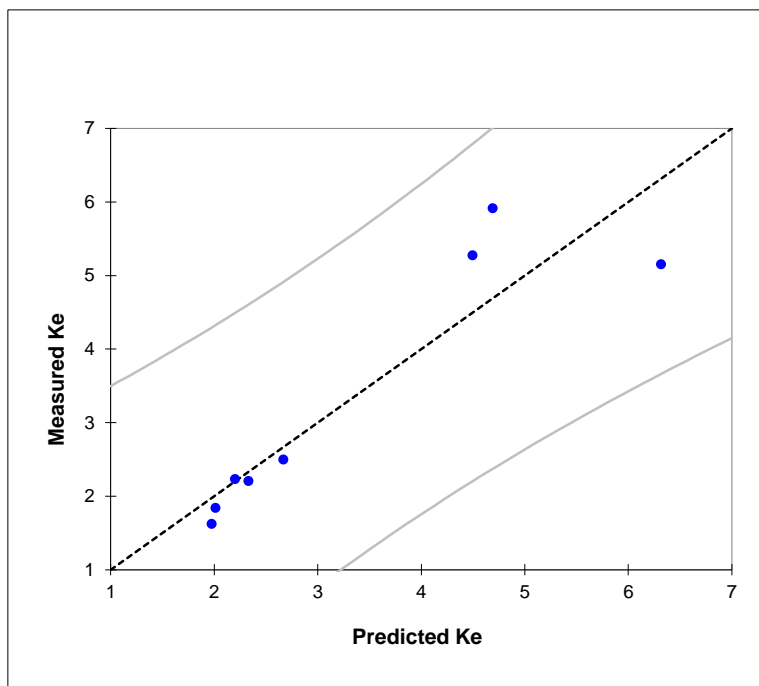


Figure 4-29. Predicted  $k_e$  versus measured  $k_e$  for  $k_e$ M6 model

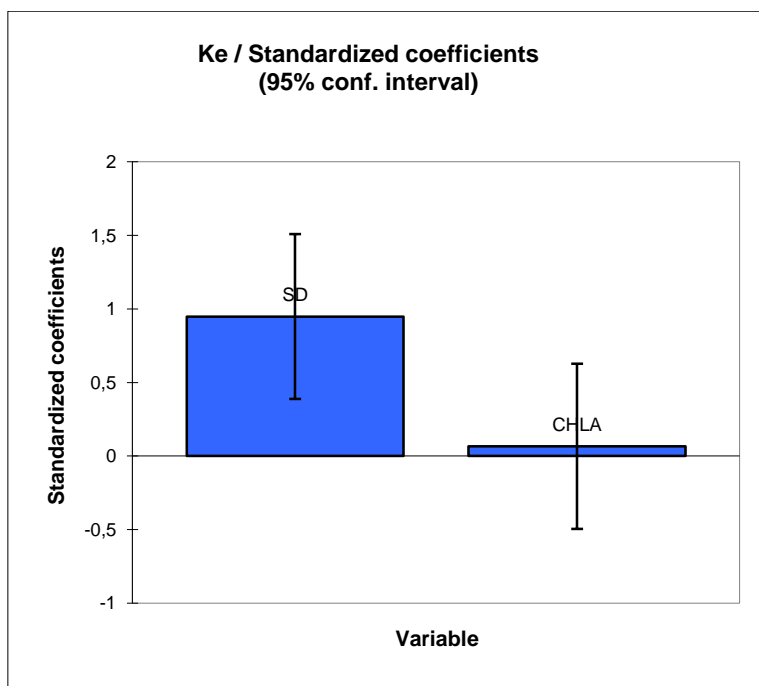


Figure 4-30. Standardized Coefficients vs. variables of  $k_e$ M6 model.

After the gate broke, according to the models  $k_eM5$  and  $k_eM6$ , it is seen that  $k_e$  is most correlated with Secchi depth. This is also an outcome of the Figure 4-28 and 4-30, Standardized Coefficients vs. variables of  $k_eM6$  model.

By examining Table 4-3 it is seen that SD and  $k_e$  is directly proportional. It is expected to be inversely proportional since as turbidity increases SD decreases while  $k_e$  increases (Christian & Sheng 2003). By this information we can say that the data obtained after the gate broke are not conforming to literature. The reason of this may be the rapidly altered water quality conditions. The data collected after the gate broke, does not involve a long time period. With this poor number of data it would not be convenient to have a detailed opinion about the lake conditions. But indisputably it can be said that the lake conditions were highly changed after the gate broke. Despite this change, Chl-a is still one of the most correlated parameter with  $k_e$ , after the gate broke.

The first part of table two is composed of linear regression model results and the 2<sup>nd</sup> part, which is below the double line is composed of non-linear regression models. That is the reason of the absence of adjusted R square and p value, because the non-linear regression model results does not have a p value and adjusted R square value.

Table 4-4. The goodness of fit statistics

Models/ Statistics	R2	Adjusted R2	RMSE	p value
k <sub>e</sub> M1	0,808	0,728	0,25	0,001
k <sub>e</sub> M2	0,782	0,736	0,246	0,0001
k <sub>e</sub> M3	0,831	0,711	0,179	0,012
k <sub>e</sub> M4	0,820	0,760	0,163	0,001
k <sub>e</sub> M5	0,976	0,943	0,424	0,009
k <sub>e</sub> M6	0,834	0,768	0,856	0,011
k <sub>e</sub> M7	0,628	0,579	0,311	0,001
CM2	0,590	0,502	15,369	0,005
CM1	0,600	0,477	15,740	0,013
CM3	0,662	0,557	19,774	0,005
k <sub>e</sub> *-all time	0,605	-	0,320	-
k <sub>e</sub> *-after gate broke	0,935	-	1,395	-
k <sub>e</sub> *-before gate broke	0,760	-	0,179	-

When Table 4-1,2 and 3 are examined, k<sub>e</sub> has the highest correlation coefficient with SD and Chl-a. It is seen that in Table 4-3 k<sub>e</sub> has the

highest correlation coefficient with depth. But as mentioned before the results obtained after the gate broke are not very representative and reliable. By this means an overall linear regression model was studied with all time data, which was named  $k_eM7$  and involved only SD and Chl-a. The  $k_eM7$  model gave the following equation;

$$k_eM7 = 1.93 - 0.80 \cdot SD + 1.07 \cdot 10^{-02} \cdot \text{Chl-a}$$

(Eq-17)

The R square of model  $k_eM7$  is 0.628, the adjusted R square is 0.579, the RMSE is 0.311 and the p value is 0.001. It is expected to obtain a lower R square value with lesser parameters. According to RMSE and p value, this model is still operative.

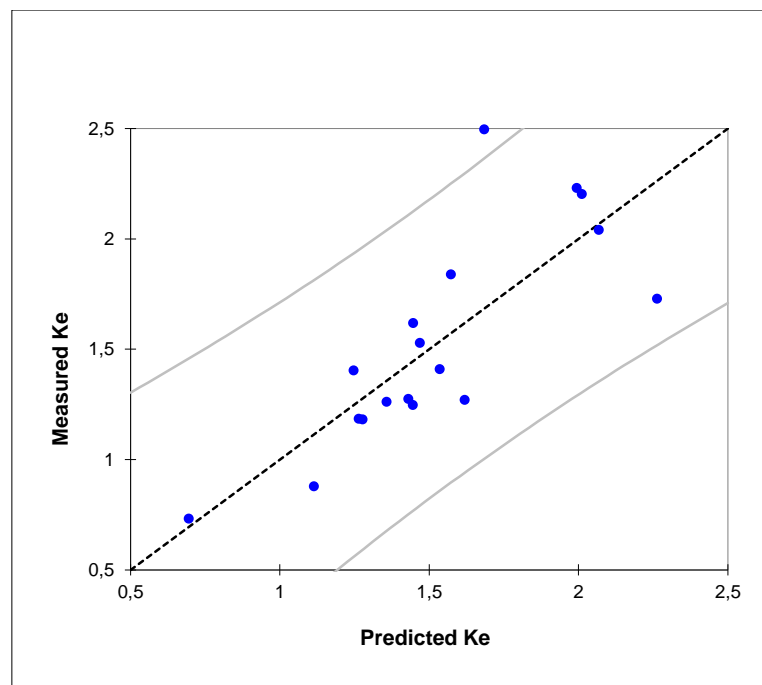


Figure 4-31. Predicted  $k_e$  versus measured  $k_e$  for  $k_eM7$  model

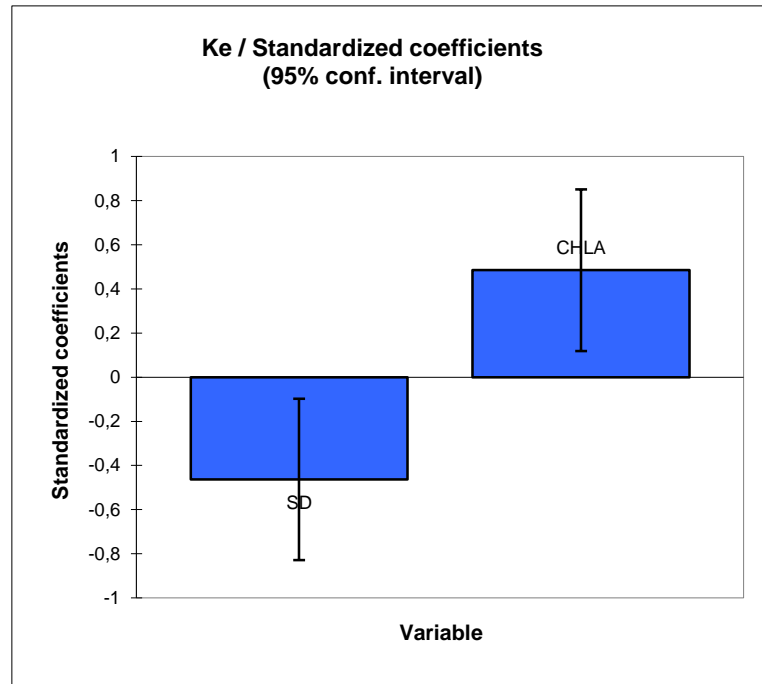


Figure 4-32. Standardized Coefficients vs. variables of  $k_e$ M7 model.

According to  $k_e$ M7 model, SD is inversely proportional with  $k_e$  as expected and it can be also seen in Figure 4-32. The predicted  $k_e$  values versus measured  $k_e$  graphic (Fig. 4-31) indicates that model is not very convenient.

As mentioned in previous chapters, it is a known fact that  $k_e$  is most correlated with turbidity (Fisher et al. 1999). And Secchi disk depth is the main indicator of turbidity and Chl-a highly contributes to turbidity (Giardino et al. 2001). With this knowledge the results obtained from this study were investigated in a way, to find the relationships of  $k_e$  with the Secchi depth and Chl-a. The data were plotted versus  $k_e$  with the average value of 5 Stations. Below in Figure 4-33. SD vs.  $k_e$  is given. On yearly base, it's seen that, as Secchi depth increase, the  $k_e$  decreases with a non-linear pattern in Lake Eymir which is an expected result (Kirk, 1994).

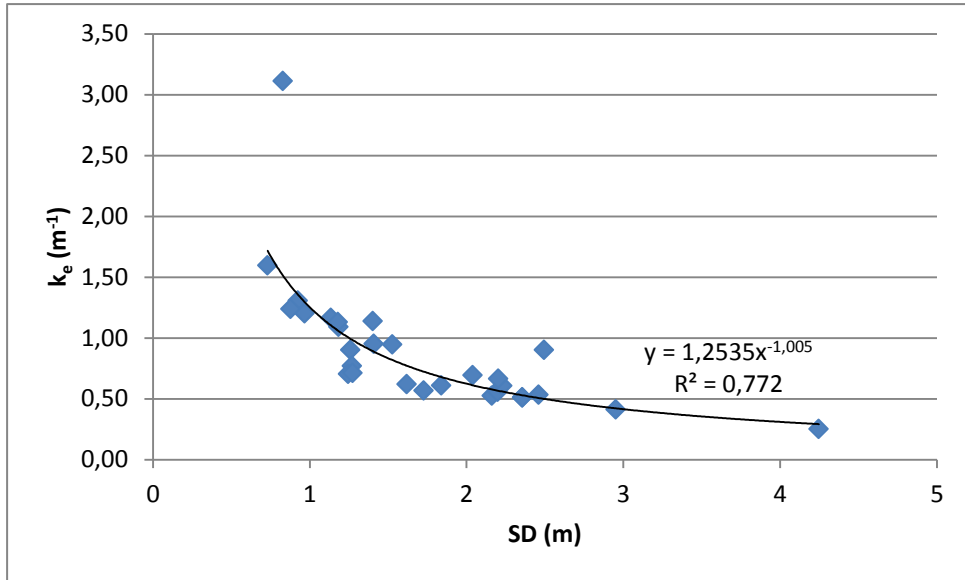


Figure 4-33:  $k_e$  vs. SD

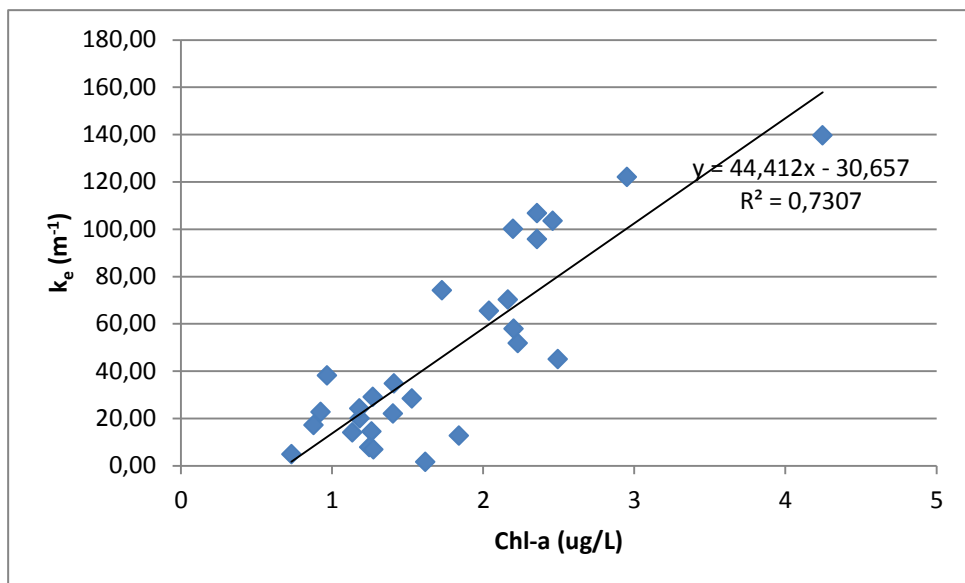


Figure 4-34:  $k_e$  vs. Chl-a

Chl-a was directly proportional with  $k_e$  according to the results of this study. In Figure 4-34, the graphic shows that as Chl-a increases,  $k_e$  also increases. Since Chl-a contributes to turbidity and  $k_e$  is correlated with

turbidity, as Chl-a increase, turbidity also increase, and light attenuation thus  $k_e$  also increases. So it is expected to make such an observation.

Figure 4-33 explains the inaccuracy in  $k_e$ M7 model. The model was run with appropriate parameters but linear regression was studied. The nonlinear regression models for every  $k_e$ M model, was also studied but the goodness of fit statistics revealed that nonlinear  $k_e$ M models are inconvenient in general. But in case of  $k_e$ M7 model it is different. In Fig 4-33 and 4-34 it is clearly seen that for year 2009-2010,  $k_e$  was linearly correlated with Chl-a, while there is a non linear correlation between  $k_e$  and SD.

A final model was derived for  $k_e$ , and named  $k_e^*$ . This  $k_e^*$  involved SD and Chl-a and ran with non-linear regression. It was ran with the data obtained before and after the gate broke, and with one-year data.

$k_e^*$  model ran with one-year data gave the following equation as result.

$$k_e^* \text{ all time} = 1.09 * SD^{-0.58} + 1.1 * 10^{-02} * \text{Chl-a}$$

(Eq-18)

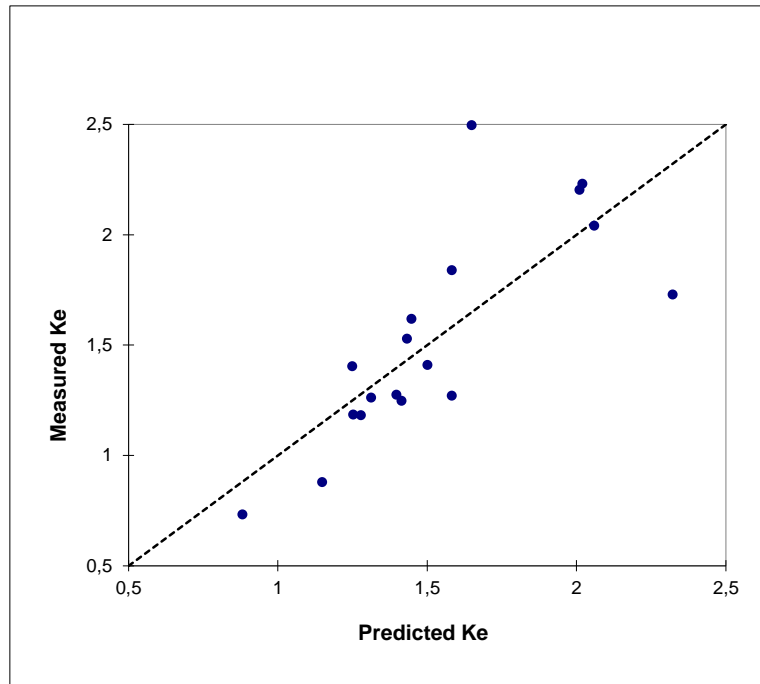


Figure 4-35. Predicted  $k_e$  versus measured  $k_e$  for  $k_e^*$  *all time* model

When Fig 4-35 is compared with Fig 4-31, it is seen that  $k_e^*$  *all time* model is much more suitable than  $k_e$ M7 model for lake Eymir. Since the data points are closer to the centered line in the graphic of measured v. predicted  $k_e^*$ . The R square of  $k_e^*$  *all time* model is 0.605 and RMSE is 0.320.

With the data obtained until the gate broke, the same model was ran.  $k_e^*$  *before gate broke* model gave the following equation as a result;

$$k_e^* \text{ before gate broke} = 1.02 \cdot SD^{-0.39} + 9.66 \cdot 10^{-03} \cdot \text{Chl-a}$$

(Eq-19)



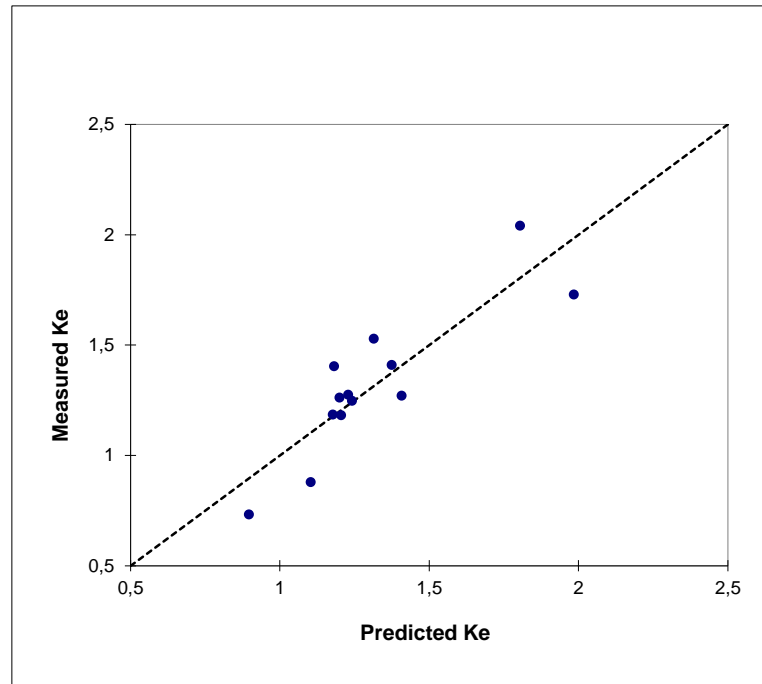


Figure 4-36. Predicted  $k_e$  versus measured  $k_e$  for  $k_e^*$  *before gate broke* model

When Fig 4-36 is examined, it can be seen that  $k_e^*$  model ran with the data obtained before the gate broke, is much convenient, especially when compared with Fig. 4-31. This reveals that the data obtained before the gate broke are more reliable and representative, and the model give better results. Another source of this conclusion is the goodness of the fit statistics, which is given in Table 4-4. The R square for  $k_e^*$  *before gate broke* is 0.760 and RMSE is 0.179. These parameters also indicate that  $k_e^*$  *before gate broke* model is more convenient than  $k_e^*$  *all time* model.

The  $k_e^*$  *after gate broke* model gave the following equation as a result.

$$k_e^* \text{ after gate broke} = 1.71 \cdot SD^{(6.65)} + 4.05 \cdot 10^{-02} \cdot \text{Chl-a}$$

(Eq-20)

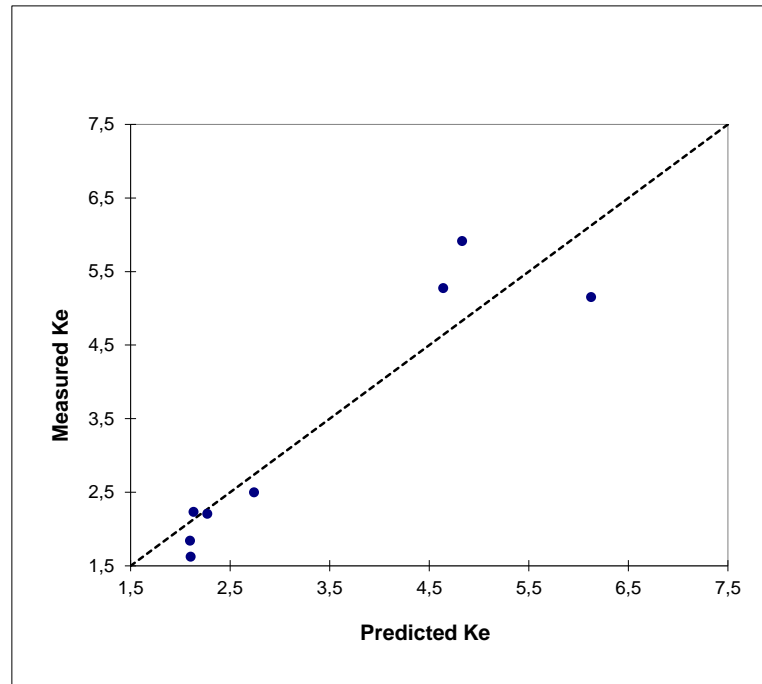


Figure 4-37. Predicted  $k_e$  versus measured  $k_e$  for  $k_e^*$  *after gate broke* model

The R square for  $k_e^*$  *after gate broke* is 0.935 and RMSE is 1.395. R square is quite high compared to  $k_e^*$  models ran with the all time data and data obtained before the gate broke. Despite this fact, RMSE is fairly high. It is also seen in Fig. 4-37 that the model ran with after gate broke data is not as convenient as the models ran for all time data and before gate broke data.

To understand the effect of  $k_e$  on Chl-a, Chl-a models were also studied. In Table 4-5 the correlation matrix of Chl-a model is given.

Table 4-5. Correlation matrix of linear regression model of Chl-a, with one-year data.

Variable	s	$k_e$	SD	TSS	NH <sub>4</sub> -N	NO <sub>3</sub> -N	Depth	PO <sub>4</sub> -P	Chl-a
$k_e$	<b>1,000</b>	<u>-0,656</u>	0,387	<u>0,641</u>	0,302	0,546	0,452	0,669	
SD	-0,656	<b>1,000</b>	-0,176	-0,529	-0,126	-0,329	-0,211	-0,398	
TSS	0,387	-0,176	<b>1,000</b>	-0,017	0,553	-0,169	0,030	0,563	
NH <sub>4</sub> -N	0,641	-0,529	-0,017	<b>1,000</b>	-0,216	<u>0,840</u>	<u>0,636</u>	0,131	
NO <sub>3</sub> -N	0,302	-0,126	0,553	-0,216	<b>1,000</b>	-0,253	-0,277	0,509	
Depth	0,546	-0,329	-0,169	0,840	-0,253	<b>1,000</b>	<u>0,688</u>	0,050	
PO <sub>4</sub> -P	0,452	-0,211	0,030	0,636	-0,277	0,688	<b>1,000</b>	0,096	
Chl-a	0,669	-0,398	0,563	0,131	0,509	0,050	0,096	<b>1,000</b>	

Two models were derived from this correlation matrix. As did previously with the  $k_e$  models, the correlation coefficients were investigated. According to the Table 4-5,  $k_e$  is correlated with SD, NH<sub>4</sub>-N. And PO<sub>4</sub>-P is correlated with NH<sub>4</sub>-N and Depth.  $k_e$  is the main parameter examined in this study, in order to keep  $k_e$  in the model, NH<sub>4</sub>-N and depth was

removed. Since  $\text{NH}_4\text{-N}$  and depth is already removed it is more logical to keep  $\text{PO}_4\text{-P}$  in the model.

First Chl-a model was named CM1 and contained  $k_e$ , TSS,  $\text{NO}_3\text{-N}$  and  $\text{PO}_4\text{-P}$ . The second was named CM2 and contained  $k_e$ , TSS and  $\text{NO}_3\text{-N}$ . CM2 was designed in such way that it would contain the parameters that have higher correlation coefficients.

CM1 model gave the equation below;

$$\text{CM1} = -21 + 26.5 * k_e + 1.19 * \text{TSS} + 3.62 * \text{NO}_3\text{-N} - 7.72 * 10^{-02} * \text{PO}_4\text{-P}$$

(Eq-21)

In Fig 4-38, standardized coefficients graphic is given. It is seen that Chl-a is most depending on  $k_e$ . Table 4-5 is another output that indicates the same fact. When the correlation coefficients are investigated, it is clearly seen that among all other parameters  $k_e$  is the parameter that has the highest correlation coefficient with Chl-a. The predicted Chl-a versus measured Chl-a graphic is given in Figure 4-39.

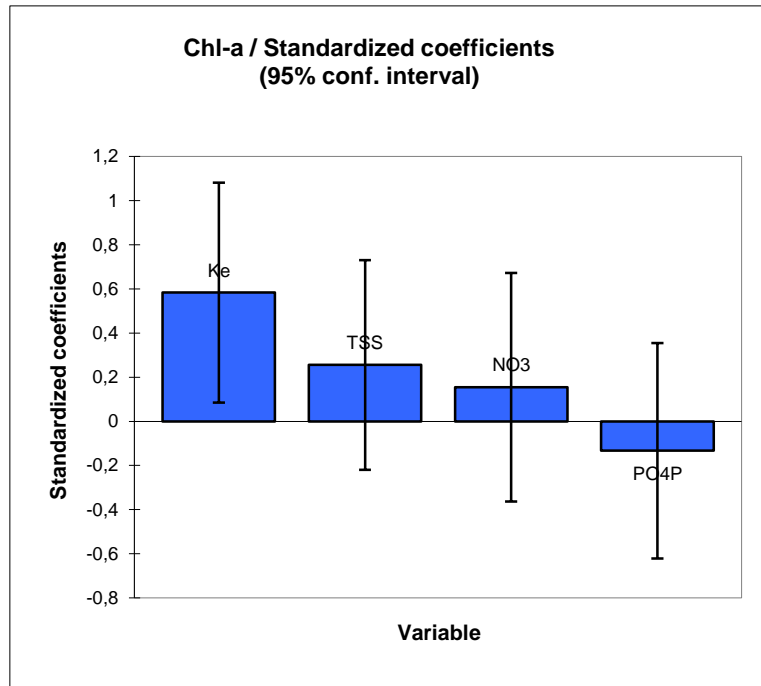


Figure 4-38. Standardized Coefficients vs. variables of CM1 model.

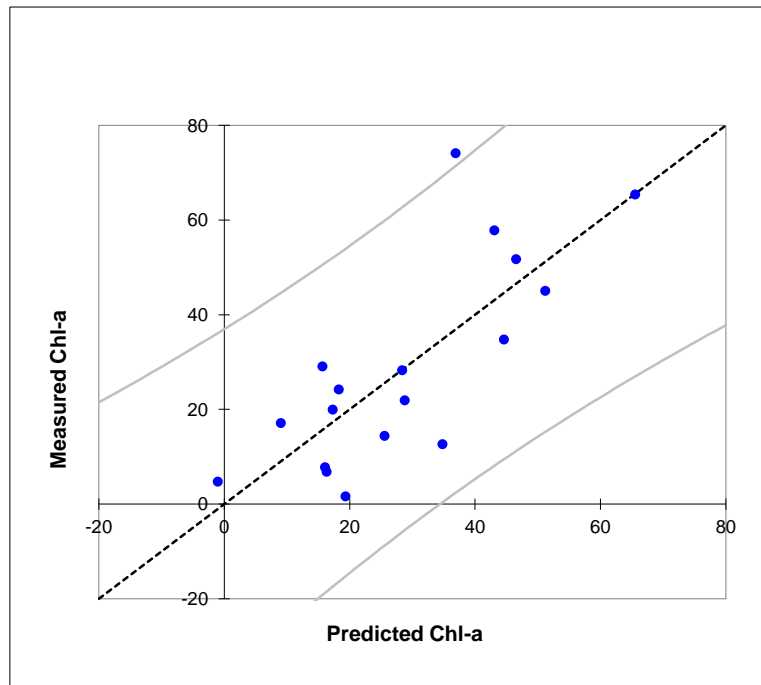


Figure 4-39. Predicted Chl-a versus measured Chl-a for CM1 model

As seen in Table 4-4 the R square of model CM1 is 0.600, the adjusted R square is 0.477, the RMSE is 15.740 and the p value is 0.013.

The second Chl-a model studied; CM2 model, gave the following equation as a result;

$$\text{CM2} = -21.84 + 23.082 \cdot k_e + 1.144 \cdot \text{TSS} + 5.16 \cdot \text{NO}_3\text{-N}$$

(Eq-22)

In this equation it is seen that  $k_e$  has the highest coefficient. Below in Fig. 4-40, the same result is seen; that Chl-a is most depended on  $k_e$ .

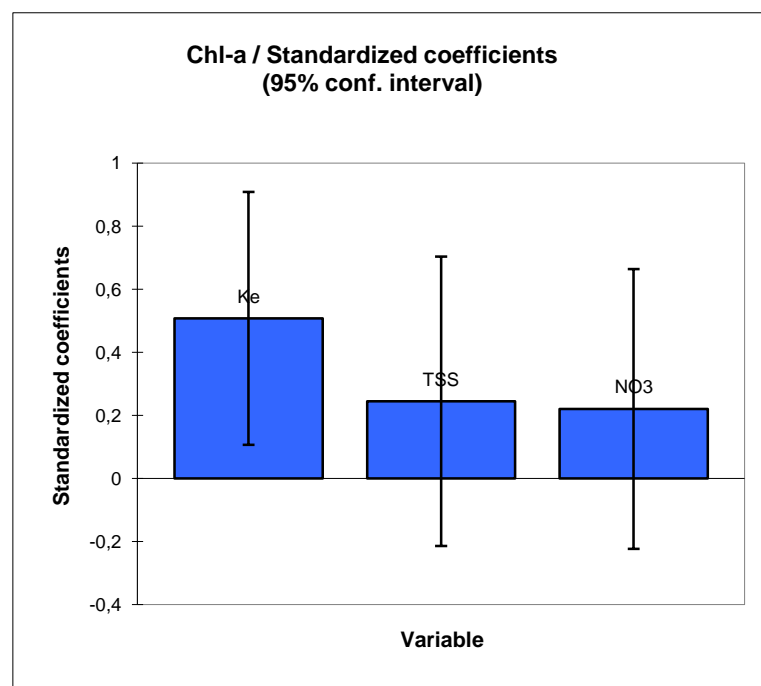


Figure 4-40. Standardized Coefficients vs. variables of CM2 model.

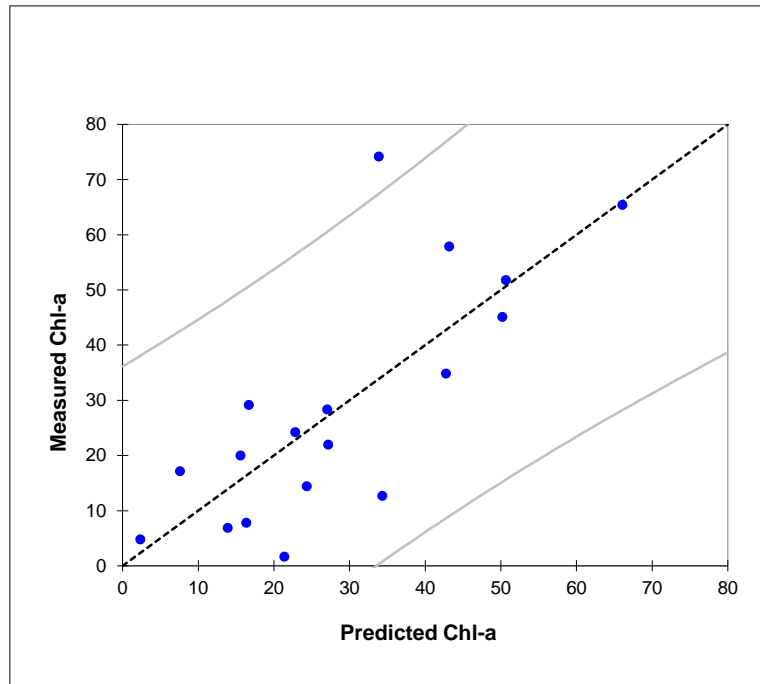


Figure 4-41. Predicted Chl-a versus measured Chl-a for CM2 model

The R square of model CM2 is 0.590, the adjusted R square is 0.502, the RMSE is 15.369 and the p value is 0.005.

When Figure 4-39 and 4-41 is considered, the dots are mostly spread, instead of being close to the center. With the goodness of fit statistics given in Table 4-4, and Fig. 4-39 and 41, it can be concluded that  $k_e$ M models are more convenient in comparison with CM models.

As different approach for investigating the  $k_e$  effect on Chl-a, among nutrients, one last CM model was studied. The model was named CM3 and contained  $\text{NO}_3\text{-N}$ ,  $\text{NH}_4\text{-N}$ ,  $\text{PO}_4\text{-P}$  and  $k_e$ .

The equation derived from CM3 model is given below.

$$\text{CM3} = 4.55 + 1.09 \cdot k_e - 0.15 \cdot \text{NH}_4\text{-N} + 0.13 \cdot \text{NO}_3\text{-N} - 0.35 \cdot \text{PO}_4\text{-P}$$

(Eq-23)

This equation and Figure 4-42 reveals that among all parameters,  $k_e$  is the parameter that contributes to Chl-a most.

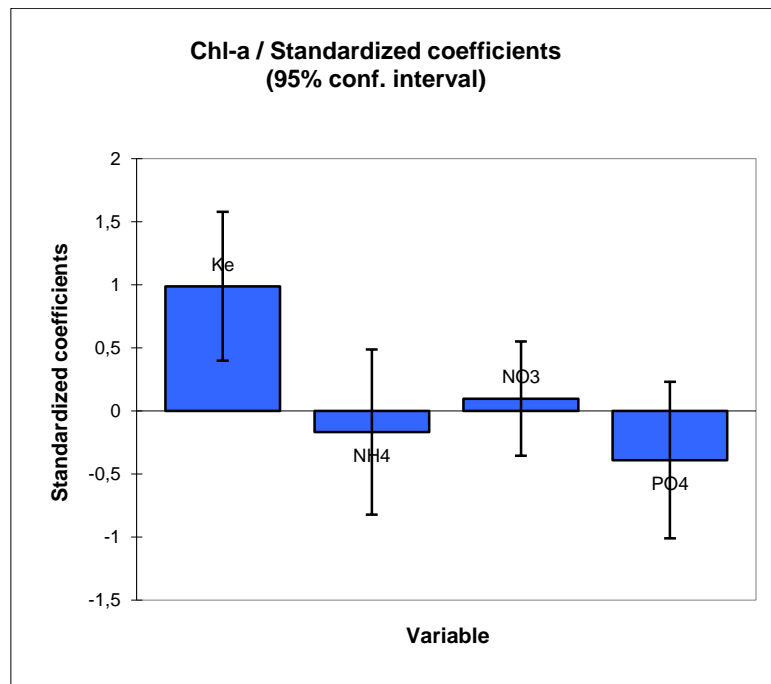


Figure 4-42. Standardized Coefficients vs. variables of CM3 model.



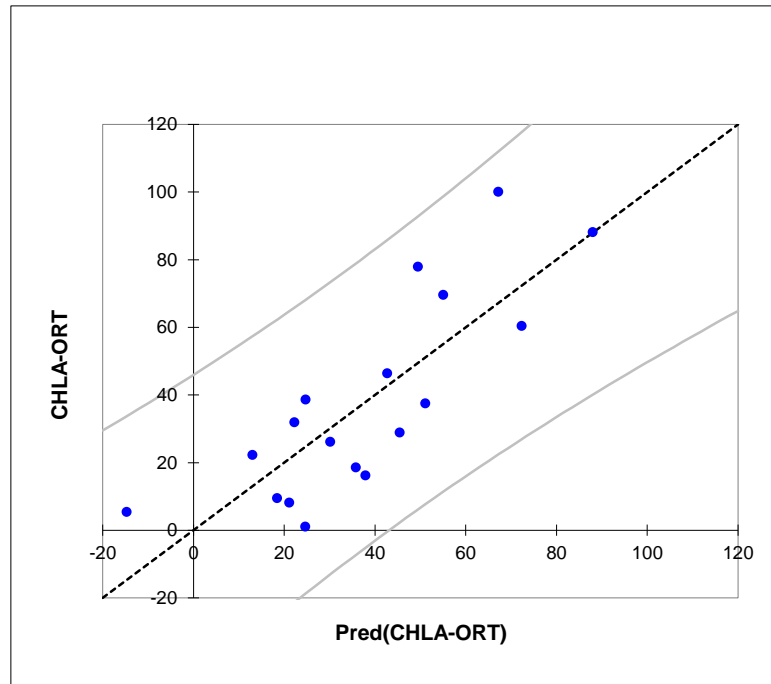


Figure 4-43. Predicted Chl-a versus measured Chl-a for CM3 model

The predicted Chl-a data versus measured Chl-a data is given in Fig. 4-43. As seen in Table 4-4, the R square of model CM3 is 0.662, the adjusted R square is 0.557, the RMSE is 19.774 and the p value is 0.005. According to these statistics and Fig 4-43, the CM3 model is slightly more convenient than CM1 and CM2 models. But compared to  $K_eM$  models, CM models are not that acceptable.

When comparing models in general, for Chl-a, by looking at the Table 4-5, it can be said that  $k_e$  is positively correlated with Chl-a and compared with nutrients,  $k_e$  has a higher role on Chl-a abundance, which is an expected situation for shallow and turbid lakes (Hairston & Fussman, 2002).  $NO_3-N$  is following  $k_e$  with a correlation coefficient of 0.509. The lake was investigated in terms of nutrient limitation. The N:P results revealed that the lake was N limited the whole time. This is the reason of the high correlation coefficient between Chl-a and  $NO_3-N$ .

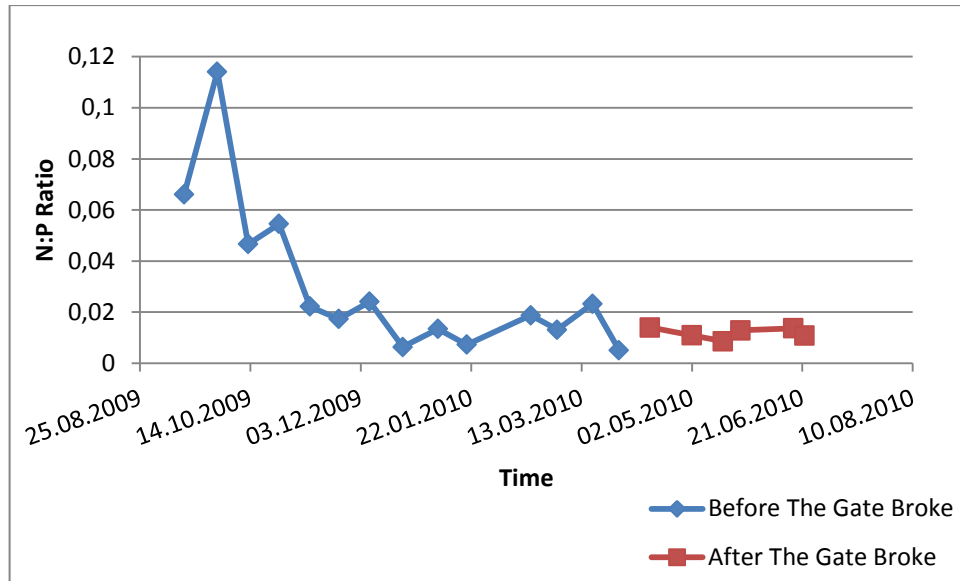


Figure 4-44. N:P Ratio of Lake Eymir.

In Fig. 4-44 it is seen that N:P ratio is not above 5 by weight. The ratio was calculated by dividing  $(\text{NO}_3\text{-N})+(\text{NH}_4\text{-N})$  to  $\text{PO}_4\text{-P}$ . According to Table 4-6 given below, Lake Eymir was N limited during whole study, including the period after the gate broke.

Table 4-6. Defining Limiting Nutrient by Dissolved N:P Ratio.

(Yenilmez, 2007)

Dissolved Nitrogen/Phosphate Phosphorus		Limiting Nutrient
By Weight	In Moles	
<5	10	N
5-12		N and/or P
>12	26,5	P

And in general,  $k_e$  models studied for all time data, indicated that  $k_e$  is most correlated with SD and Chl-a. Besides SD and Chl-a, there is also a high correlation between  $\text{NO}_3\text{-N}$  and  $k_e$ , which can be seen when the Table 4-2 is investigated. This is due to the dependence of Chl-a on  $\text{NO}_3\text{-N}$  as limiting nutrient. Eventhough in Table 4-5 it is clearly seen that  $k_e$  has a higher correlation coefficient with Chl-a, compared to  $\text{NO}_3\text{-N}$ ,  $\text{NO}_3\text{-N}$  is still an important parameter for Chl-a. So since when  $k_e$  is modeled, Chl-a is the most important parameter, due to its dependence on  $\text{NO}_3\text{-N}$ ,  $\text{NO}_3\text{-N}$  is one of the parameters that  $k_e$  depends on.

In Table 4-7 the summary of this study is given, with the parameters used in the model and the goodness of fit statistics of the model results.

Table 4-7. The Summary of the Models Studied

Models	Used Parameters in Model					R <sup>2</sup>	Adjusted R <sup>2</sup>	RMSE	p value
k <sub>e</sub> M1	SD	Chl-a	TSS	NO <sub>3</sub>	Depth	0,808	0,728	0,25	0,001
k <sub>e</sub> M2	SD	Chl-a	Depth	-	-	0,782	0,736	0,246	0,0001
k <sub>e</sub> M3	SD	Chl-a	TSS	PO <sub>4</sub>	Depth	0,831	0,711	0,179	0,012
k <sub>e</sub> M4	SD	Chl-a	TSS	-	-	0,82	0,76	0,163	0,001
k <sub>e</sub> M5	SD	Chl-a	NH <sub>4</sub>	PO <sub>4</sub>	-	0,976	0,943	0,424	0,009
k <sub>e</sub> M6	SD	Chl-a	-	-	-	0,834	0,768	0,856	0,011
k <sub>e</sub> M7	SD	Chl-a	-	-	-	0,628	0,579	0,311	0,001
CM1	k <sub>e</sub>	TSS	NO <sub>3</sub>	PO <sub>4</sub>	-	0,6	0,477	15,74	0,013
CM2	k <sub>e</sub>	TSS	NO <sub>3</sub>	-	-	0,59	0,502	15,369	0,005
CM3	k <sub>e</sub>	NH <sub>4</sub>	NO <sub>3</sub>	PO <sub>4</sub>	-	0,662	0,557	19,774	0,005
k <sub>e</sub> *-all time	SD	Chl-a	-	-	-	0,605	-	0,32	-
k <sub>e</sub> *-after gate broke	SD	Chl-a	-	-	-	0,935	-	1,395	-
k <sub>e</sub> *-before gate broke	SD	Chl-a	-	-	-	0,76	-	0,179	-

Models given in blue column was executed with all time data, the red columns are the models which were ran with the data obtained before the gate broke and the yellow columns are the models which were examined with the data obtained after the gate broke.

In the beginning of this study, it was assumed that our data conformed to Lambert Beer law. In order to investigate this, the In PAR versus depth graphics were monitored. Higher the R square of the graphics indicated that the data conformed to Lambert Beer equation. On some certain days the graphics seemed to be slightly non linear. Which R squares were lesser than other days data. To understand the reason, the relationship of  $k_e$  and Chl-a was investigated. The normalized R squares of the In PAR versus depth graphics were plotted with normalized Chl-a data, and Fig. 4-45 was obtained.

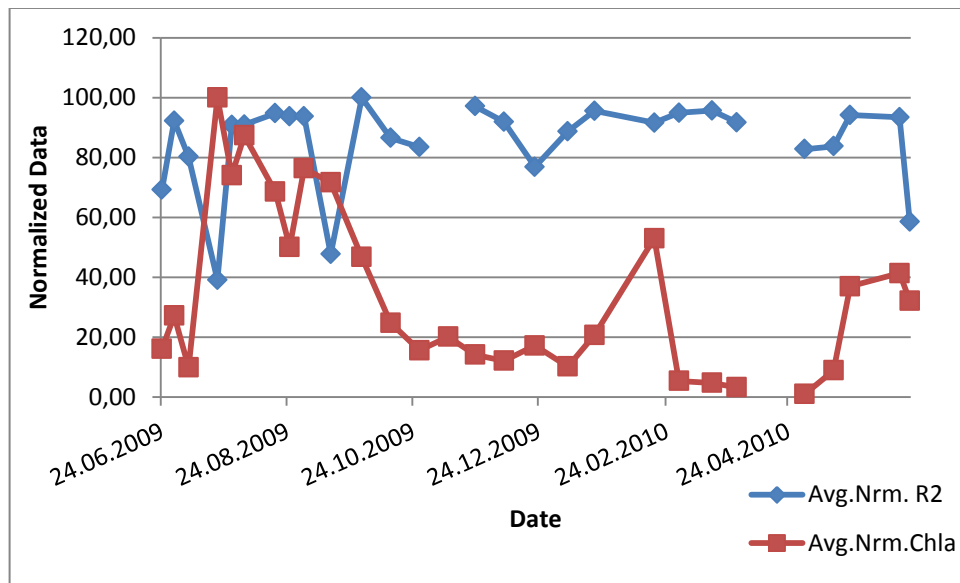


Figure 4-45. Normalized Chl-a and Normalized R square values versus time.

Normalization was done with the following formula;

$$y = a + (X - A)(b - a)/(B - A)$$

(Eq-24)

Where  $a$  and  $b$  are the lowest and the highest values of the normalized data set, which in this case it is 1 and 100 respectively.  $A$  and  $B$  are the lowest and the highest values of the original data set respectively. And  $X$  is a random data in the original data set, and  $y$  is the corresponding value of  $X$  in the normalized data set (URL10). When this Fig. 4-45 is investigated, it is seen that as Chl-a concentration showed a peak, R squares draw away from 1. So it can be said that as Chl-a increases the data is not conforming to Lambert Beer law. Gallegos (2001) showed in his study that  $k_e$  might be nonlinear and might not obey to Lambert Beer law in Case 2 waters; in which optical properties are affected substantially by non-algal particulate matter and coloured dissolved organic matter. But  $k_e$  would obey perfectly to Lambert Beer law in Case 1 waters (Gallegos, 2001). With our data, the R squares of  $\ln$  PAR versus Depth graphics were very close to 1, in other words; almost perfectly linear, thus Lamberts Beer law is generally appropriate to be used in this study.

Another reason of accepting that  $k_e$  conforms to the Lambert Beer law in this study is because, in Fig 4-45 the data used is for from June 2009 to June 2010. But to work with XL STAT, only the data of the days at which all analyzes were done are used. For example,  $\text{NH}_4\text{-N}$  analyses were not done until September 29<sup>th</sup> 2009. So the data before that date was not involved to the CM and  $k_e\text{M}$  models. And when we check Fig. 4-45, the deviations in R square is before Sept 29<sup>th</sup>. So it is safe to say that it is

appropriate to assume that  $k_e$  conforms to Lambert Beer law for the data collected from Lake Eymir in this study.

## CHAPTER 5

### CONCLUSION & RECCOMENDATIONS FOR FUTURE STUDIES

This study shows that in Lake Eymir, water quality parameters act as expected among seasons. In warmer seasons, the parameters such as depth, Secchi disk depth decreased while the Chl-a, TSS and  $k_e$ , increased. And vice versa at the months where there were precipitation and melted snow input to the lake.

Due to the breaking of the gate that connects Lake Eymir and Mogan, after March 20<sup>th</sup>, 2010, lake level increased. This additional water affected other parameters, for example SD reached its peak value while TSS and Chl-a decreased after the gate broke.

In this study besides investigating the yearly path that the measured parameters follow, mainly XL-STAT models were conducted. Besides the model, the graphics plotted  $k_e$  versus SD and Chl-a also showed that Chl-a has a very high linear correlation with  $k_e$ , while SD has an exponential relationship with  $k_e$ . This conclusion and the studied models led us to derive more representative models.

It was assumed that the data conformed to Lambert Beer law, and  $k_e$  were calculated by this method. It was seen that, except for the times where Chl-a concentrations were relatively high, the data does conform to Lambert Beer law. Equations derived from the linear regression models and and goodness of fit statistics of  $k_e$  and Chl-a models were examined. In general, all  $k_e$  models gave similar results. The model results revealed that  $k_e$  is negatively proportional with SD, and positively correlated with



TSS and Chl-a. In some of the models studied,  $k_e$  was also correlated with  $\text{NO}_3\text{-N}$ . The correlation between Chl-a and SD, TSS,  $\text{NO}_3\text{-N}$  and  $k_e$ , was a known fact and also observed in this study. Based on this knowledge and also considering that Lake was N limited during the study period, it is expected to observe such a relationship between  $k_e$  and SD, Chl-a, and  $\text{NO}_3\text{-N}$ .

Chl-a model results were not as good as  $k_e$  results but it were still acceptable. Similar to  $k_e$  model results, according to Chl-a model, Chl-a is most correlated with  $k_e$ , TSS and  $\text{NO}_3\text{-N}$ , respectively.

The studied models revealed that the effect of  $k_e$  is as important as nutrients on the Chl-a concentration, and it should not be ignored. Among all parameters investigated, Chl-a had the highest correlation matrix with  $k_e$ . The correlation matrixes derived from the models, showed that  $k_e$  has the biggest role on Chl-a abundance among all the other parameters.

XL STAT model results are reliable according to the statistical parameters. Results indicate that the XL-STAT model is an effective model that is appropriate to use for water quality analysis purposes.

As a recommendation for future studies, more sampling stations may be chosen. More sampling station would represent the lake better and the results would be much accurate. But it must be noted that, the more the sample Stations are, the more the study will be hard and complicated to conduct. Besides working with more sampling stations, more frequent sampling would provide more representative results.

As another recommendation, more parameters might be added to the study, such as dissolved oxygen and pH. This way it would be easier to understand the interactions  $k_e$  with other parameters. The more the number of parameters used, the better the result of the model is. The goodness fit of the model result will be better with various parameters. But

it should be also recorded that higher number of parameters might cause complications.

## REFERENCES

- Altınbilek, D., Usul, N., Yazıcıođlu, H., Kutođlu, Y., Merzi, N., Gögüş, M., Doyuran, V. & Günyaktı, A., (1995) "Gölbaşı-Mogan-Eymir gölleri için su kaynaklar ve çevre yönetim planı projesi," Mogan ve Eymir Gölleri 1. Çevre Kurultayı
- Ansari, A.A., Singh Gill, S., Lanza, G.R., Rast, W. (2011) "Eutrophication: Causes, consequences and control", *Springer*, 1<sup>st</sup> edition.XIII, 394 p.
- Antonopoulos, V., Gianniou, S. (2003) "Simulation of water temperature and dissolved oxygen distribution in Lake Vergoritis, Greece", *Ecol. Mod.* 160, 39–53
- Armengol, J., Caputo, L., Comerma, M., Feijoo, C., Garcia, J. C., Marce, R., Navarro, E. and Ordonez, J., (2003) "Sau Reservoir's light climate: relationships between Secchi depth and light extinction coefficient", *Limnetica* 22: 195–210.
- Asaeda, T., Trung, V.K., Manatunge, J., Van Bon, T., (2001) "Modelling macrophyte–nutrient–phytoplankton interactions in shallow eutrophic lakes and the evaluation of environmental impacts", *Ecol. Eng.* 16, 341–357.
- Beklioglu, M., Ince, Ö. & Tüzün I., (2002) "Restoration of eutrophic Lake Eymir, Turkey, by biomanipulation undertaken following a major external nutrient control", I. *Hydrobiologia* 489: 93–10
- Brivio, PA., Giardino, C., Pepe, M., Ghezzi, P., Zilioli, E. (2001) "Detecting chlorophyll, Secchi disk depth and surface temperature in a sub-alpine lake using Landsat imagery", *Sci Total Environ*; 268:19–29

- Brock, T.D. & Brock, M.L. (1969) "Effect of light intensity on photosynthesis by thermal algae adapted to natural and reduced sunlight", *Limnol. Oceanogr.* 14:334–341.
- Camur M.Z, Yazicigil H, Altinbilek D., (1997) "Hydrogeochemical Modeling of Waters in Mogan and Eymir Lakes Special Environmental", *Water Environment Research*, 69(6), 1144-1153.
- Chapra, S .C., (1997) "Surface Water-Quality Modelling", *McGrawHill*, New York, 560-576. 844 p
- Chong, L. (2005) "Modeling deep chlorophyll maxima in oligotrophic lakes", Bachelor's dissertation, The University of Australia
- Christian D., & Sheng Y. P. (2003) "Relative influence of various water quality parameters on light attenuation in Indian River Lagoon", *Estuarine Coastal and Shelf Science*, 57(5–6), 961–971.
- Clark, E. H., Haverkamp J. A., and Chapman W. (1985). "Eroding Soils. The Off-Farm Impacts." *The Conservation Foundation*, Washington D.C., 252 pp.
- Clarke, G. I. (1941) "Observations on the transparency of a S.W. section of the North Atlantic". *J. Mar. Res.* 4: 221-230.
- Cloern, J. E. (1999), "The relative importance of light and nutrient limitation of phytoplankton growth: a simple index of coastal ecosystem sensitivity to nutrient enrichment", *Aquat. Ecol.* 33: 3–16.
- Danilov R., Ekelund N.G.A. (1999) "The efficiency of seven diversity and one similarity indices based on phytoplankton data for assessing the level of eutrophication in lakes in central Sweden", *Sci Total Environ* 234:15–23

- Davies-Colley, R. J. and W. N. Vant, (1988). "Estimation of Optical Properties of Water From Secchi Disk Depths", *Water Resources Bulletin* 24: 1329-1335.
- Davies-Colley, R.J., Smith, D.G. (2001) "Turbidity, suspended sediment, and water clarity: a review" *J. Am. Water Res. Assoc.* 37, 1085–1101
- de Jonge, V. N. (1997) "High remaining productivity in the Dutch Wadden Sea despite decreasing nutrient inputs from riverine sources", *Marine Pollution Bulletin* 34, 427–436.
- Demirci, G., Aslan, M., Elahdab, T., & Aksoy, A. (2005) "Eymir Gölü'ndeki Su Kalitesinin İzlenmesi ve Değerlendirilmesi" *Proceedings of 6th National Environmental Engineering Congress* (pp. 72-76). Istanbul: CMO.
- Devlin, M., Barry J., Foden J., Sivyer D., Mills D., Gowen R. & Tett, P. (2008) "Relationships between suspended particulate material, light attenuation and Secchi depth in UK marine waters", *Estuarine Coastal and Shelf Science* 79: 429–439.
- Diker, Z. (1992) "A Hydrobiological and ecological study in Lake Eymir", MSc thesis, METU, Ankara
- Domingues R. B., Anselmo T. P., Barbosa A. B., Sommer U. & Galvao H. M (2010) "Light as a driver of phytoplankton growth and production in the freshwater tidal zone of a turbid estuary", *Estuarine Coastal and Shelf Science* 91(4) 526-535.
- Effler, S. W., Wodka M. C., and Field S. D., (1984) "Scattering and Adsorption of Light in Onondaga Lake", *Journal of Environmental Engineering, ASCE* 110:1134-1145.

- Elahdab, T. (2006) "Investigation of algae distribution in Eymir Lake using site measurements and remotely sensed data", MSc thesis, METU, Ankara
- Fisher, T. R., Gustafson, A. B., Sellner, K., Lacouture, R., Haas, L. W., Wetzel, R. L., (1999) "Spatial and temporal variation of resource limitation in Chesapeake Bay", *Marine Biology*, 133(4), 763–778.
- Gallegos CL (2001) "Calculating optical water quality targets to restore and protect submersed aquatic vegetation: overcoming problems in partitioning the diffuse attenuation coefficient for photosynthetically active radiation", *Estuaries* 24:381–397
- Geldiay, R., (1949) "Çubuk Barajı ve Emir Gölünün Makro ve Mikro Faunasinin Mukayeseli İncelenmesi", *Ankara Üniversitesi, Fen Fakültesi Mecmuası* 2: 146–252
- Giardino C., Brivio P.A., Zilioli E. (2001) "Validation of satellite data for quality assurance in lake monitoring applications", *Sci Total Environ*;268:3 –13.
- Graham, M.H., (2003) "Confronting multicollinearity in ecological multiple regression". *Ecology* 84: 2809–1
- Gregory, S.V., (1980) "Effects of Light, Nutrients and Grazing on Periphyton Communities in Streams" Ph.D. thesis, Oregon State University, Corvallis, OR
- Grobbelaar, J. U., (2009), "Turbidity", *Encyclopedia of Inland Waters*, 699-704
- Hairston, N. G. & Fussman, G. F., (2002) "Lake Ecosystems", *Encyclopedia of life sciences*, New York; Wiley-Interscience

- Hanaoka, T., Furukawa A. and Nogami K., (1956) "Studies on suspended matter in the sea I On suspension factor and its meaning", *Bull. Jap. Soc. of Scient. Fish.* 22 (4), 213-244
- Hansson L.A., Brönmark C. (2009). "Biomanipulation of aquatic ecosystems", *Encyclopedia of inland waters*, 242-248
- Harrison, P. J., Whitney F. A., Tsuda A., Saito H., and Tadokoro K. (2004), "Nutrient and Plankton Dynamics in the NE and NW Gyres of the Subarctic Pacific Ocean", *J. Oceanogr.*, 60, 93-117.
- Hasegawa H, Rahman MA, Kitahara K. (2010) "Seasonal changes of arsenic speciation in lake waters in relation to eutrophication", *Sci Total Environ* 408(7):1684-1690
- Havens, K. E., Fukushima T., Xie P., Iwakuma T., James R. T., Takamura N., Hanazato T. & Yamamoto T., (2001) "Nutrient dynamics and the eutrophication of shallow lakes Kasumigaura (Japan), Donghu (PR China), and Okeechobee (USA)", *Environmental Pollution* 111: 263–272
- Hein, L., (2006) "Cost-efficient eutrophication control in a shallow lake ecosystem subject to two steady states" *Ecological Economics* 59, 429–439.
- Hoyer, M.V., Jones, J.R. (1983) "Factors affecting the relation between phosphorus and chlorophyll a in midwestern reservoirs", *Canadian Journal of Fisheries and Aquatic Sciences* 40, 192-199.
- Jamu, D.M., Lu, Z., Piedrahita, R.H., (1999) "Relationship between Secchi disk visibility and chlorophyll a in aquaculture ponds", *Aquaculture* 170, 205 – 214
- Jaun, L., Finger D., Zeh M., Schurter M. and West A., (2007) "Effects of upstream hydropower operation and oligotrophication on the light

regime of a turbid peri-alpine lake”, *Aquat. Sci.* 69: doi 10.1007/s00027-007-0876-3.

Jeppesen, E., Jensen, P., Sondegaard, M., Lauridsen, T., Landkildehus, F. (2000) “Trophic structure, species richness and biodiversity in Danish lakes: changes along a phosphorus gradient”, *Freshwater Biology* 45, 201–218

Johnstone, I. M. & Robinson P. W. (1987), “Light level variation in Lake Tutira after transient sediment inflow and its effect of the submersed macrophytes”, *New Zealand Journal of Marine Freshwater Research* 21: 47–53.

Karakoc, G., Erkoc, F. U. and Katircoglu, H. (2003) “Water quality and impacts of pollution sources for Eymir and Mogan Lakes (Turkey)”, *Environ. Int.* 29(1), 21–27

Karlsson J, Byström P, Ask J, Ask P, Persson L, Jansson M (2009) “Light limitation of nutrient-poor lake ecosystems”, *Nature*, 460, 506–509.

Karul C. & Soyupak S., (2003) “A comparison between neural network based and multiple regression models for chlorophyll-a estimation Ecological Informatics. Understanding Ecology by Biologically-Inspired Computation”, *Springer*, New York

Karul, C., Soyupak, S., Cilesiz, A. F., Akaby, N., Germen, E. (2000) “Case studies on the use of neural networks in eutrophication modeling”, *Ecological Modelling* 134, 145 –152.

Kirk, J. T. O., (1994) “Light and Photosynthesis in Aquatic Eco systems. (Second Edition)”, *Cambridge University Press*, New York, 509

Kitsiou, D., & Karydis, M. (2011). “Coastal marine eutrophication assessment: A review on data analysis”, *Environment International*, 37, 778–801



- Kudoh, S., Robineau, B., Suzuki, Y., Fujiyoshi, Y. and Takahashi, M. (1997) "Photosynthetic acclimation and estimation of temperate ice algal primary production in Saroma-Ko Lagoon, Japan", *J. Mar. Syst.*, 11, 93-109
- Lau, S. S. S. & Lane S. N. (2002) "Biological and chemical factors influencing shallow lake eutrophication: A long-term study", *Science of the Total Environment* 3: 167-181
- Le Grand, Y. (1939) "La pénétration de la lumière dans la mer", *Annls Inst. Oceanogr.*, Monaco 19: 393-436
- Lee RW, Rust W. (1997) "Light attenuation in a shallow, turbid reservoir, Lake Houston Texas", *US Geological Survey, Water Resources Investigation Report* 97-4064.
- Li Y., Cao W., Su C., Hong H. (2011) "Nutrient sources and composition of recent algal blooms and eutrophication in the northern Jiulong River, Southeast China", *Mar Pollut Bull* 63:5-12
- Lloyd, D. S., J. P. Koenings and J. D. La Perriere, (1987). "Effects of Turbidity in Fresh Waters of Alaska", *North American Journal of Fisheries Management* 7:18-33.
- Loiselle S. A., Cozar A., Dattilo A. D., Bracchini L. and Galvez J. A. (2007) "Light limitations to algal growth in tropical ecosystems", *Freshwater Biol.*, 52, 305–312.
- MacIntyre, H.L. and Cullen, J.J. (1995). "Fine-scale vertical resolution of chlorophyll and photosynthetic parameters in shallow-water benthos", *Mar. Ecol. Prog. Ser.* 122,227-237.
- Megard, R. O. (1972). "Phytoplankton, photosynthesis, and phosphorus in Lake Minnetonka, Minnesota", *Limnol. Oceanogr.* 17: 68-87.

- Nyenje, P.M., Foppen, J.W., Uhlenbrook, S., Kulabako, R. and Muwanga, A. (2010) "Eutrophication and nutrient release in urban areas of sub-Saharan Africa – A review", *Sci. of the Total Env.*, 408(3), 447-455
- Otto, L. (1966), "Light attenuation in the North Sea and the Dutch Wadden Sea in relation to Secchi disk visibility and suspended matter", *Netherlands Journal of Sea Research* 3: 28-51
- Ozaydin V., Sendil U. & Altınbilek D. (2001) "Stable isotope mass balance method to find the water budget of a lake", *Turk. J. Engin. Environ. Sci.* 25, 329–44.
- Ozen, A. (2006) "Role of hydrology, nutrients and fish predation in determining the ecology of a system of shallow lakes", MSc thesis, METU, Ankara
- Ozen, A., Karapınar B., Kucuk I., Jeppesen E. & Beklioglu M. (2010) "Drought-induced changes in nutrient concentrations and retention in two shallow Mediterranean lakes subjected to different degrees of management", *Hydrobiologia* 646: 61–72.
- Pillsbury, R.W., Lowe, R.L., Pan, Y.D., and Greenwood, J.L. (2002) "Changes in the benthic algal community and nutrient limitation in Saginaw Bay, Lake", *Huron, Journal of the North American Benthological Society*, 21(2), 238 – 252.
- Rodhe, W. (1965). Standard correlations between pelagic photosynthesis and light. *Mem. Ist. Ital. Idrobiol.* 18(suppl.): 365-381
- Schanz, F. (1985) "Vertical light attenuation and phytoplankton development in Lake Zurich", *Limnol. Oceanogr.* 30: 299–310.
- Scheffer M., Van Nes E.H. (2007) "Shallow lakes theory revisited: Various alternative regimes driven by climate, nutrients, depth and lake size", *Hydrobiologia* 584:455–466.

- Schindler DW (1978) "Factors regulating phytoplankton production and standing crop in the world's freshwaters", *Limnol Oceanogr* 23:478–486.
- Schwarz, A.-M., Markager, S., (1999) "Light absorption and photosynthesis of a benthic moss community: importance of spectral quality of light and implications of changing light attenuation in the water column", *Fresh. Biol.* 42, 609–623
- Smith, G. (2012) "Essential Statistics, Regression, and Econometrics", Elseiver, Sandiego, CA.
- Smith, VH, Tilman GD, Nekola JC. (1999) "Eutrophication: impacts of excess nutrient inputs on freshwater, marine, and terrestrial ecosystems", *Environ Pollut* 1999;100:179–96.
- Smith, D. G., G. F. Croker and K. McFarlane, (1995a) "Human Perception of Water Appearance. 1. Clarity and Colour for Bathing and Aesthetics", *New Zealand Journal of Marine and Freshwater Research* 29:29-43
- Sorokin, C. & Krauss. R. W. (1958) "The effect of light intensity on the growth rates of green algae", *Plant Physiology*, 33:109-113
- Tan C, and Beklioglu M. (2005). Catastrophic-like shifts in shallow Turkish lakes: a modeling approach. *Ecological Modeling*, 183(4), 425-434.
- Tan, C. O. (2002) "The roles of hydrology and nutrients in alternative equilibria of two shallow lakes of Anatolia, lake Eymir and lake Mogan: Using monitoring and modeling approaches", MSc thesis, METU, Ankara.
- Tessier, A. (1992) "Sorption of Trace Elements on Natural Particles in Oxic Environments; In Environmental Particles", *Lewis Publishers*, Boca Raton, Florida, pp. 425-453.

- Tibby, R. B. and Barnard J. L., (1963) "Some physical and biological characteristics of open coastal waters and their relationship to waste discharge", *Air and Water Pollution*, 7 (8), 865-888.
- Tilzer M. M. (1983) "The importance of fractional light absorption by photosynthetic pigments for phytoplankton productivity in Lake Constance", *Limnol. Oceanogr.* 28: 833-846
- Underwood G. J. C., Kromkamp J. (1999) "Primary production by phytoplankton and microphytobenthos in estuaries", *Adv Ecol Res* 29:93–154
- Van Vierssen, W., Hootsmans, M.J.M., Vermaat, J. (1994) "Lake Veluwe, A Macrophyte-dominated System under Eutrophication Stress", *Kluwer Academic Publ.*, Dordrecht, p. 374
- Vitousek, P.M., Mooney, H.A., Lubchenko, J., Melillo, J.M. (1997a) "Human domination of Earth's ecosystems". *Science* 277, 494±499.
- Vogel, J. L. and Beauchamp D. A. (1999) "Effects of Light, Prey Size, and Turbidity on Reaction Distances of Lake Trout (*Salvelinus namaycush*) to Salmonid Prey", *Canadian Journal of Fisheries and Aquatic Sciences* 56:1293-1297.
- Walmsley, R. D., Butty M., Van Der Piepen H., and Grobler D., (1980) "Light Penetration and the Inter-relationships Between Optical Parameters in a Turbid Subtropical Impoundment", *Hydrobiologia* 70:145-157
- Yagbasan O, Yazicigil H. (2009) "Sustainable management of Mogan and Eymir Lakes in Central Turkey", *Env Geol* 56(6):1029–1040
- Yang X., Wu X., Hao H. and He Z. (2008) "Mechanisms and assessment of water eutrophication", *Journal of Zhejiang University. Science. B.* Vol. 9.

Yang H. J., Shen Z. M., Zhu S. H., Wang W. H., (2007) "Vertical and temporal distribution of nitrogen and phosphorus and relationship with their influencing factors in aquatic-terrestrial ecotone: a case study in Taihu Lake, China." *J Environ Sci*,19(6): 689–695.

Yang, R.J., Wang, N., Tho, C.H., Bobineau, J.P., and Wang, B.P., (2001) "Metamodeling Development for Vehicle Frontal Impact Simulation," *ASME Design Engineering Technical Conference*, DETC2001/DAC-21012, Pittsburgh, PA.

Yenilmez F., (2007) "Modeling the water quality in Ulubat Lake", MSc thesis, METU, Ankara

Yenilmez F., Keskin P., Aksoy A. (2010) "Water quality trend analysis in Eymir Lake, Ankara", *Physics and Chemistry of the Earth*, 36(5-6),135-140.

Yuzugullu, O., (2011) "Determination of chlorophyll-a distribution in Lake Eymir using regression and artificial neural network models with hybrid inputs", MSc thesis, METU, Ankara

URL1: <http://www.eymir.org/eymir-golu-harita-uydu.jpg> Retrieved on Nov 15<sup>th</sup>, 2011.

URL2: <http://www.resmigazete.gov.tr/eskiler /2011/04/20110429-5-1.pdf> Retrieved on Jan 3<sup>rd</sup>, 2012.

URL3: [http://www.golbasitaraf.com/news\\_detail.php?id=2235](http://www.golbasitaraf.com/news_detail.php?id=2235) Retrieved on Sep 15<sup>th</sup>, 2011.

URL4: [http://www.weather-sensors.com/images/li-cor\\_2009s.jpg](http://www.weather-sensors.com/images/li-cor_2009s.jpg) Retrieved on Oct 3<sup>rd</sup>, 2011

URL5: [http://www.hydrolab.com/web/ott\\_hach.nsf/gfx/ Sensor\\_Li-Cor.jpg /\\$file/Sensor\\_Li-Cor.jpg](http://www.hydrolab.com/web/ott_hach.nsf/gfx/ Sensor_Li-Cor.jpg /$file/Sensor_Li-Cor.jpg) Retrieved on Oct 3<sup>rd</sup>, 2011

URL6: [http://www.advancedaquarist.com/2005/7/review\\_album/TitlePhoto.jpg](http://www.advancedaquarist.com/2005/7/review_album/TitlePhoto.jpg) Retrieved on Oct 3<sup>rd</sup>, 2011

URL7: <http://www.Secchidipin.org/images/Secchi%20Disk.jpg> Retrieved on Sept 21<sup>st</sup>, 2011

URL8: [http://www.kc-denmark.dk/public\\_html/11.200\\_-\\_11.300\\_Van\\_Dorn\\_-\\_3\\_og\\_5\\_liter\\_water\\_sampler.jpg](http://www.kc-denmark.dk/public_html/11.200_-_11.300_Van_Dorn_-_3_og_5_liter_water_sampler.jpg) Retrieved on Sept 25<sup>th</sup>, 2011.

URL9: <http://www.iczm.sabah.gov.my/reports/Sandakan%202/mst06.jpg> Retrieved on Oct 4<sup>th</sup>, 2011.

URL10: <http://www.howcast.com/videos/359111-How-To-Normalize-Data>

## APPENDIX

### A-ke CALCULATIONS

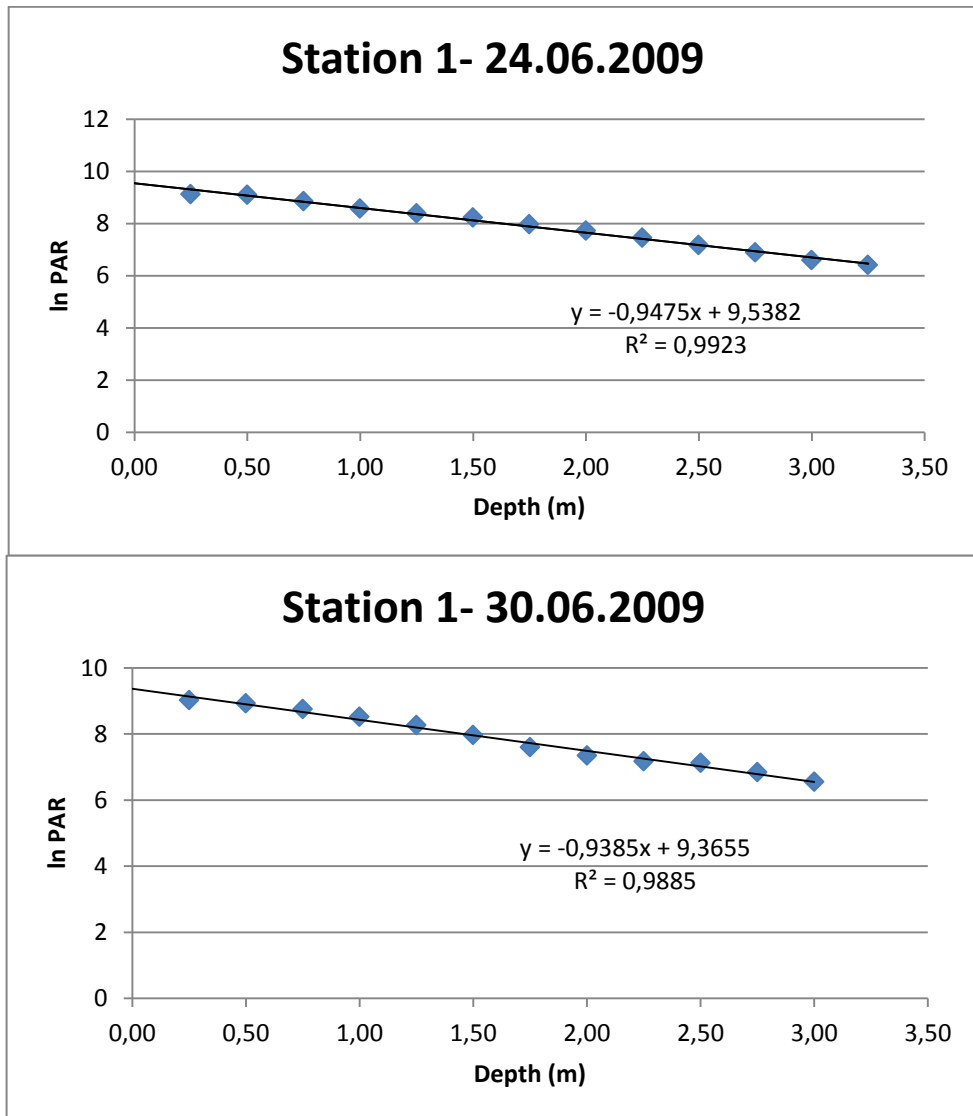


Figure A-1: Station 1 In PAR values versus Depth For June, 2009.

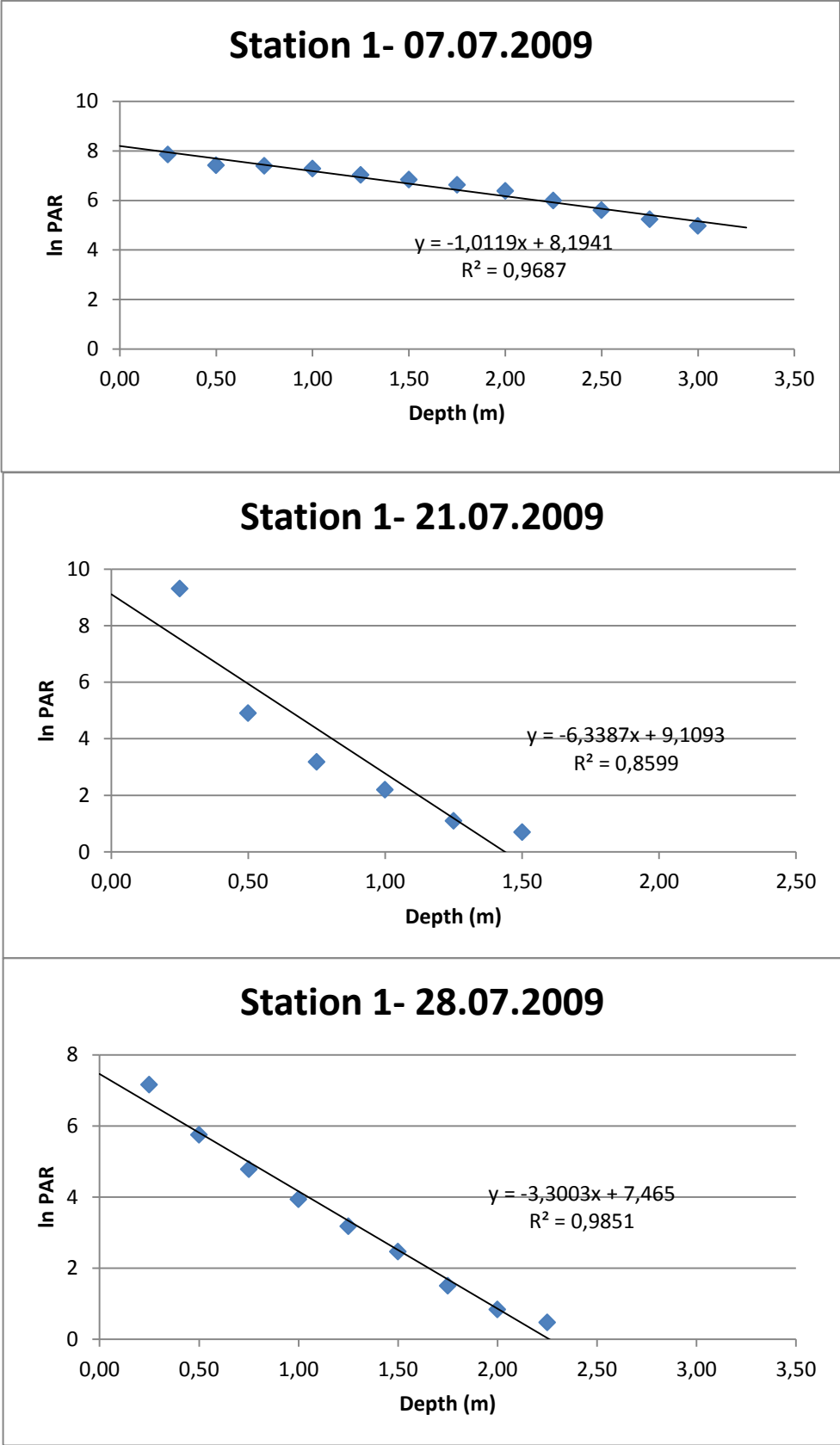


Figure A-2: Station 1 In PAR values versus Depth, For July, 2009.



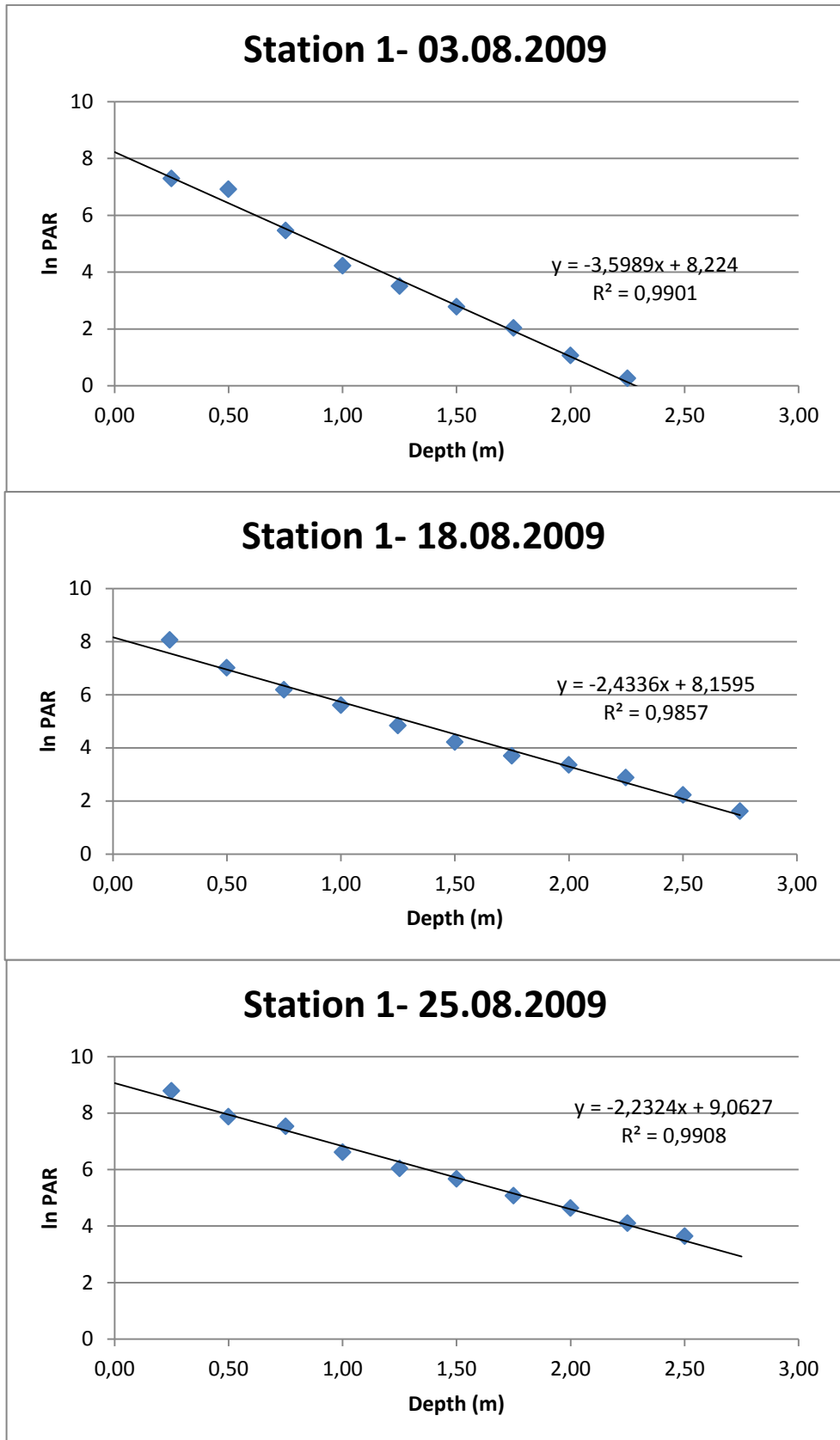


Figure A-3: Station 1 In PAR values versus Depth, For August, 2009.

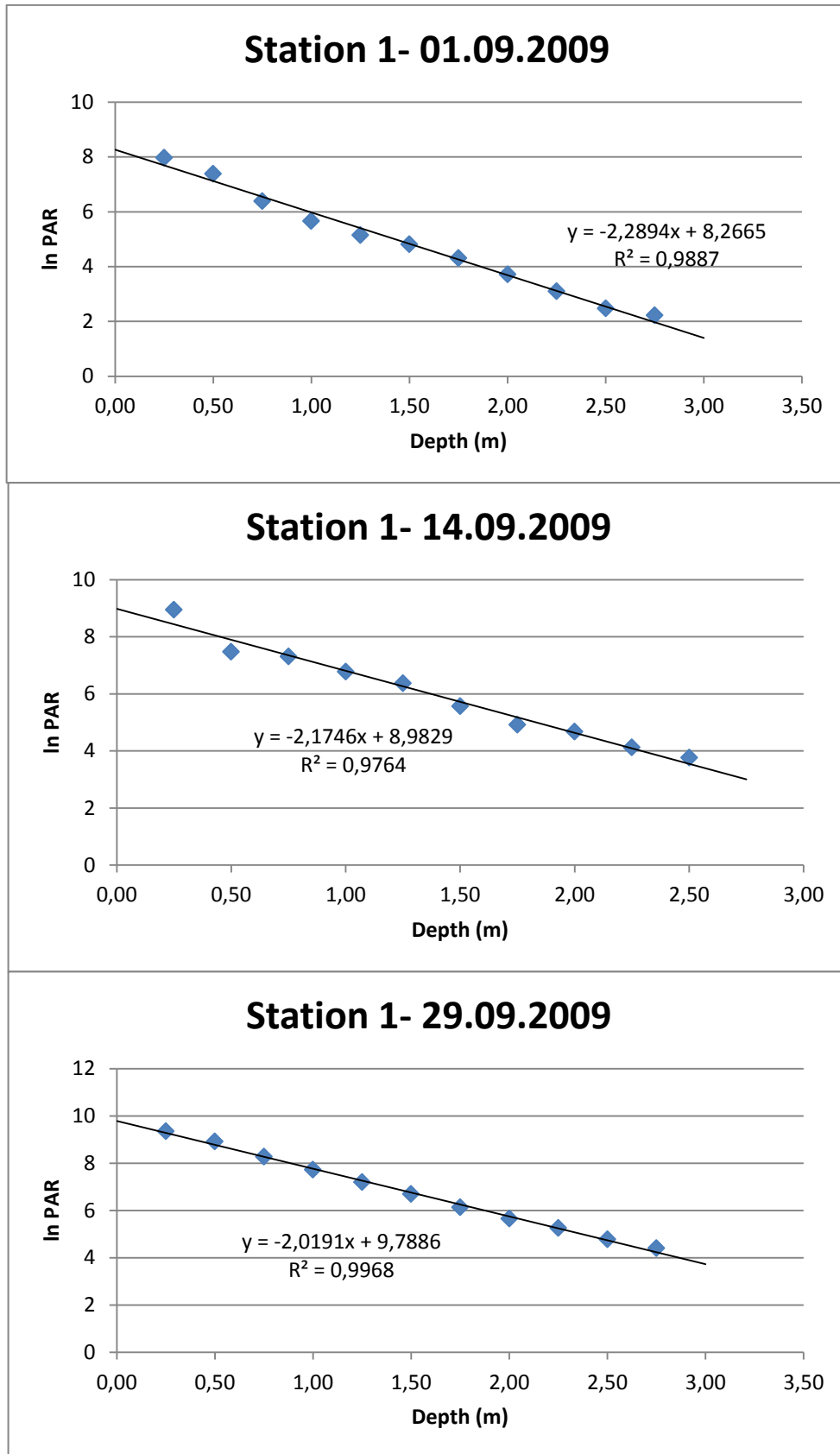


Figure A-4: Station 1 In PAR values versus Depth, For September, 2009.

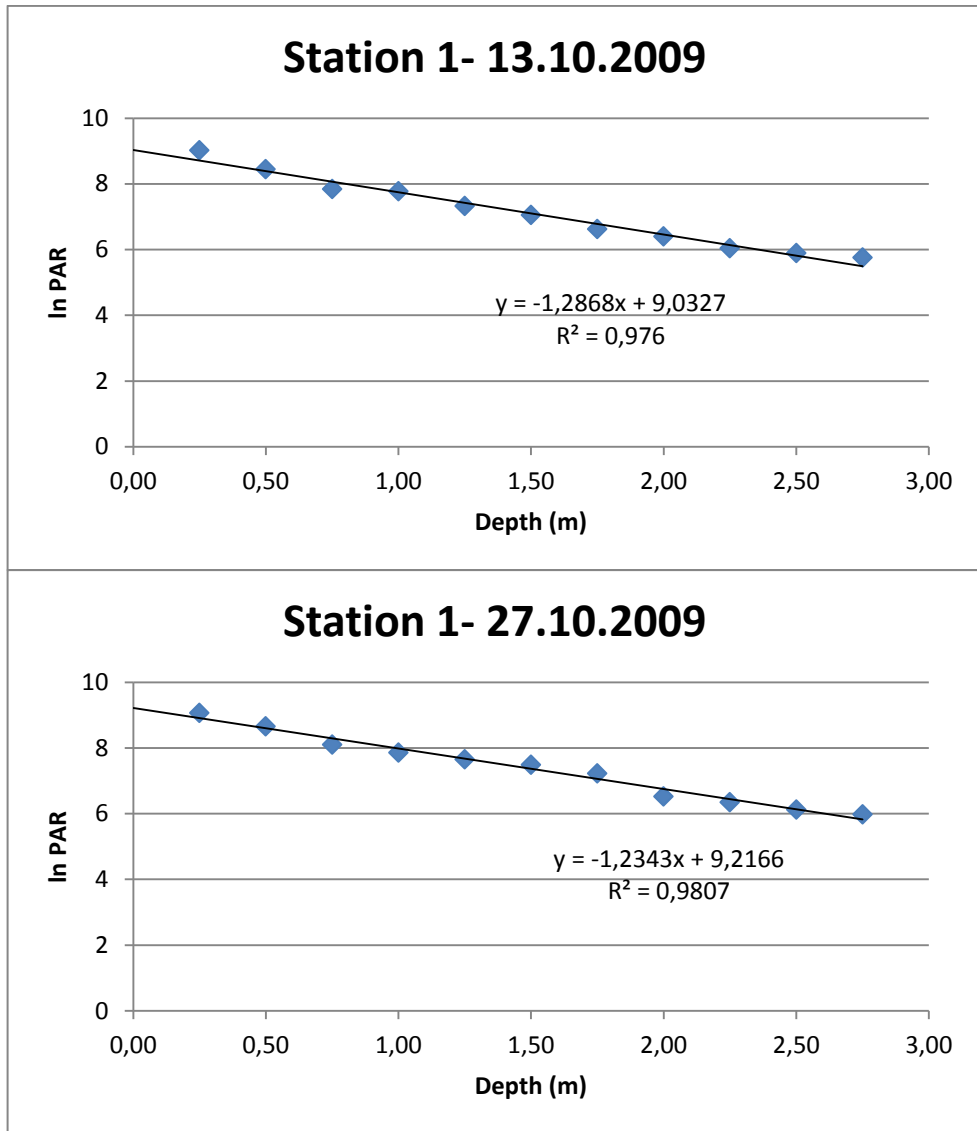


Figure A-5: Station 1 In PAR values versus Depth, For October, 2009.

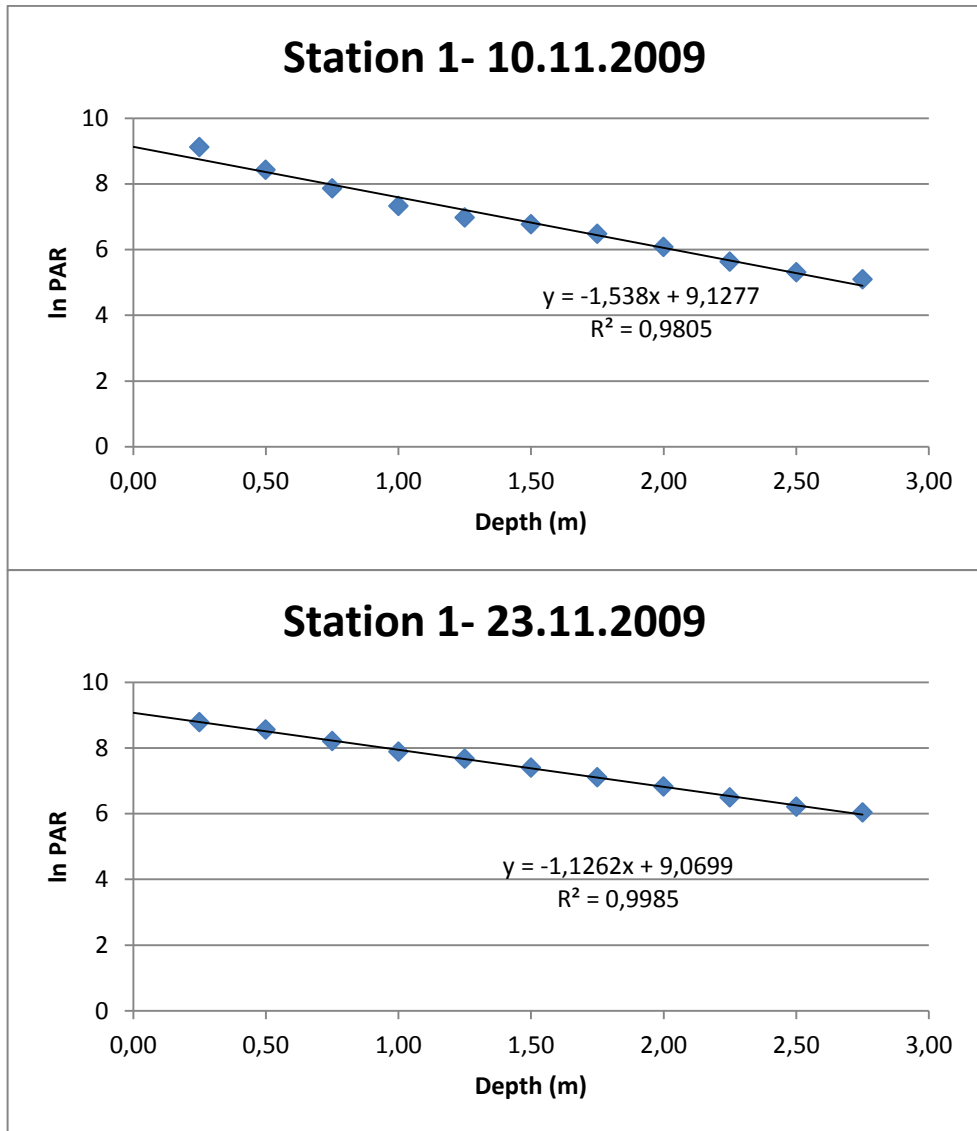


Figure A-6: Station 1 In PAR values versus Depth, For November, 2009.

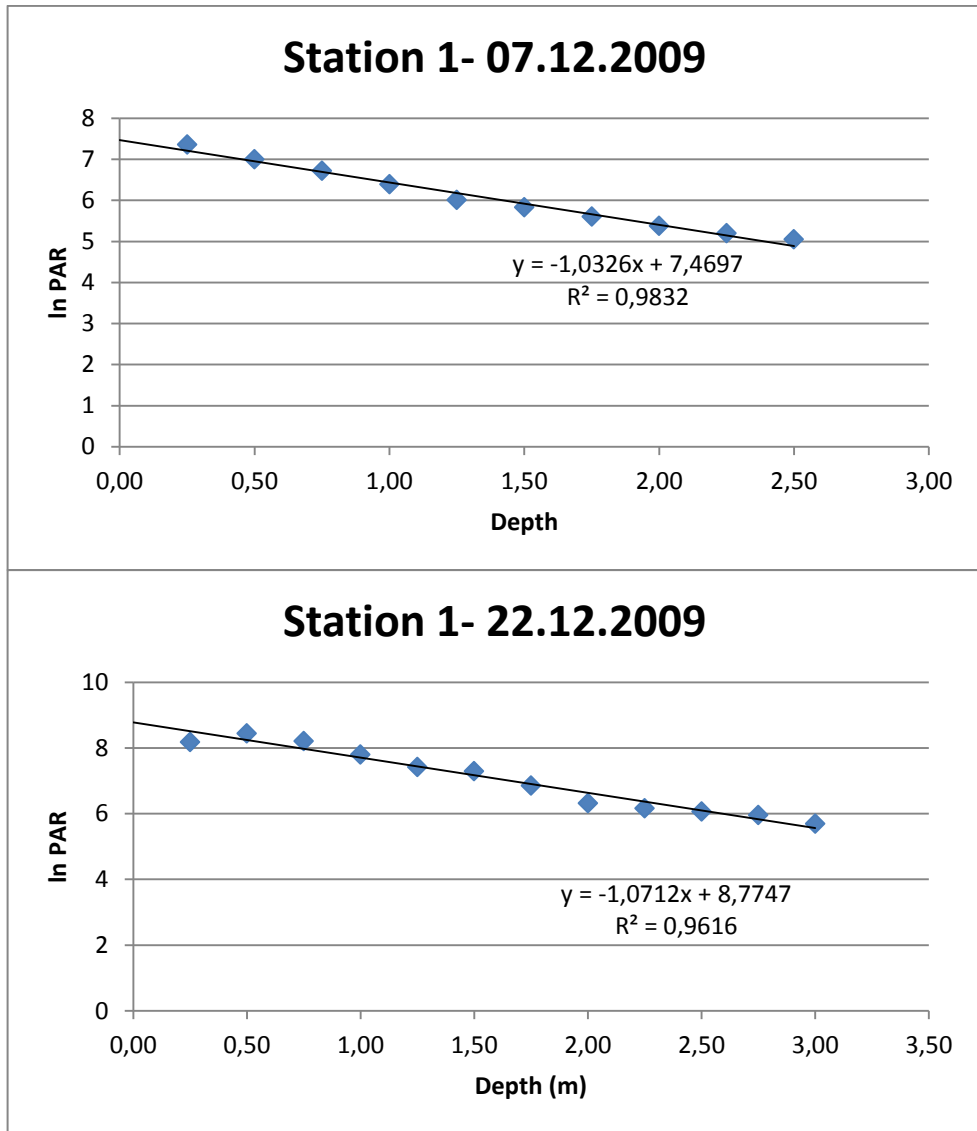


Figure A-7: Station 1 In PAR values versus Depth, For December, 2009.

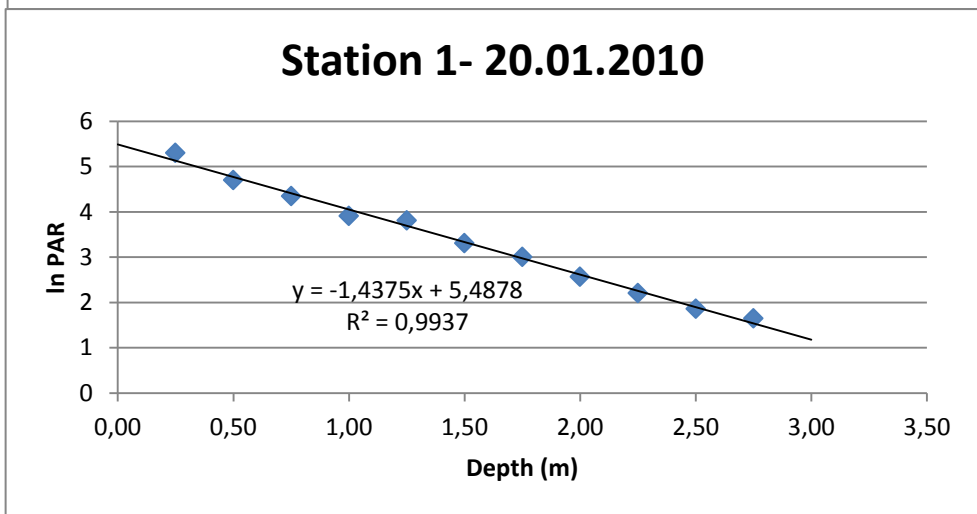
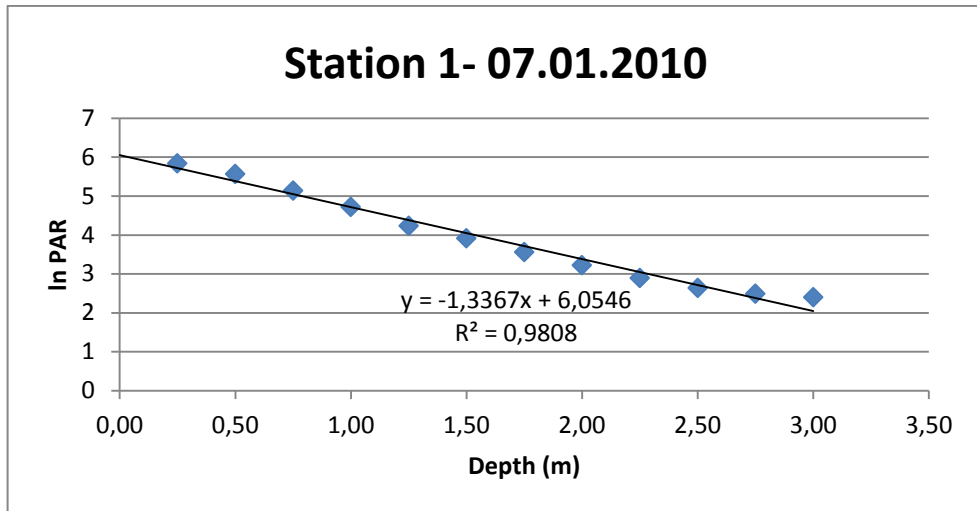


Figure A-8: Station 1 In PAR values versus Depth, For January, 2010

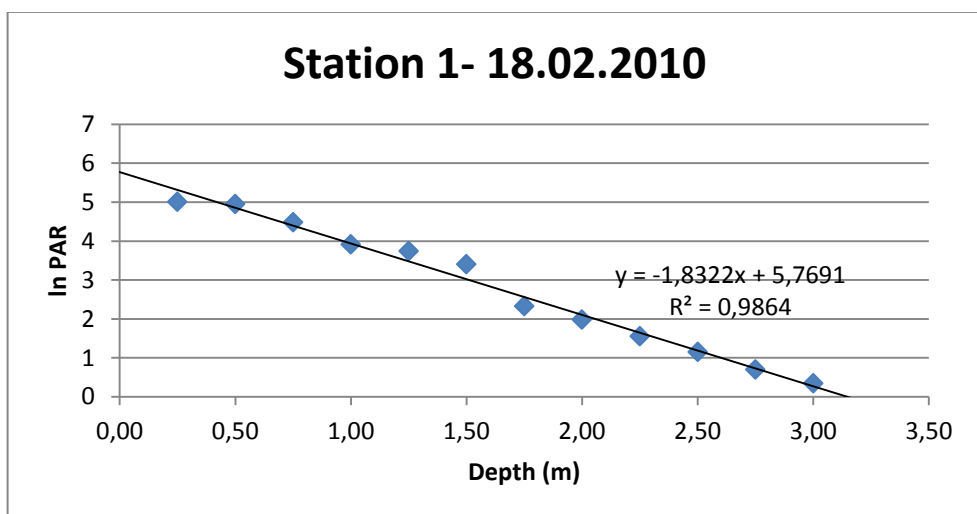


Figure A-9: Station 1 In PAR values versus Depth, For February, 2010

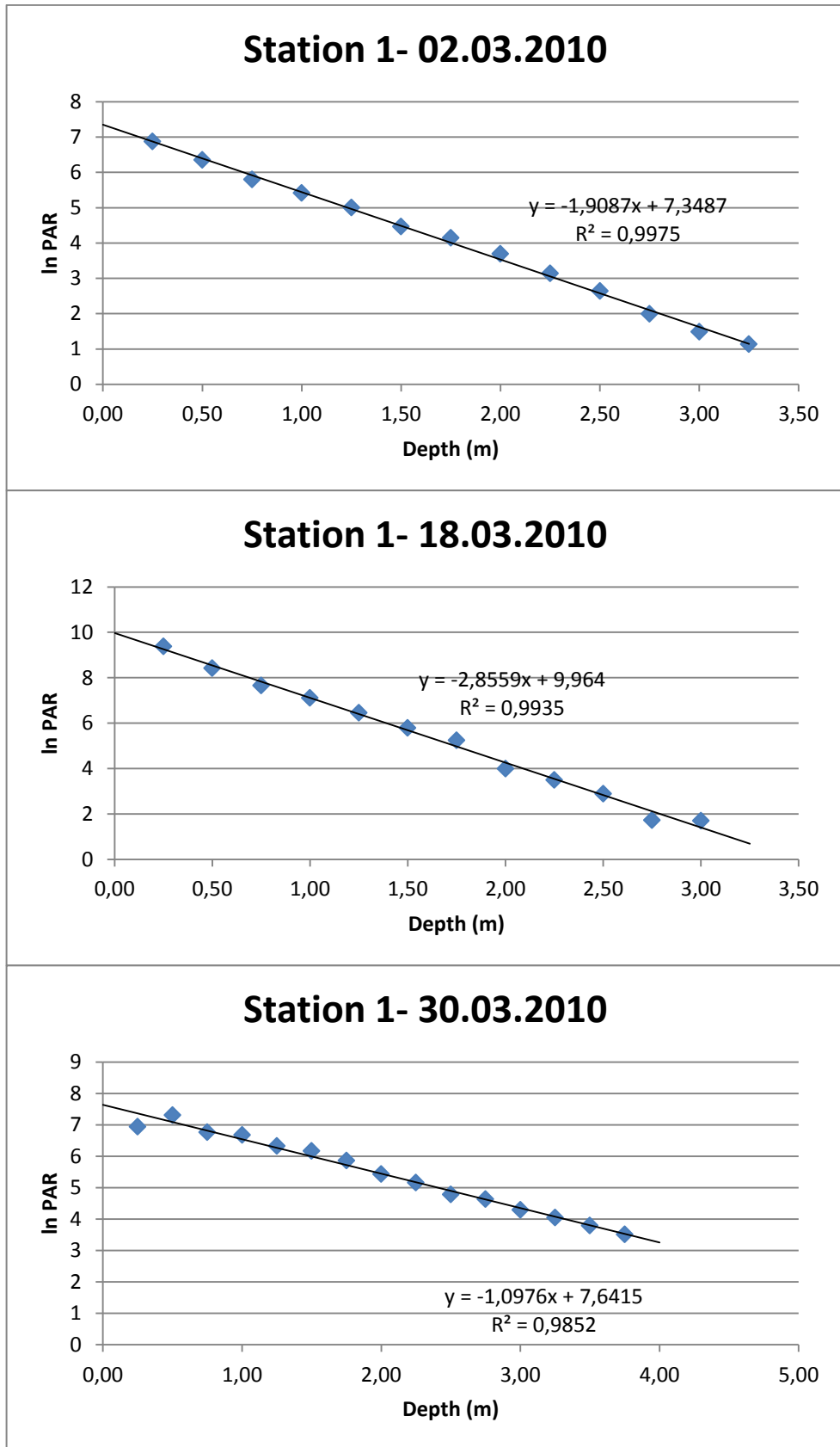


Figure A-10: Station 1 In PAR values versus Depth, For March, 2010

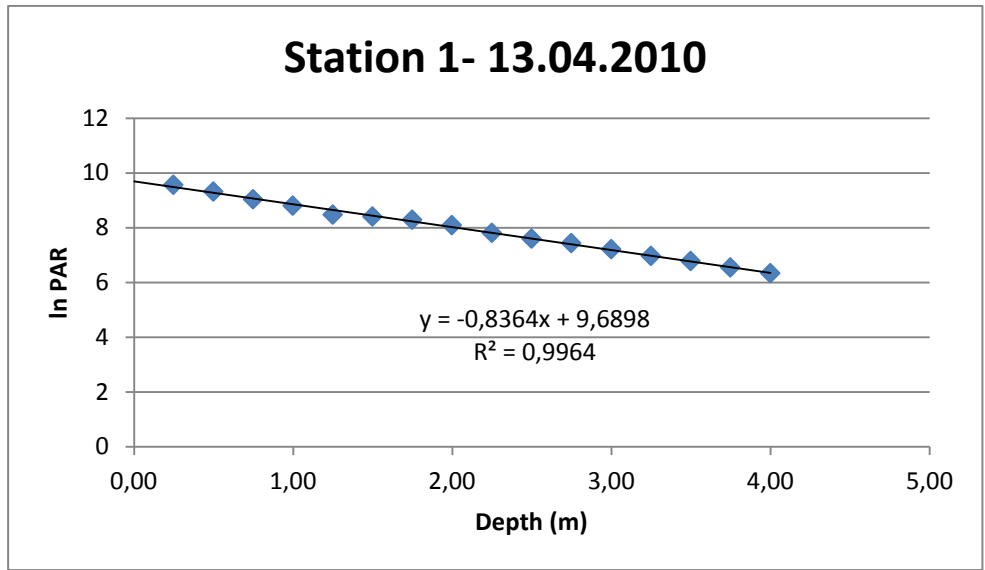


Figure A-11: Station 1 ln PAR values versus Depth, For April, 2010



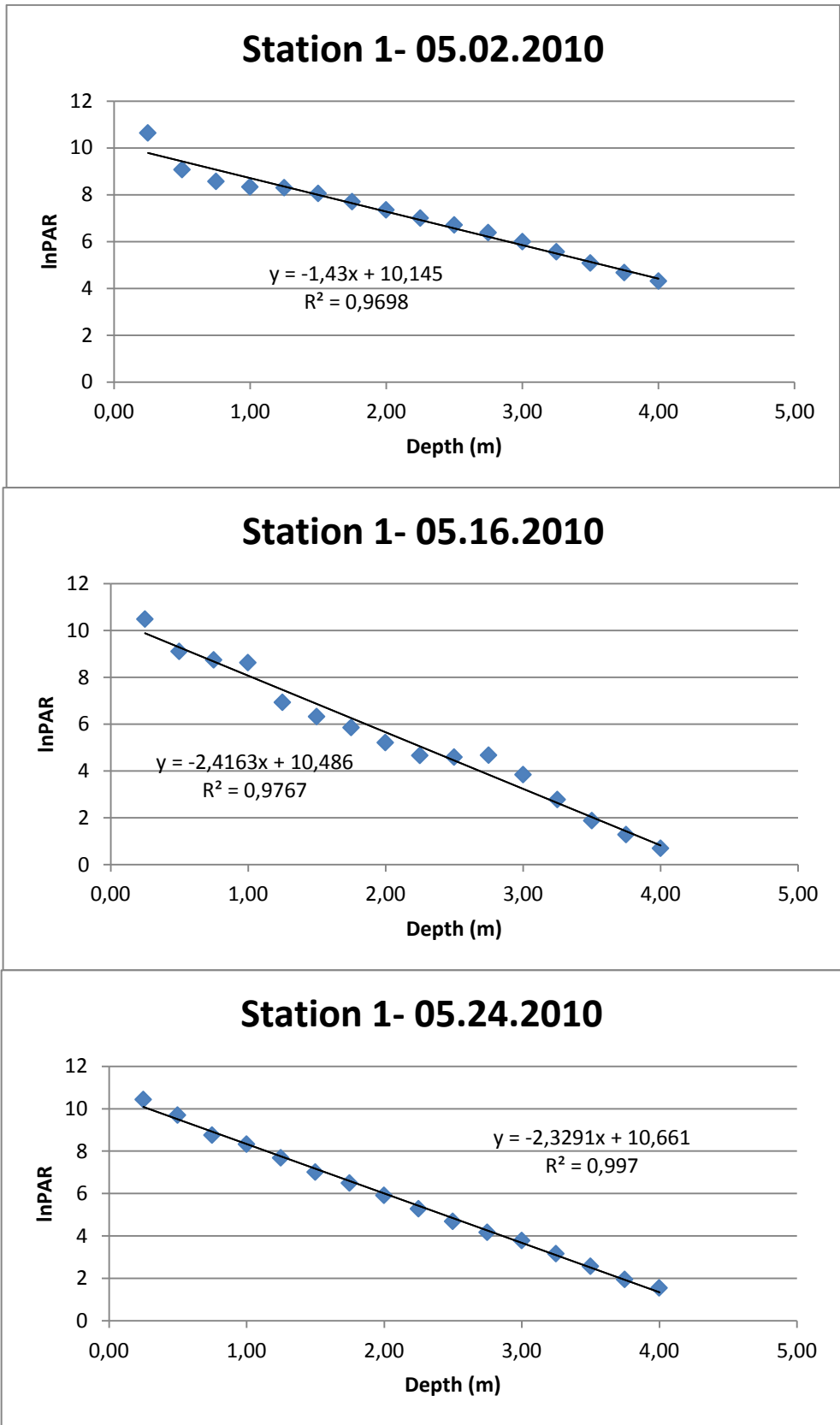


Figure A-12: Station 1 In PAR values versus Depth, For May, 2010

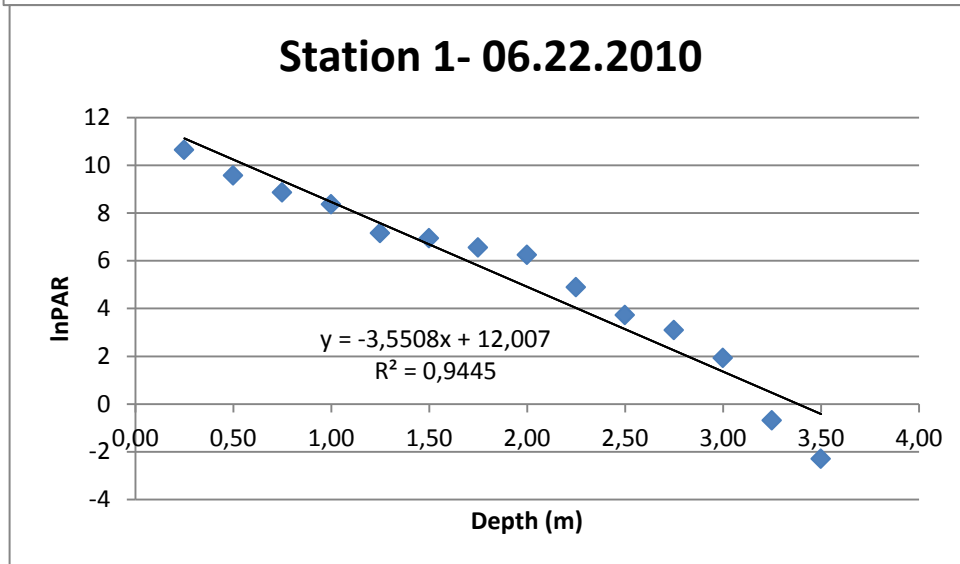
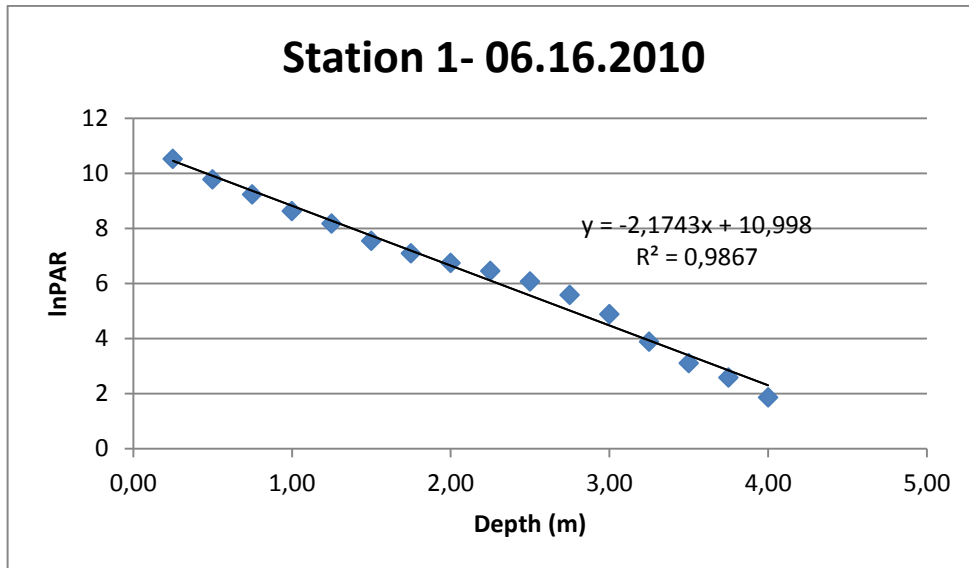


Figure A-13: Station 1 In PAR values versus Depth, For June, 2010

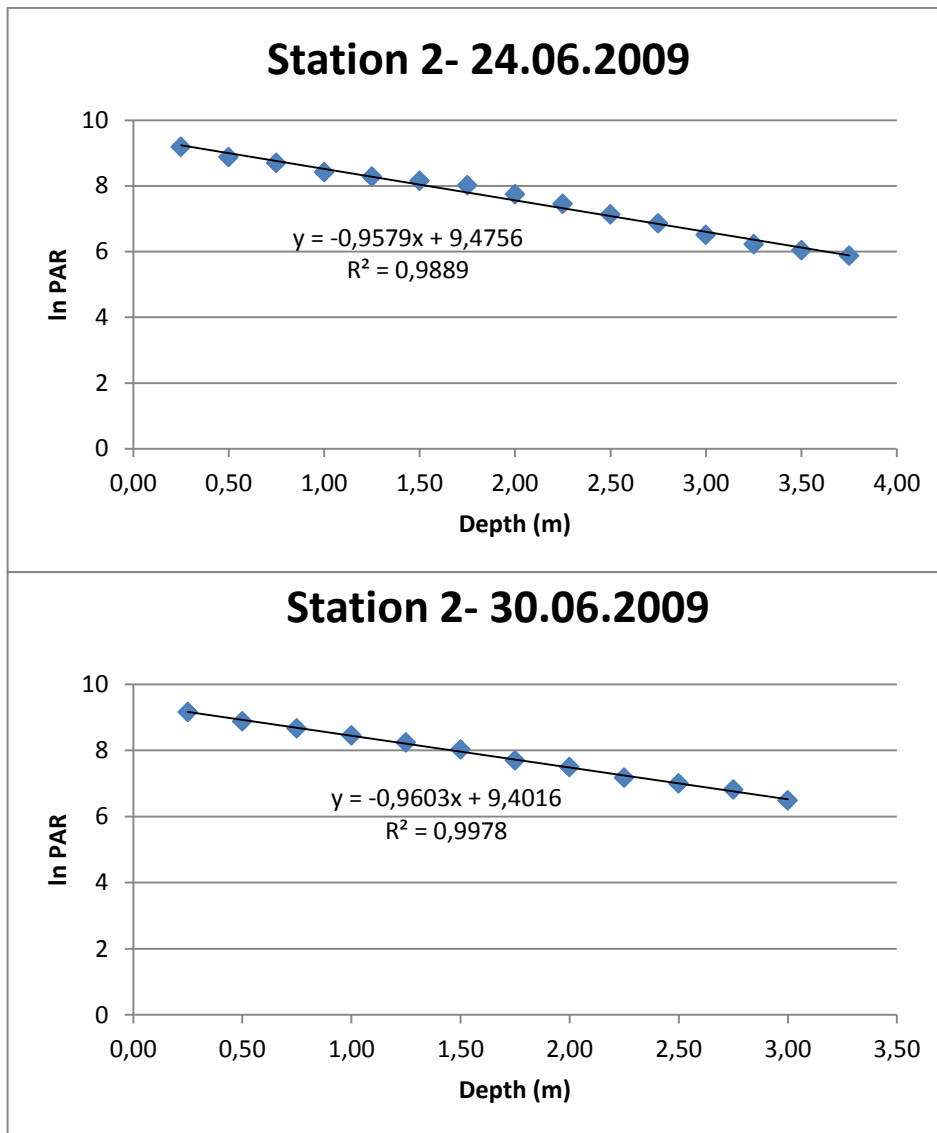


Figure A-14: Station 2 In PAR values versus Depth, For June, 2009

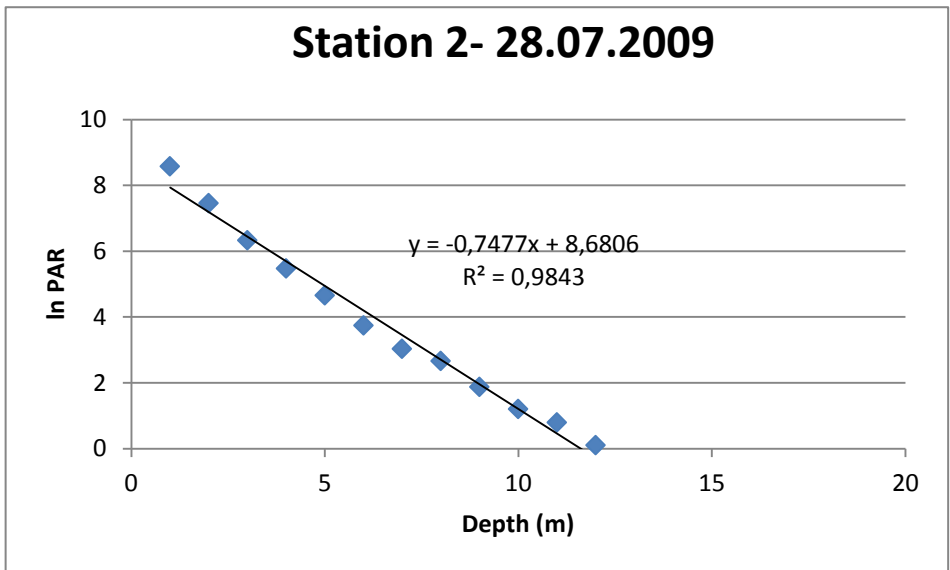
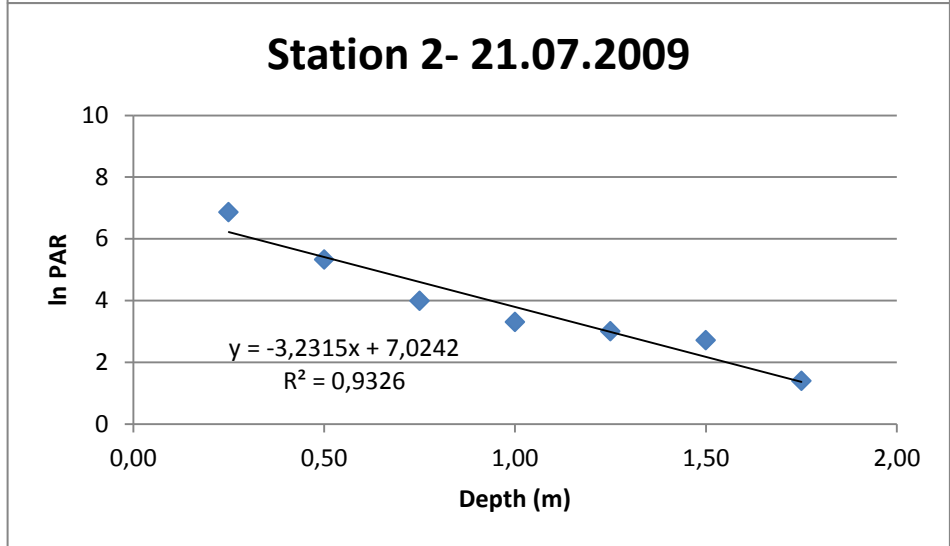
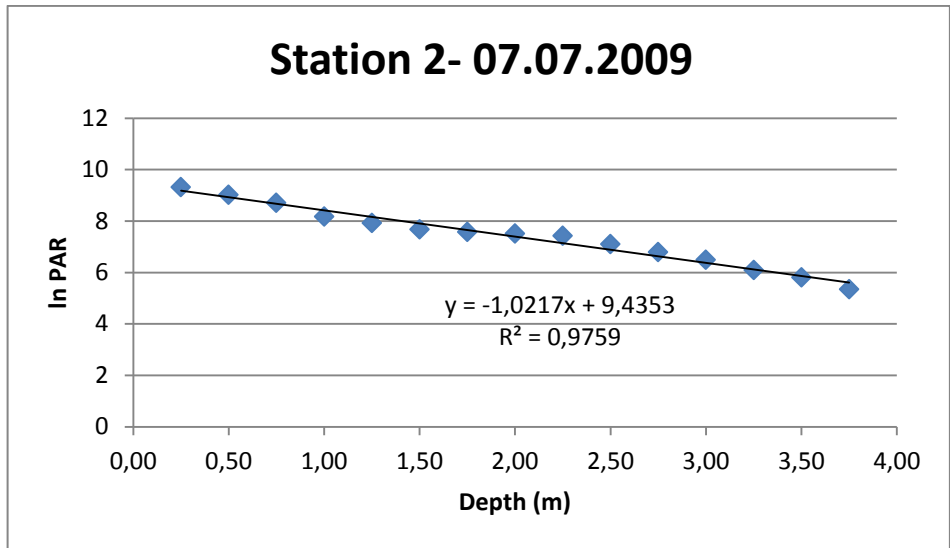


Figure A-15: Station 2 In PAR values versus Depth, For July, 2009

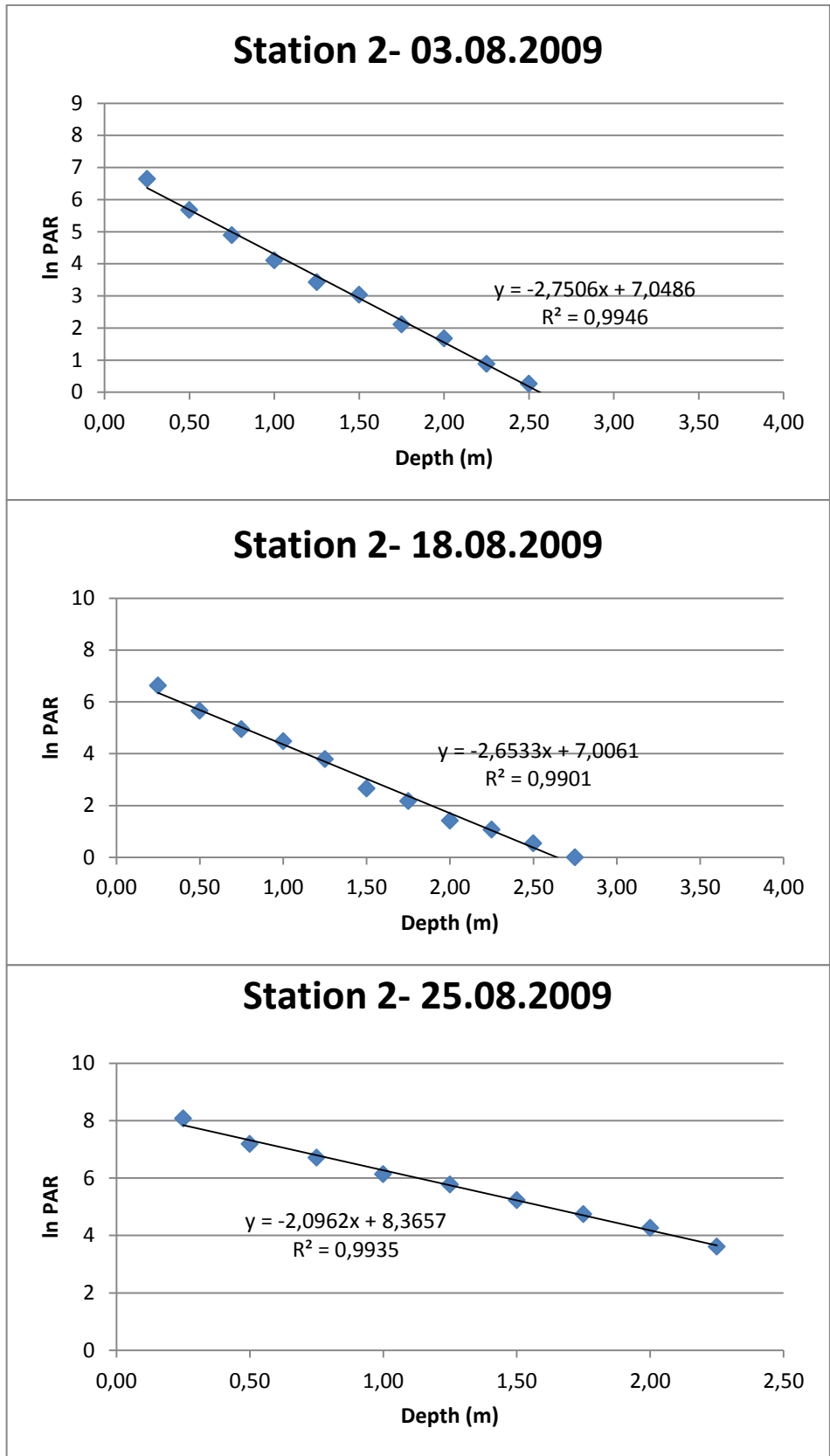


Figure A-16: Station 2 In PAR values versus Depth, For August, 2009

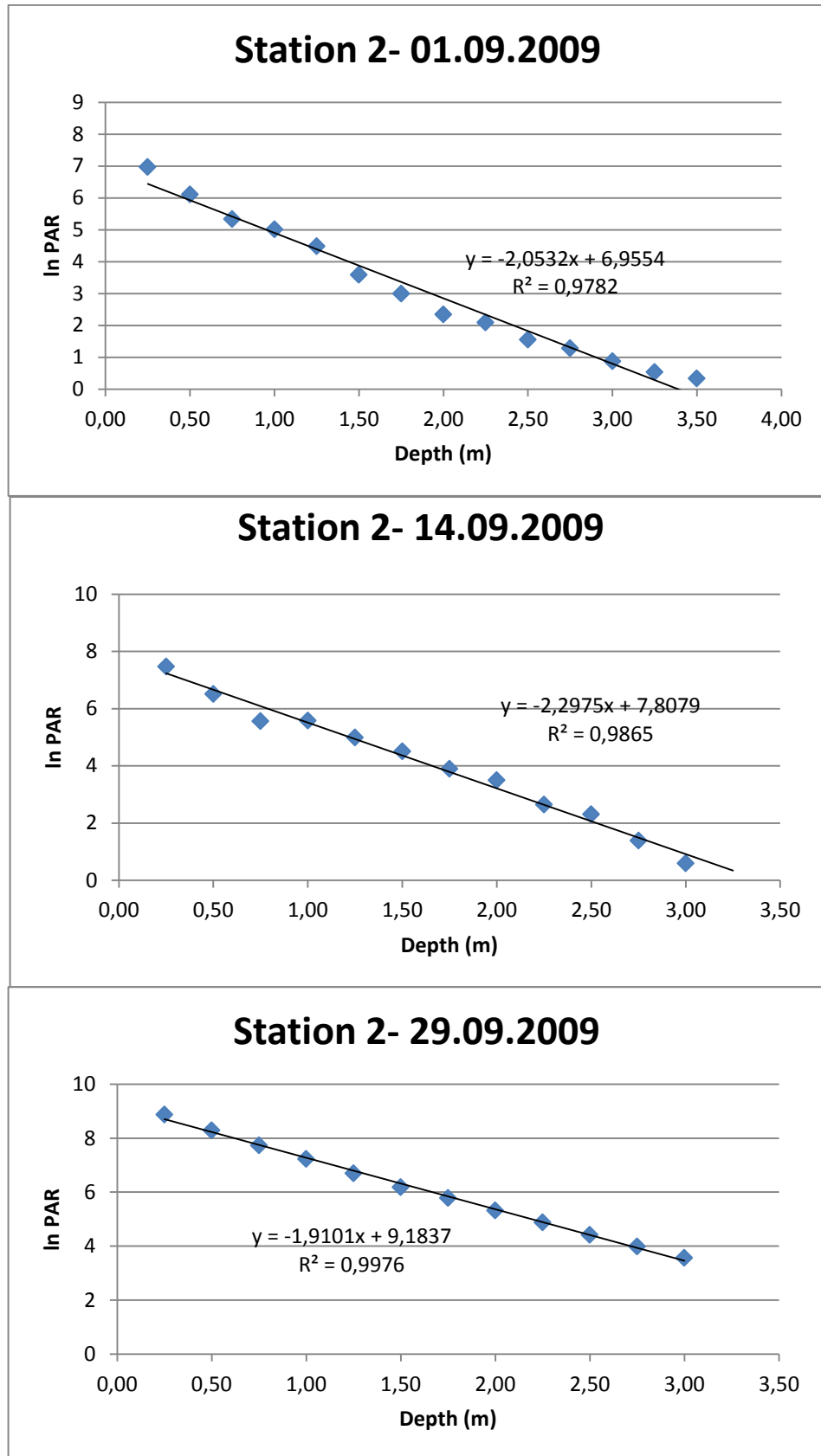


Figure A-17: Station 2 In PAR values versus Depth, For September, 2009

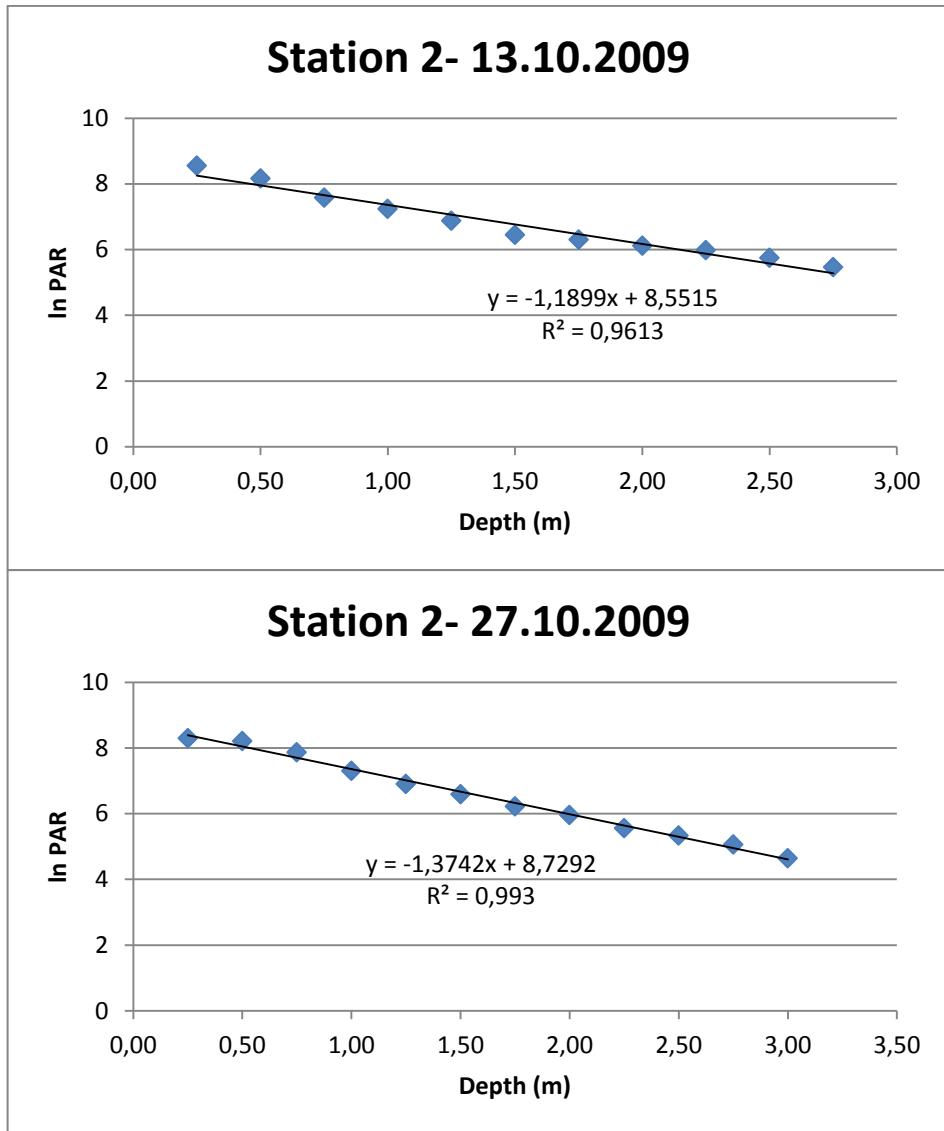


Figure A-18: Station 2 In PAR values versus Depth, For October, 2009

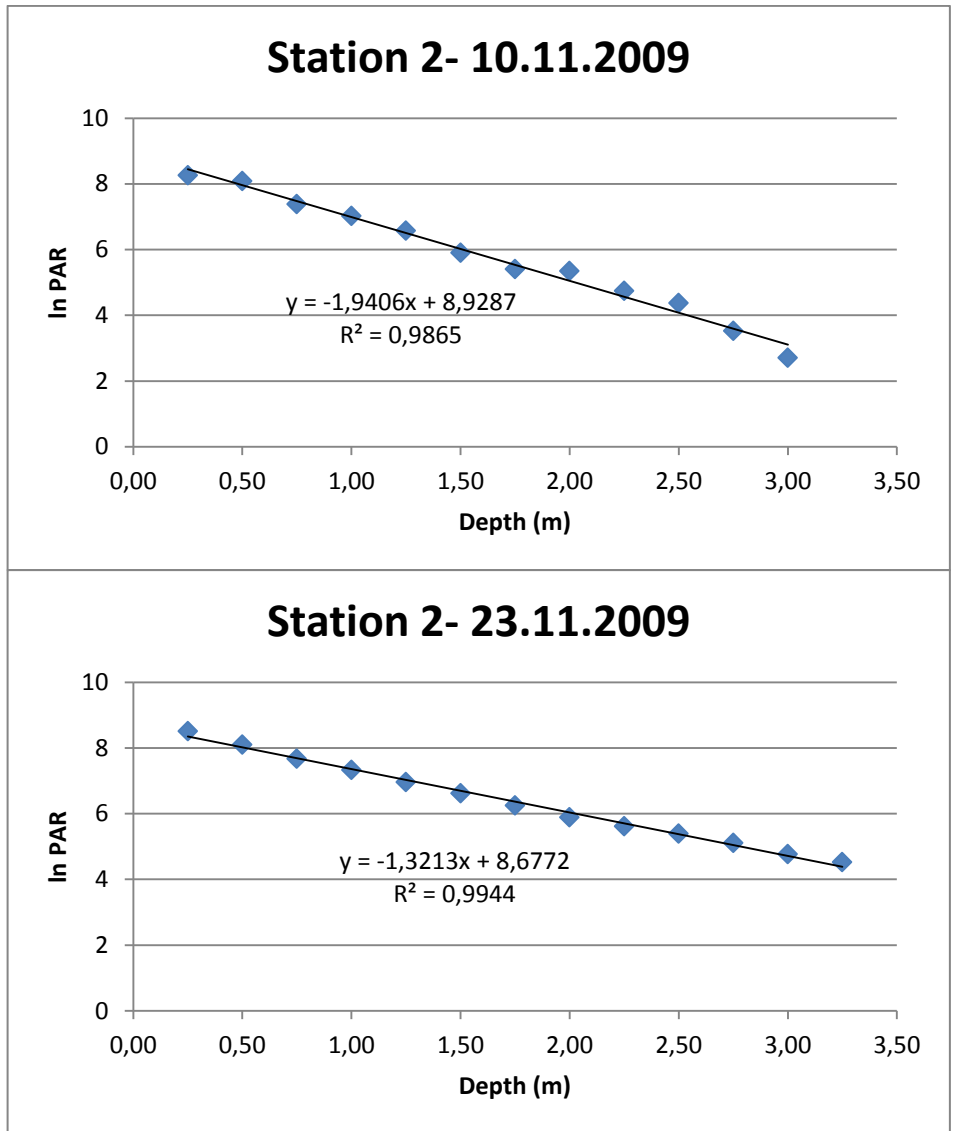


Figure A-19: Station 2 In PAR values versus Depth, For November, 2009



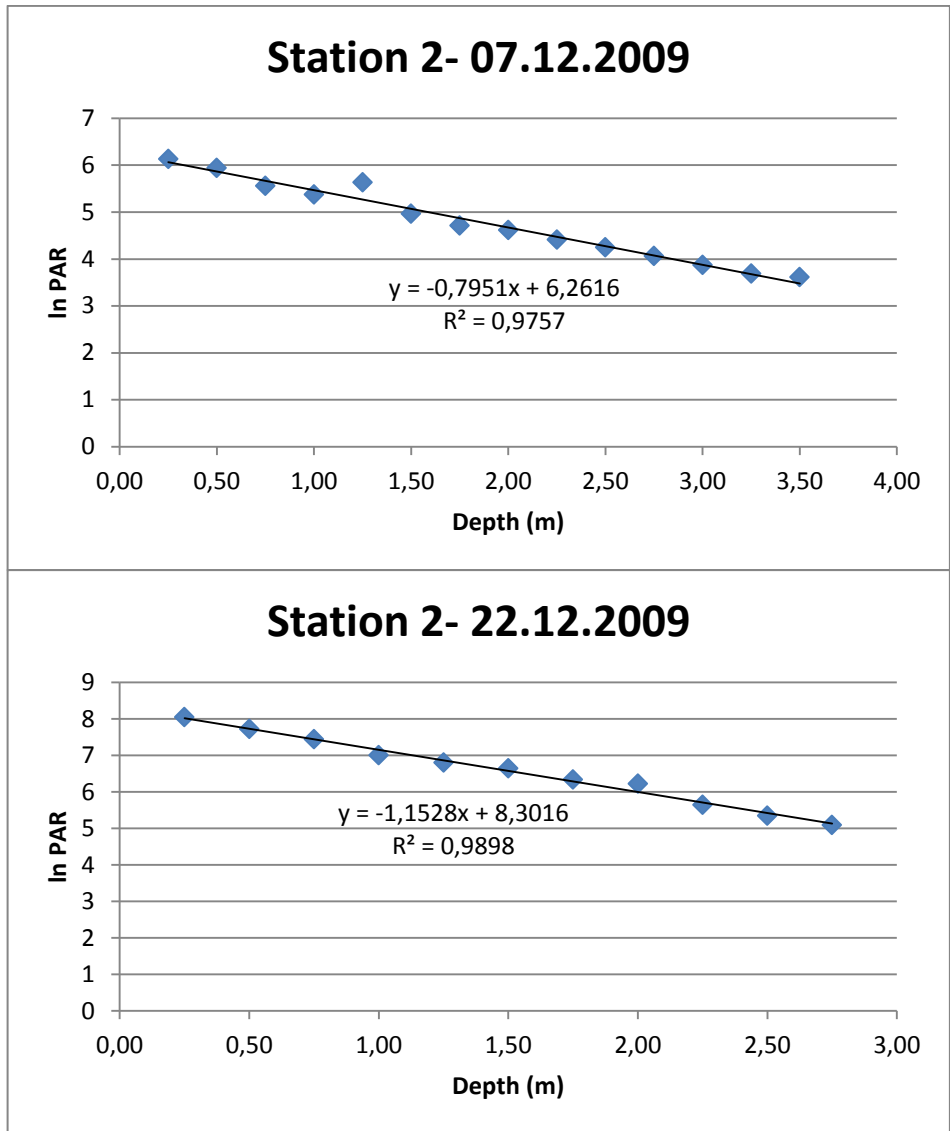


Figure A-20: Station 2 In PAR values versus Depth, For December, 2009

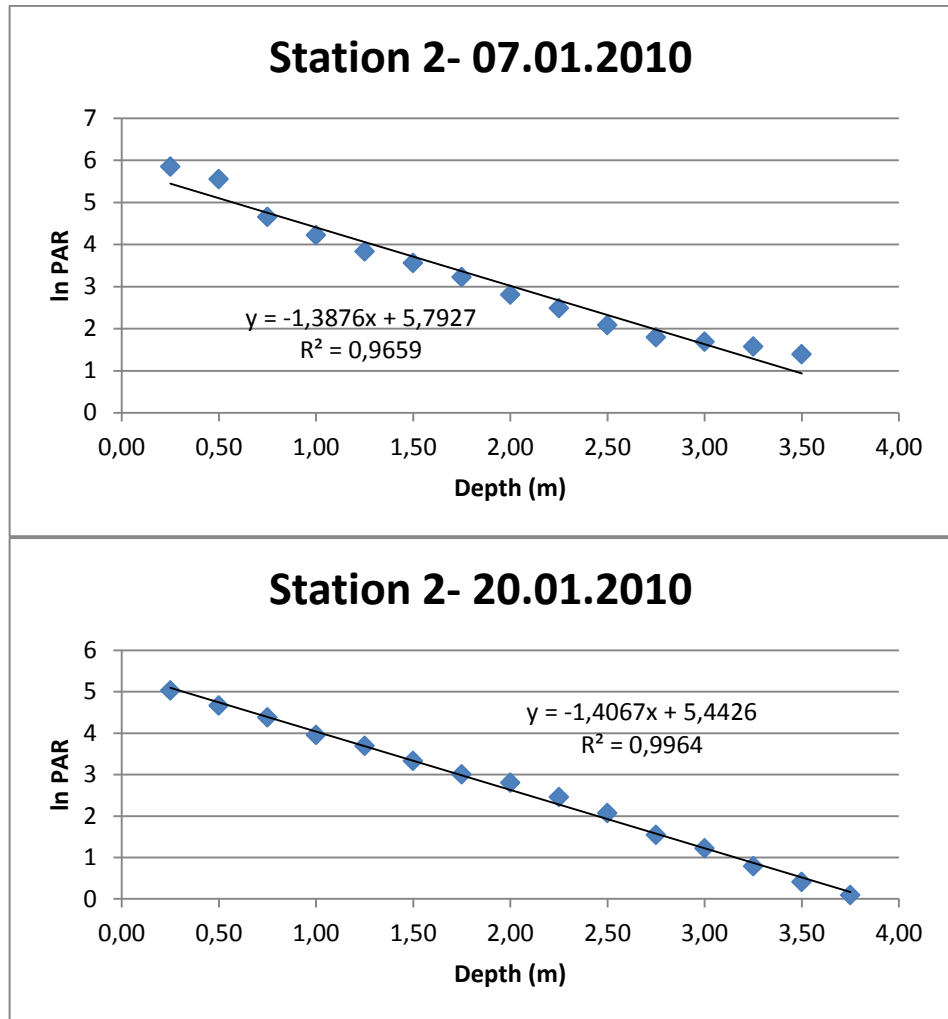


Figure A-21: Station 2 In PAR values versus Depth, For January, 2010

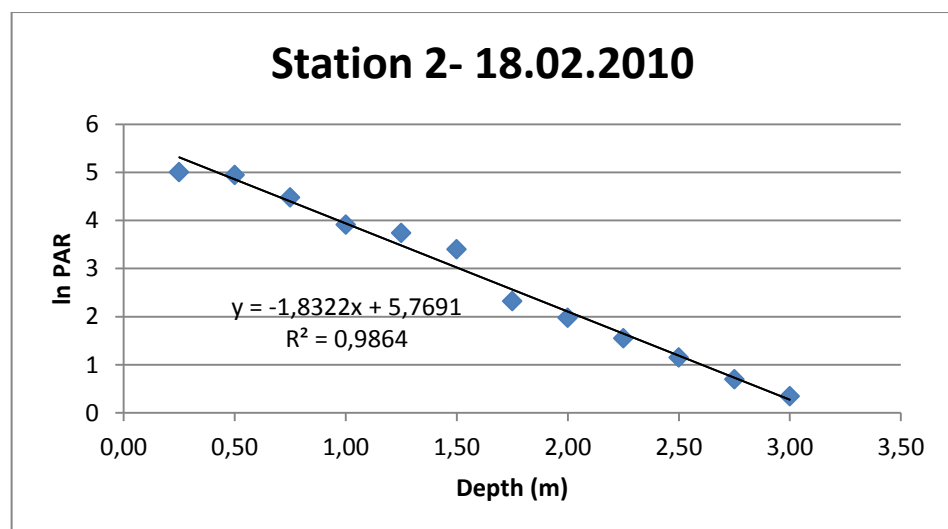


Figure A-22: Station 2 In PAR values versus Depth, For February, 2010

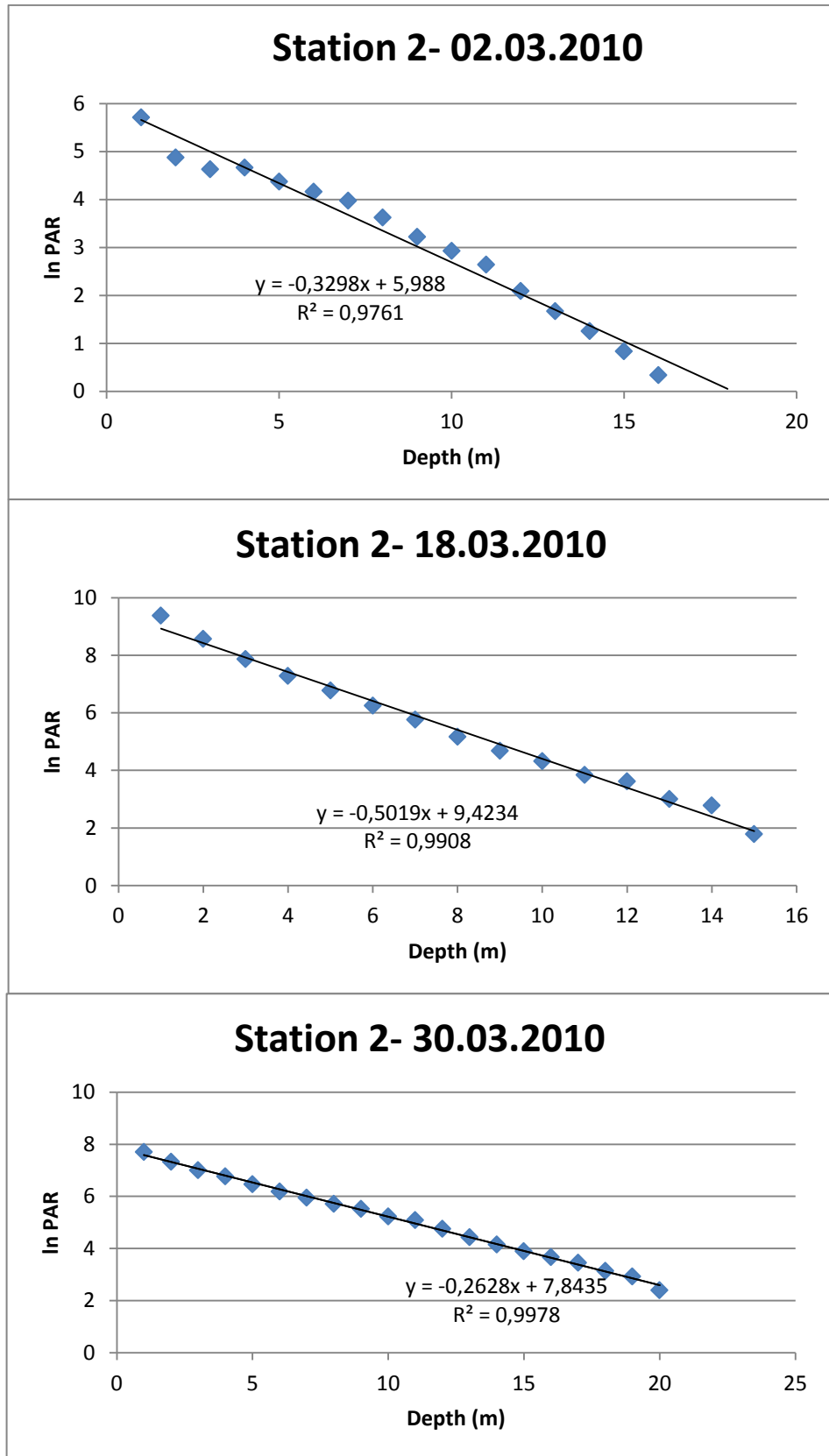


Figure A-23: Station 2 In PAR values versus Depth, For March, 2010

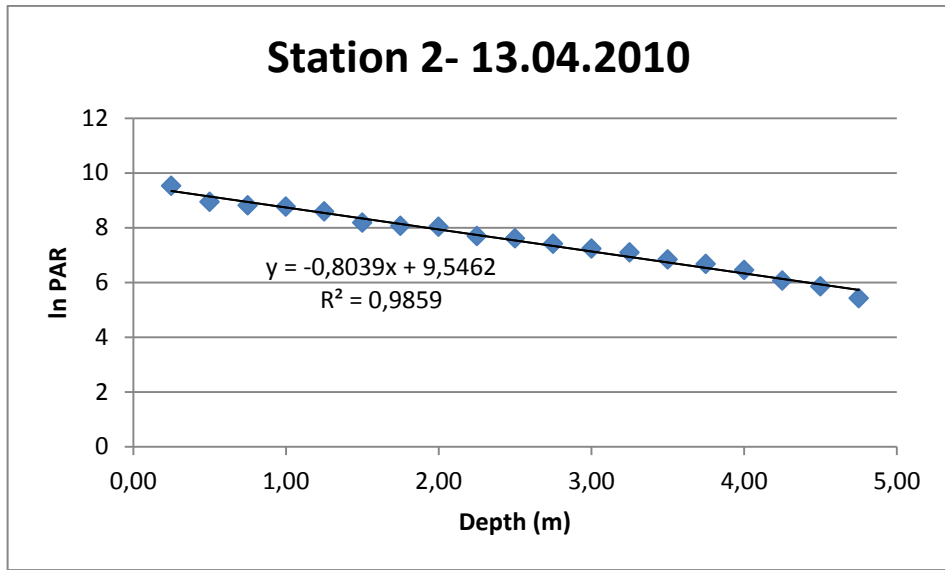


Figure A-24: Station 2 ln PAR values versus Depth, For April, 2010

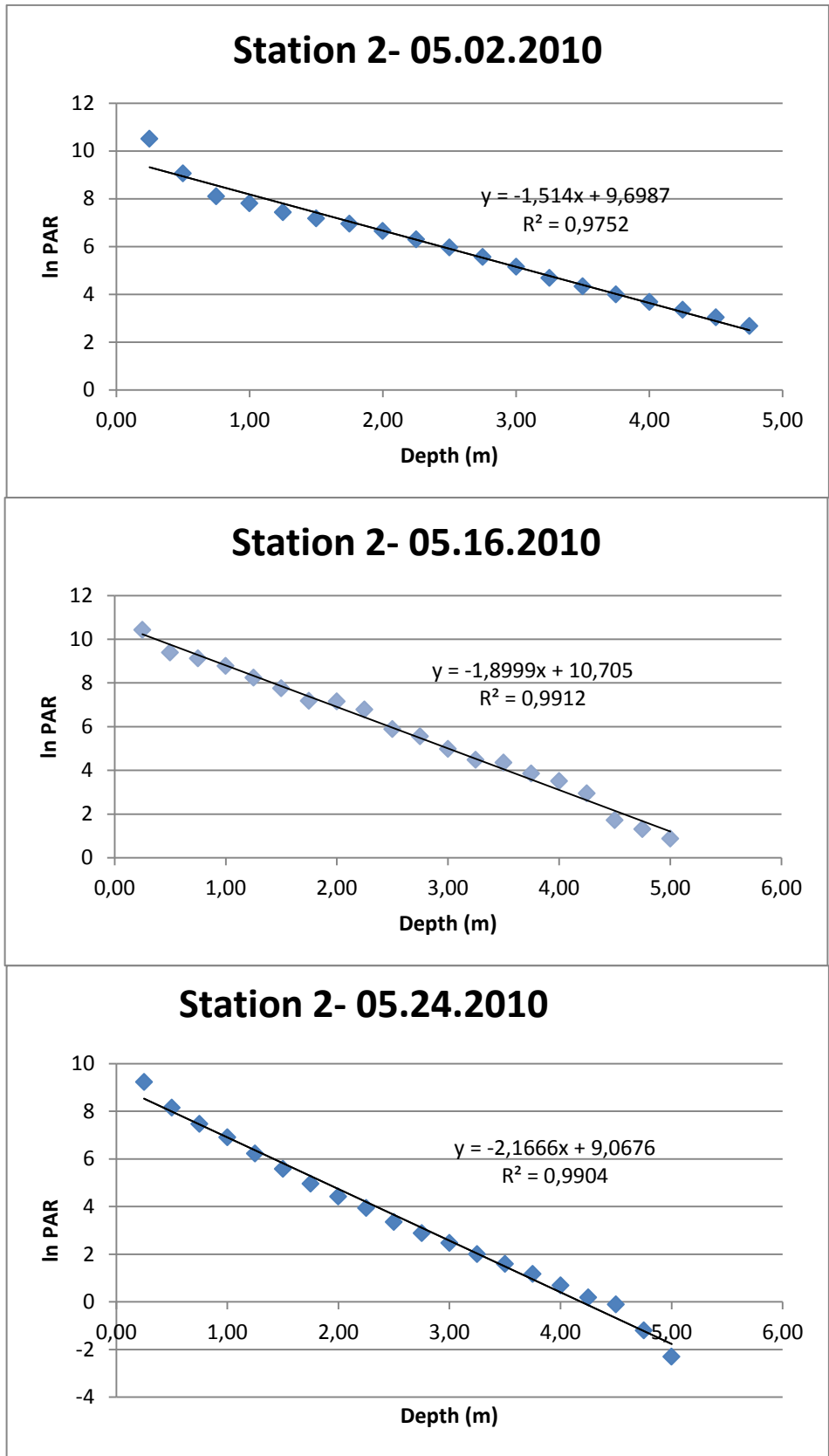


Figure A-25: Station 2 In PAR values versus Depth, For May, 2010

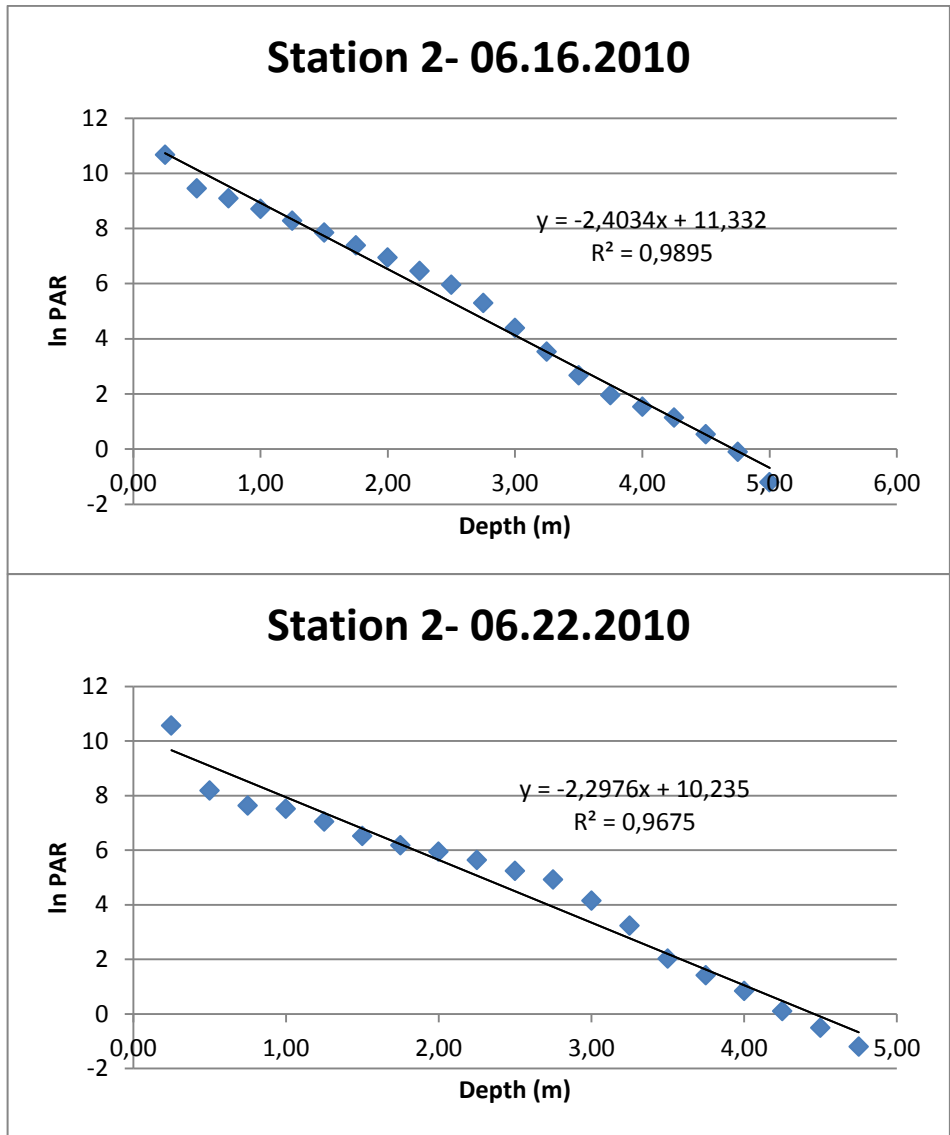


Figure A-26: Station 2 In PAR values versus Depth, For June, 2010

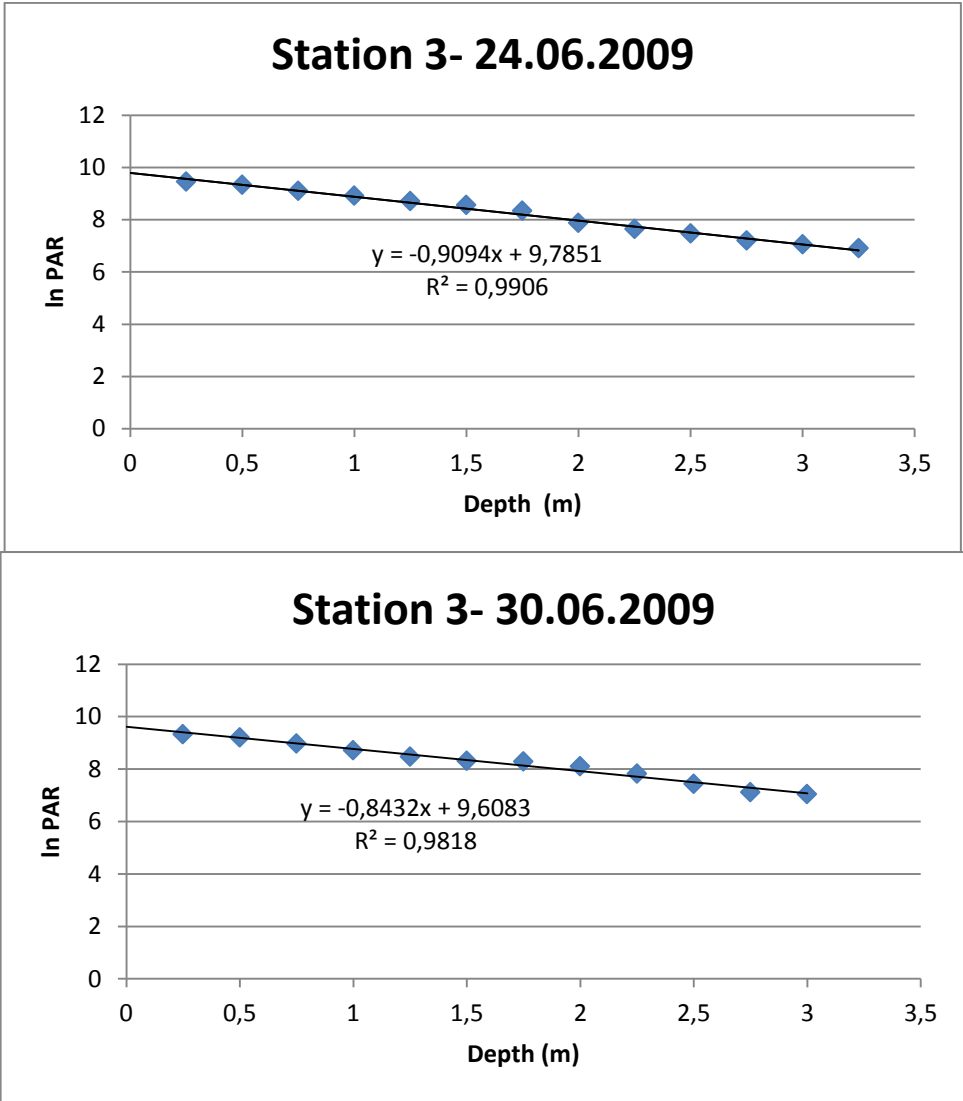


Figure A-27: Station 3 In PAR values versus Depth, For June, 2009

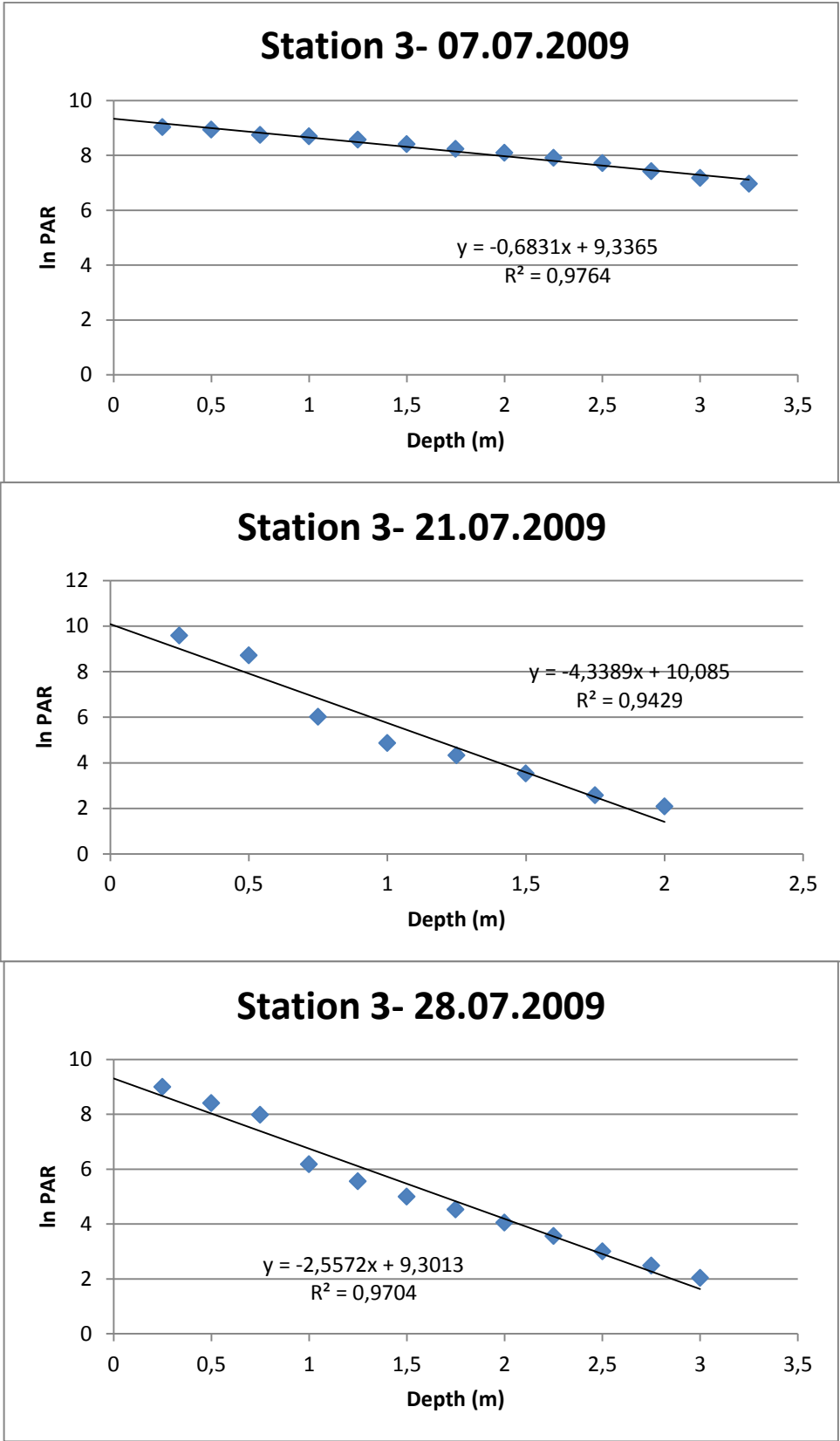


Figure A-28: Station 3 In PAR values versus Depth, For July, 2009



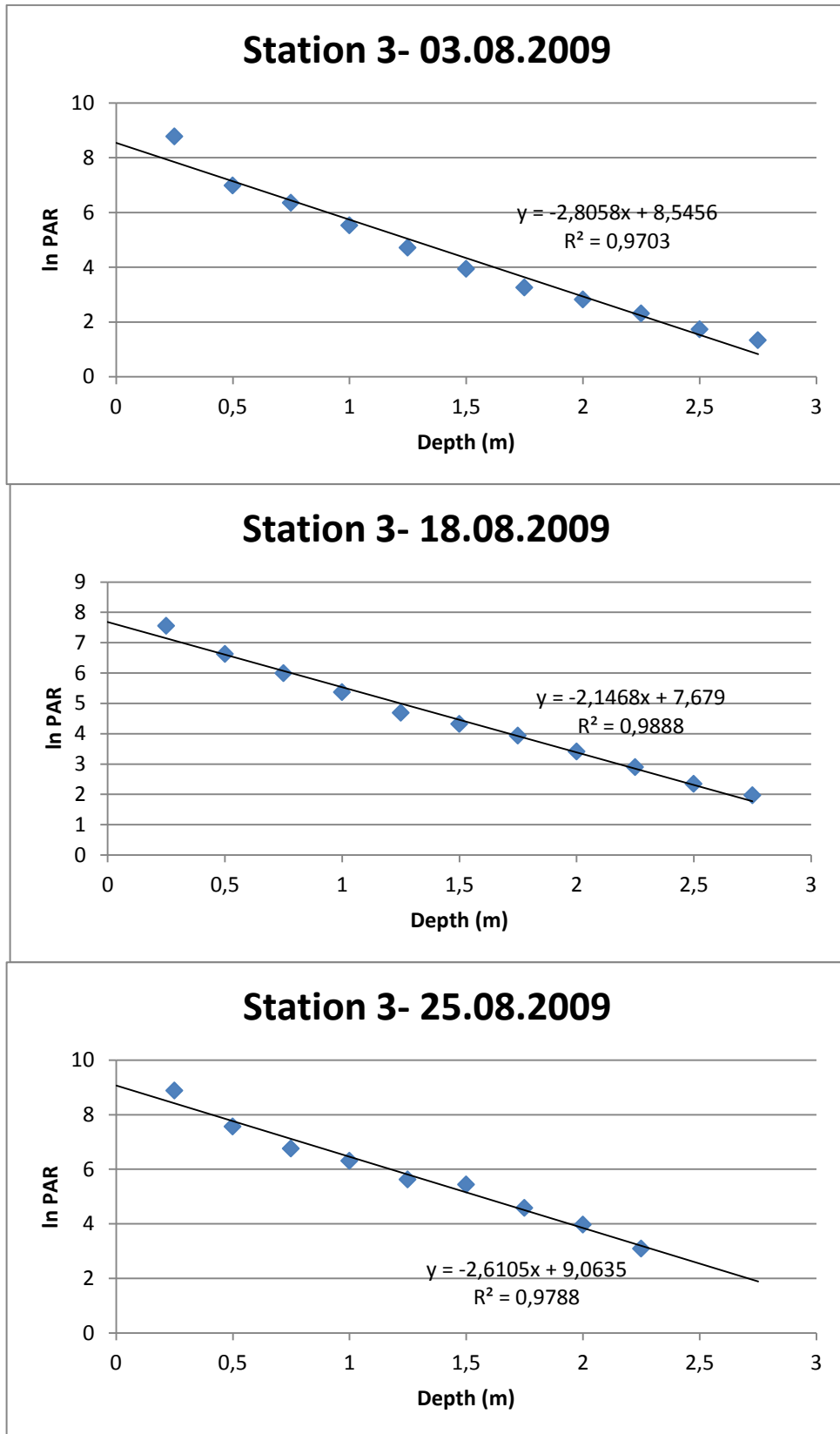


Figure A-29: Station 3 In PAR values versus Depth, For August, 2009

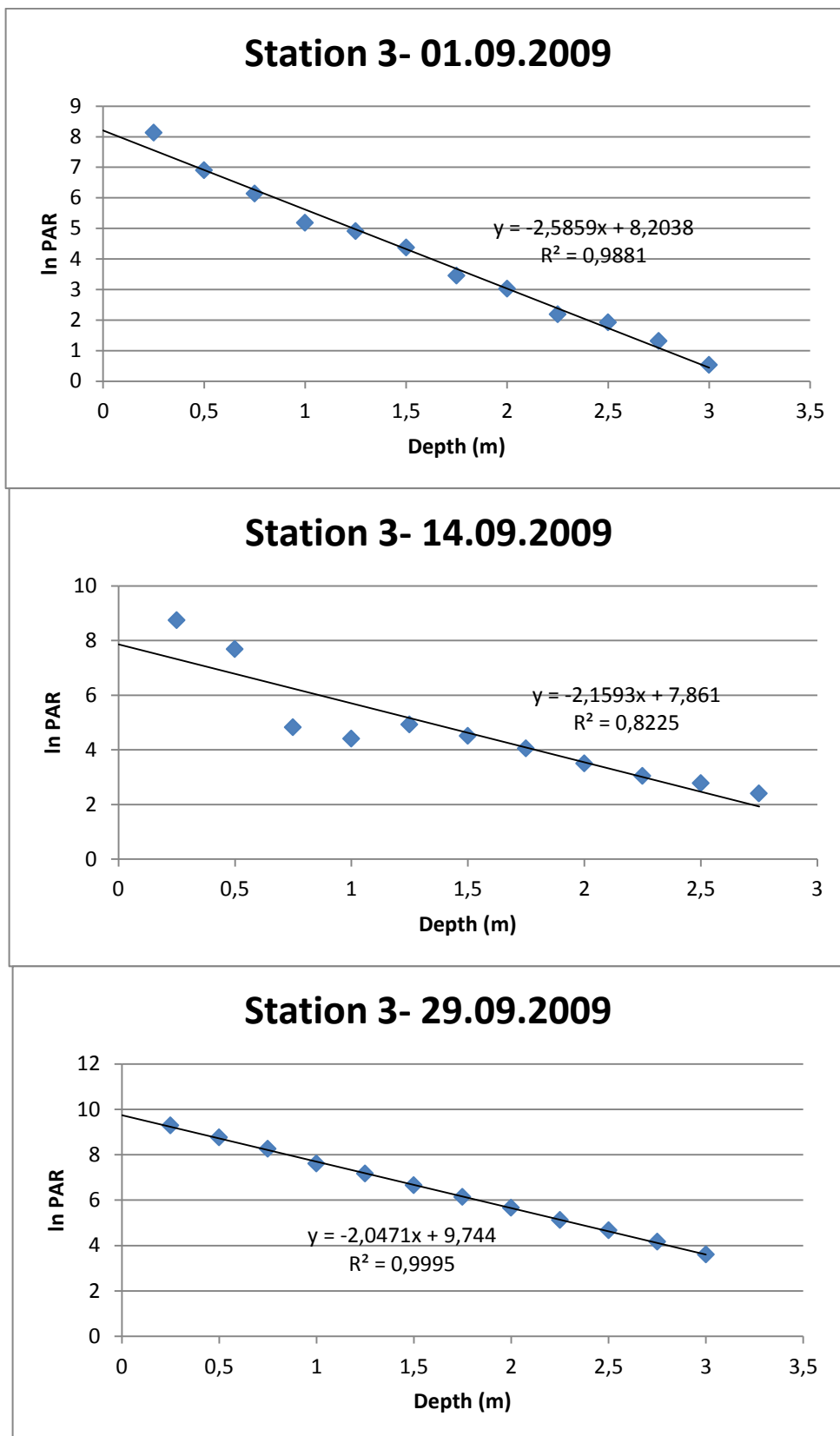


Figure A-30: Station 3 In PAR values versus Depth, For September, 2009

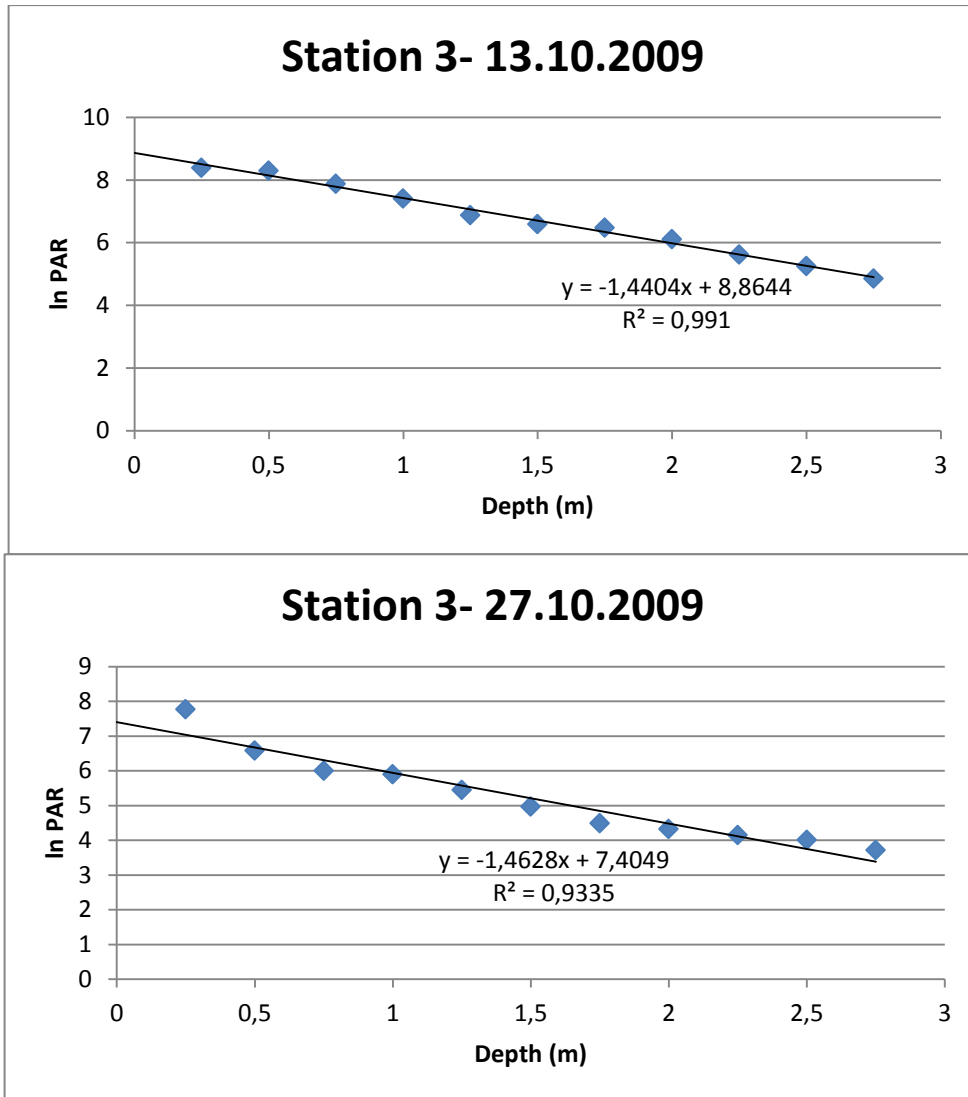


Figure A-31: Station 3 In PAR values versus Depth, For October, 2009

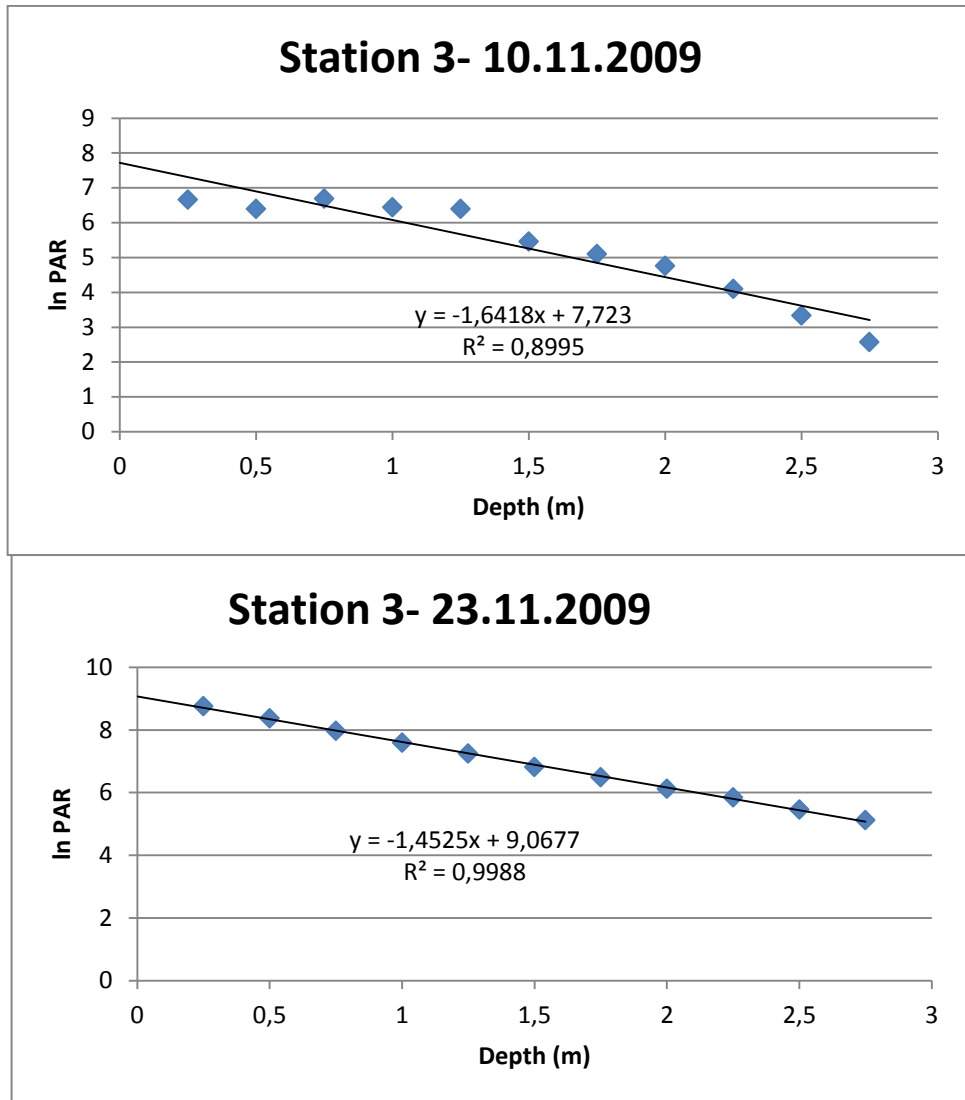


Figure A-32: Station 3 In PAR values versus Depth, For November, 2009

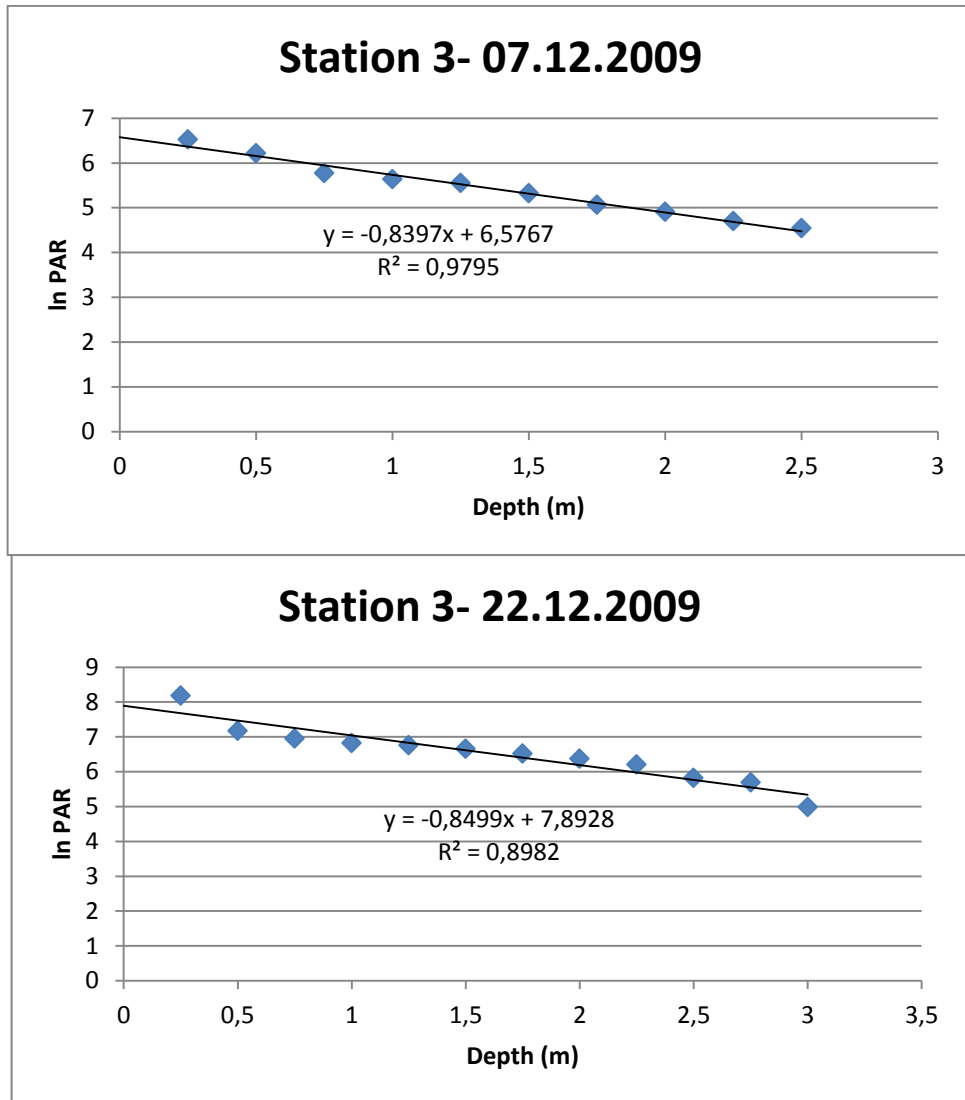


Figure A-33: Station 3 In PAR values versus Depth, For December, 2009

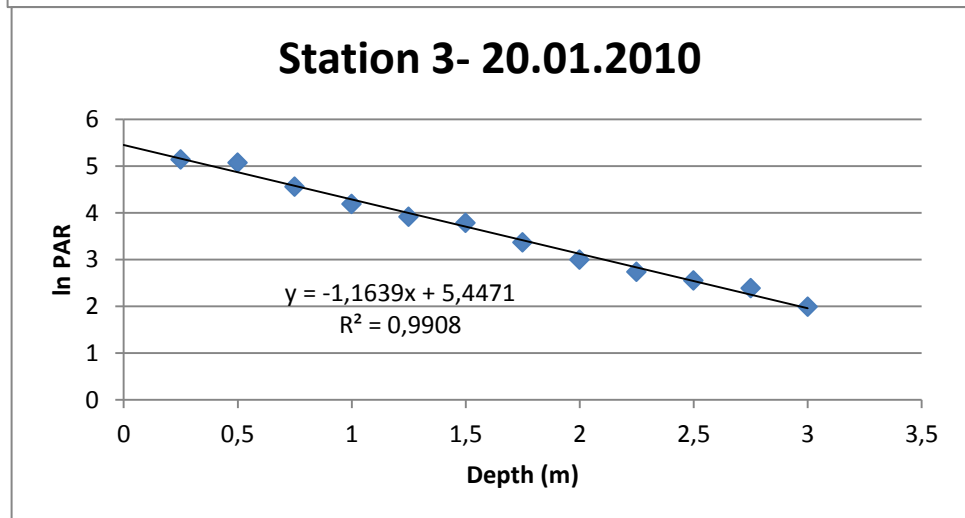
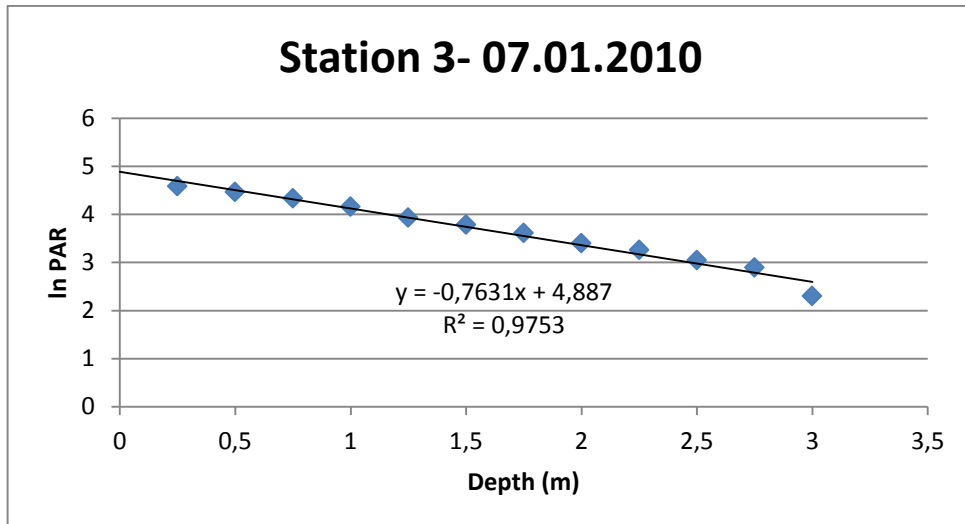


Figure A-34: Station 3 In PAR values versus Depth, For January, 2010

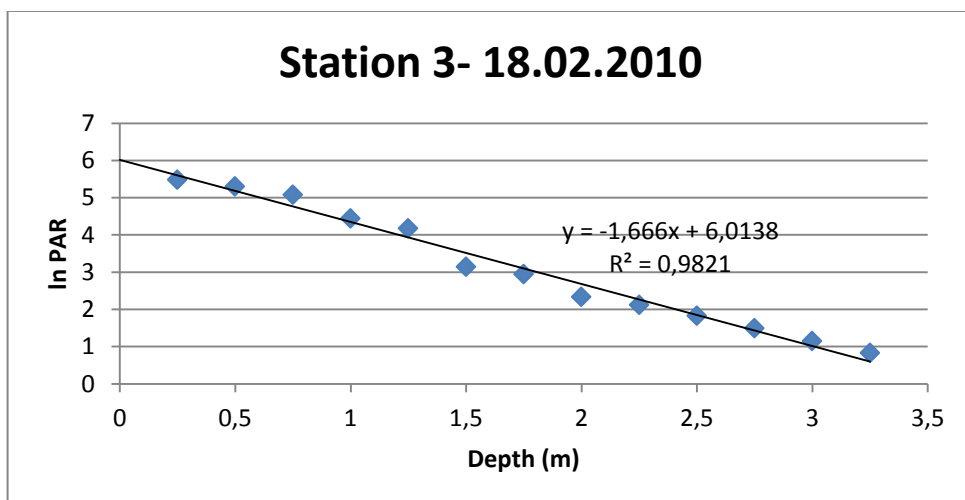


Figure A-35: Station 3 In PAR values versus Depth, For February, 2010

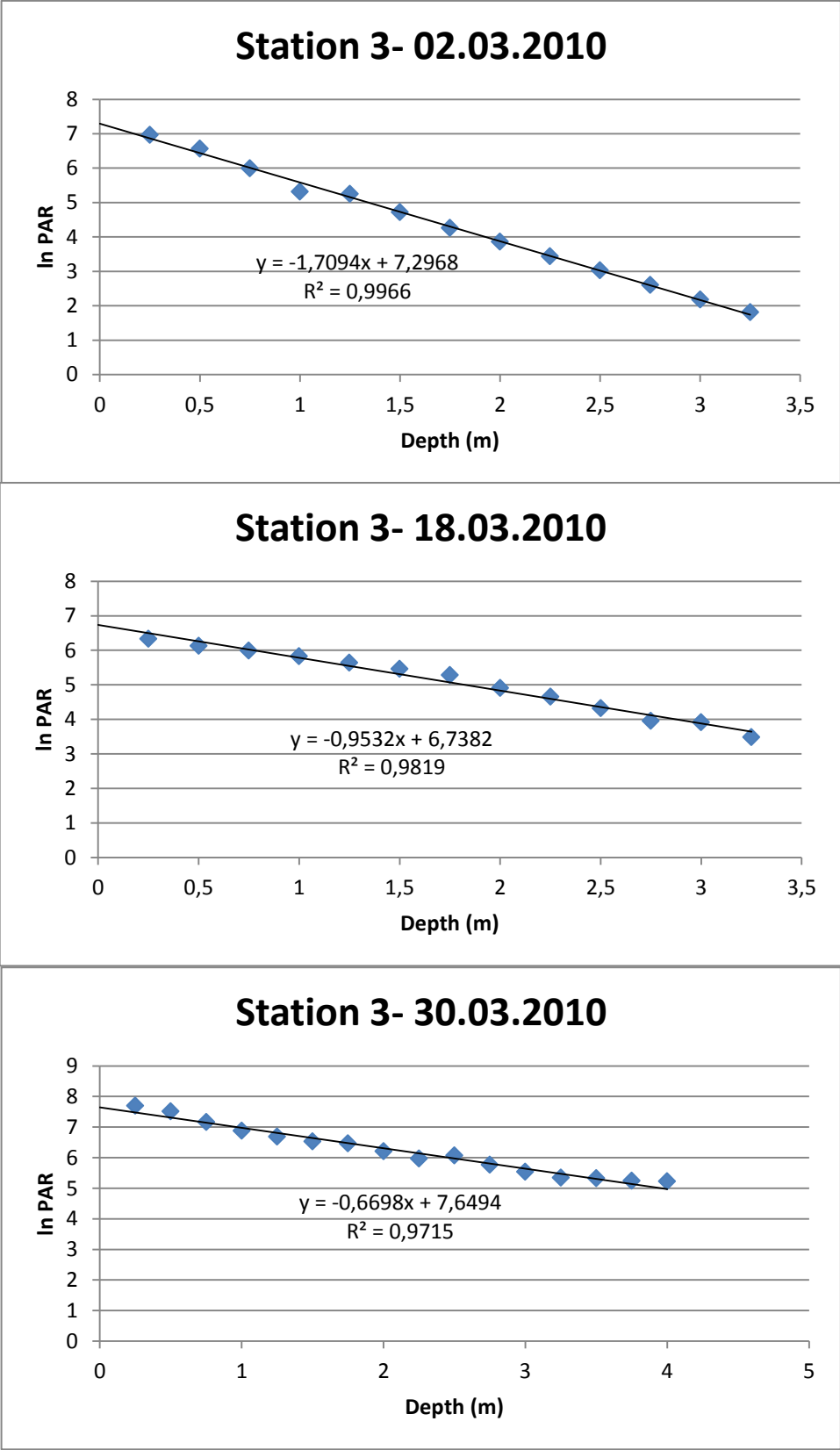


Figure A-36: Station 3 In PAR values versus Depth, For March, 2010

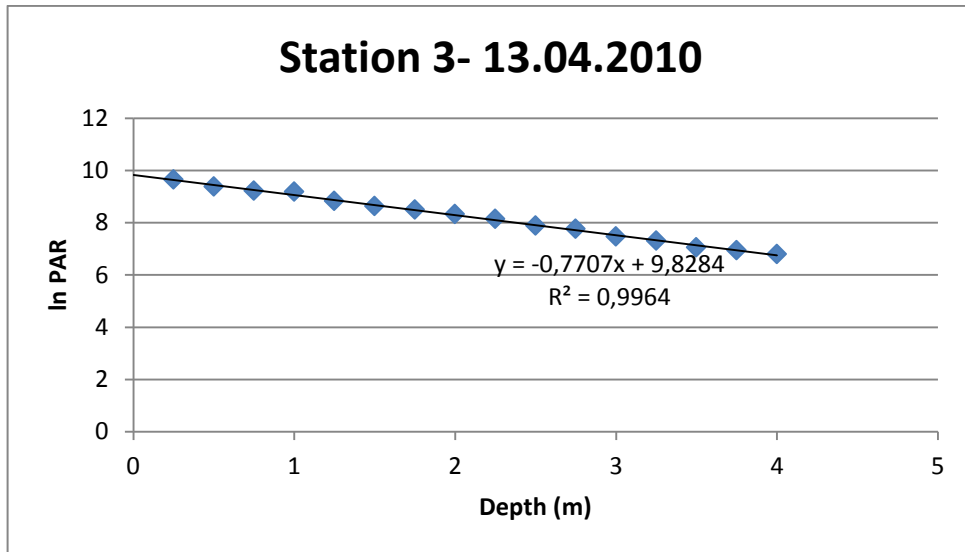


Figure A-37: Station 3 ln PAR values versus Depth, For April, 2010



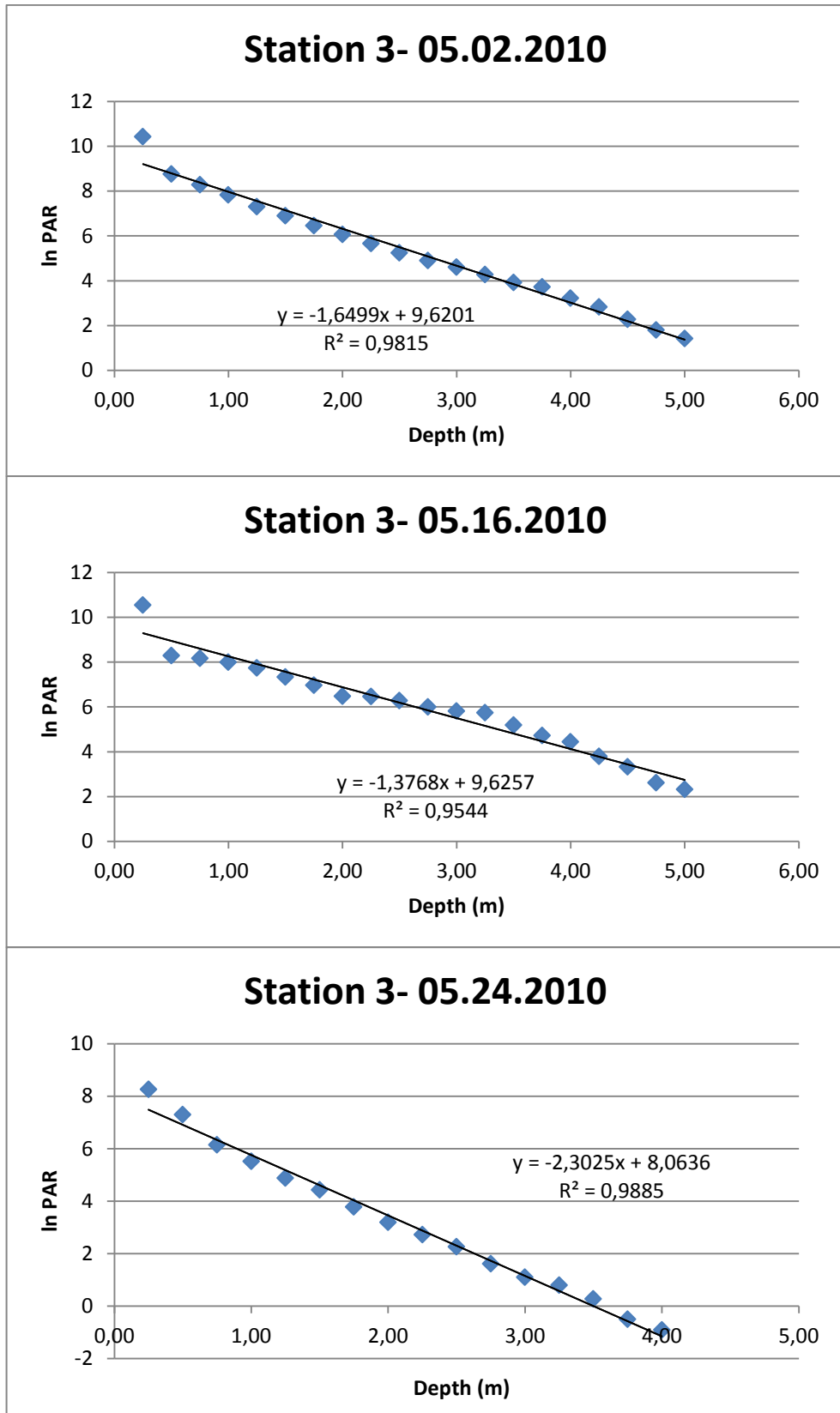


Figure A-38: Station 3 In PAR values versus Depth, For May, 2010

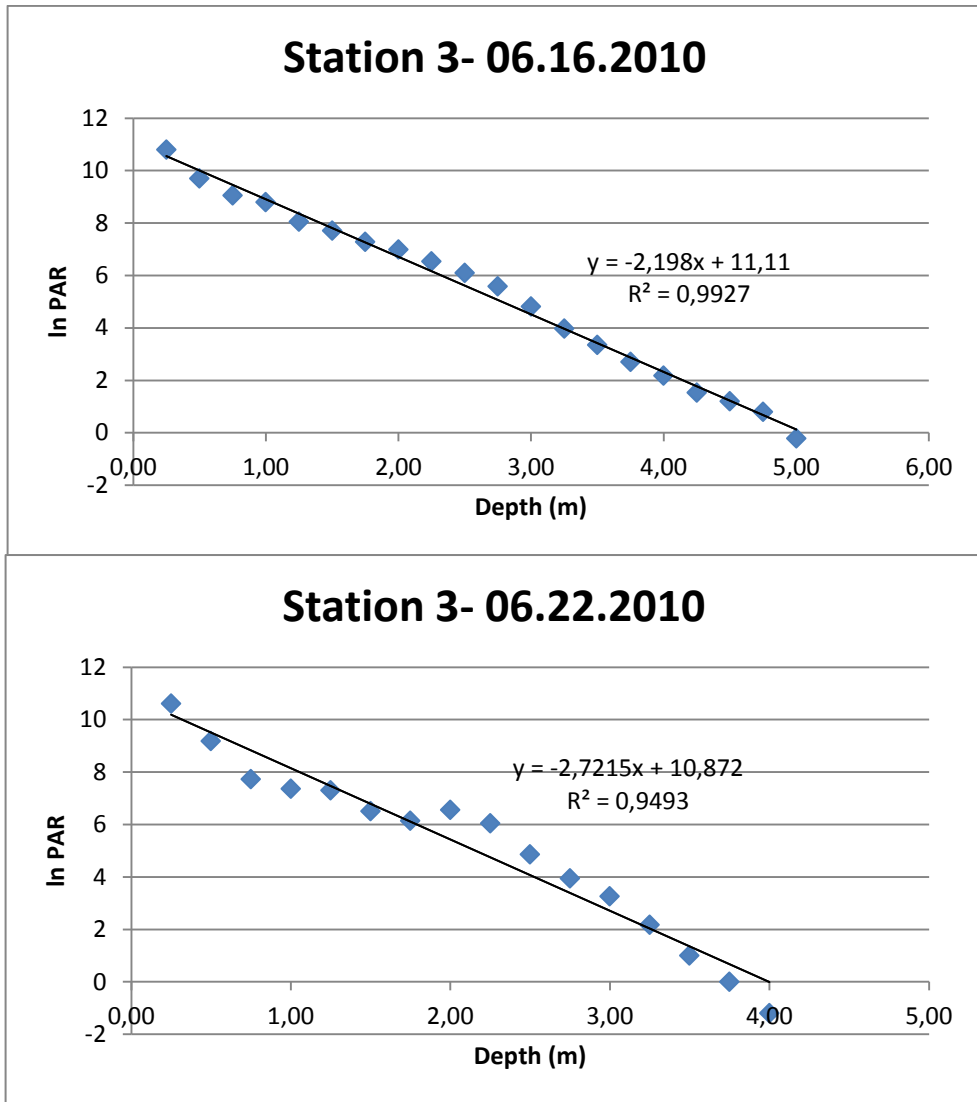


Figure A-39: Station 3 In PAR values versus Depth, For June, 2010

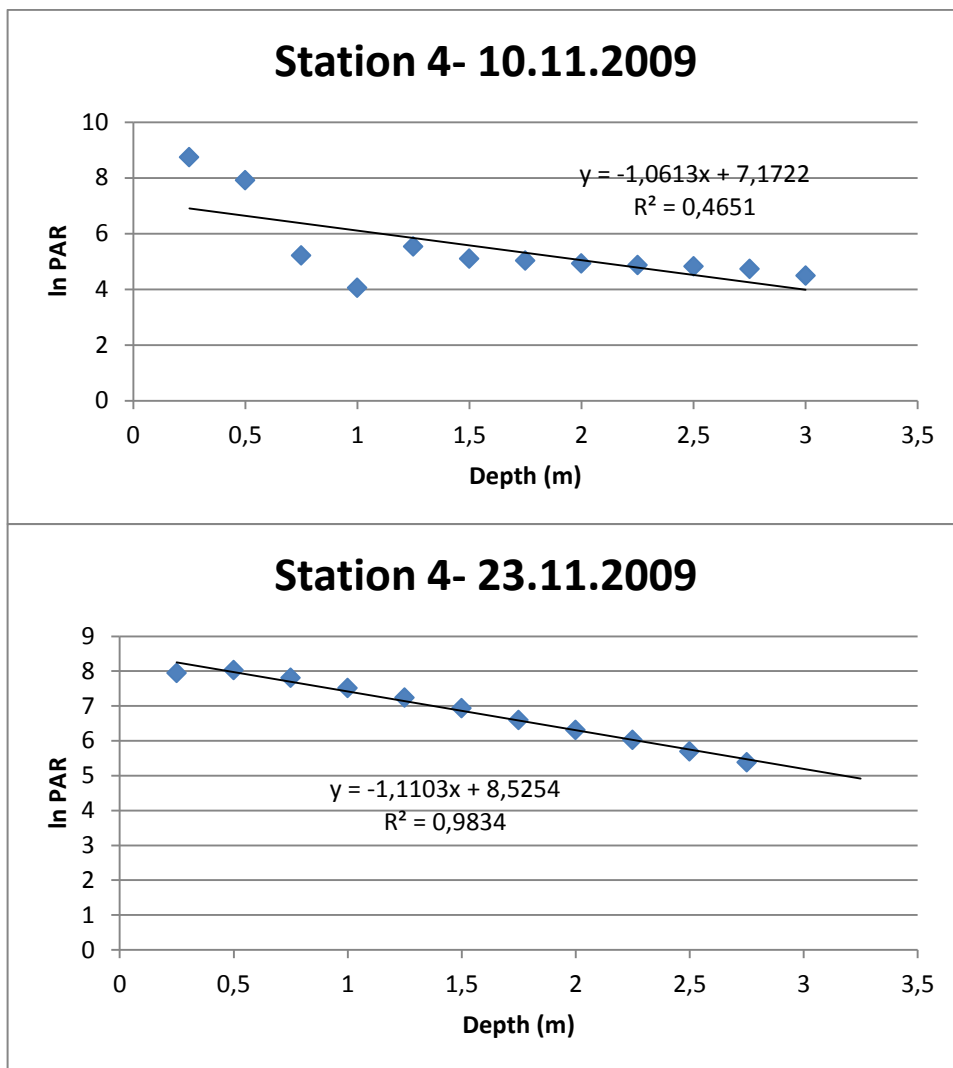


Figure A-40: Station 4 In PAR values versus Depth, For November, 2009

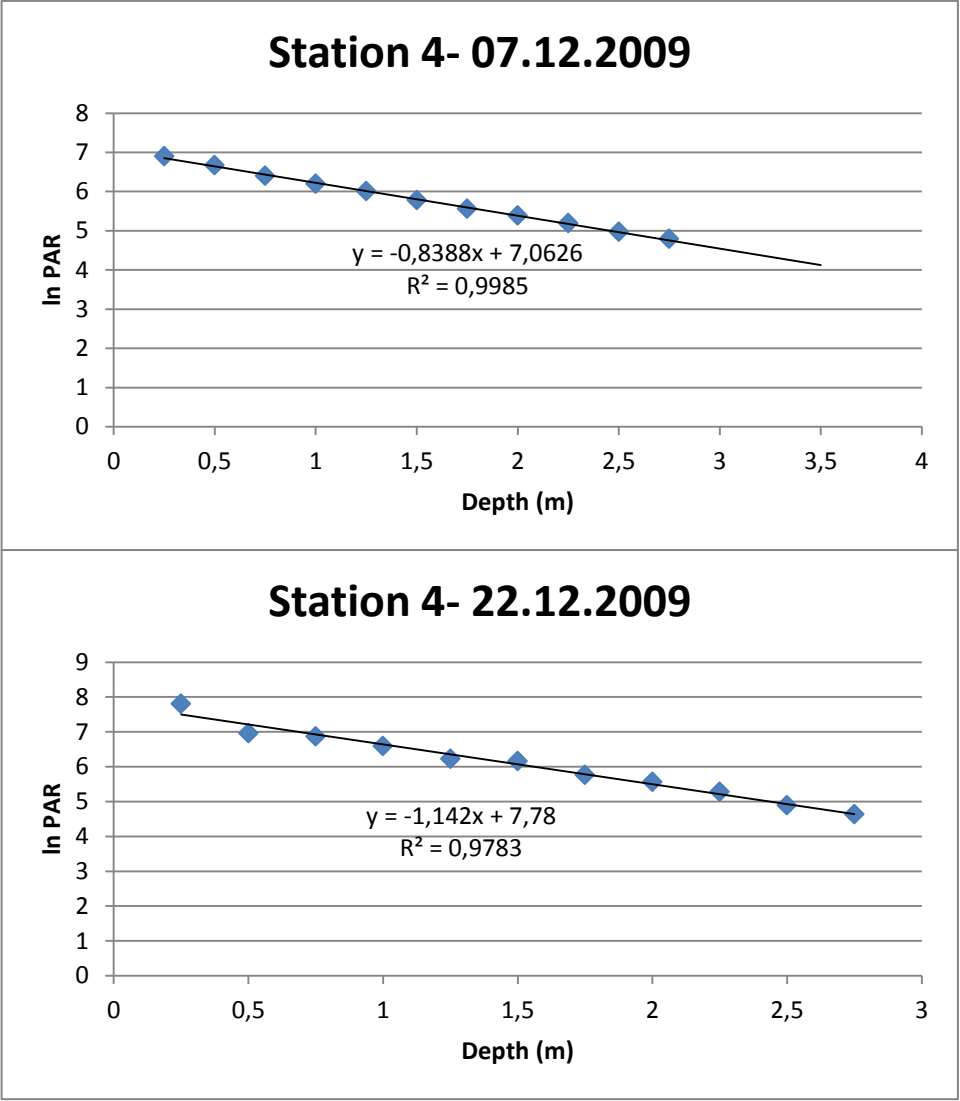


Figure A-41: Station 4 In PAR values versus Depth, For December, 2009

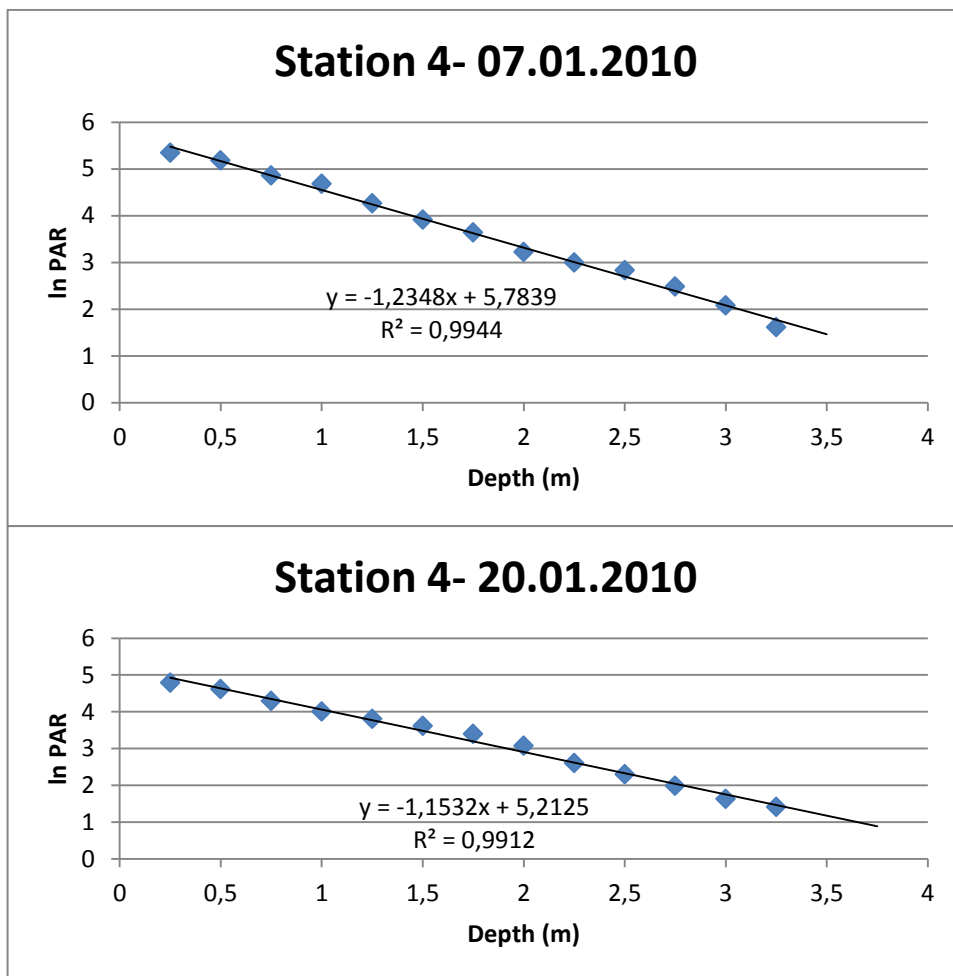


Figure A-42: Station 4 In PAR values versus Depth, For January, 2010,

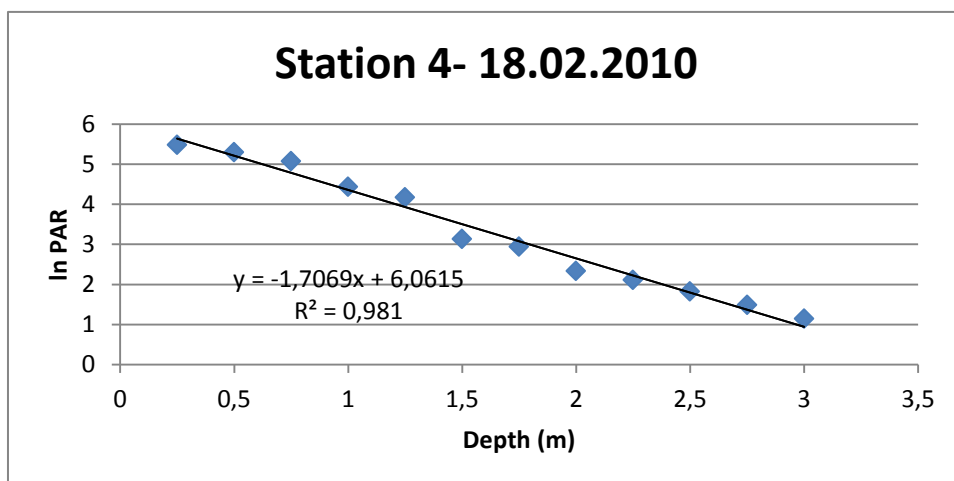


Figure A-43: Station 4 In PAR values versus Depth, For February, 2010

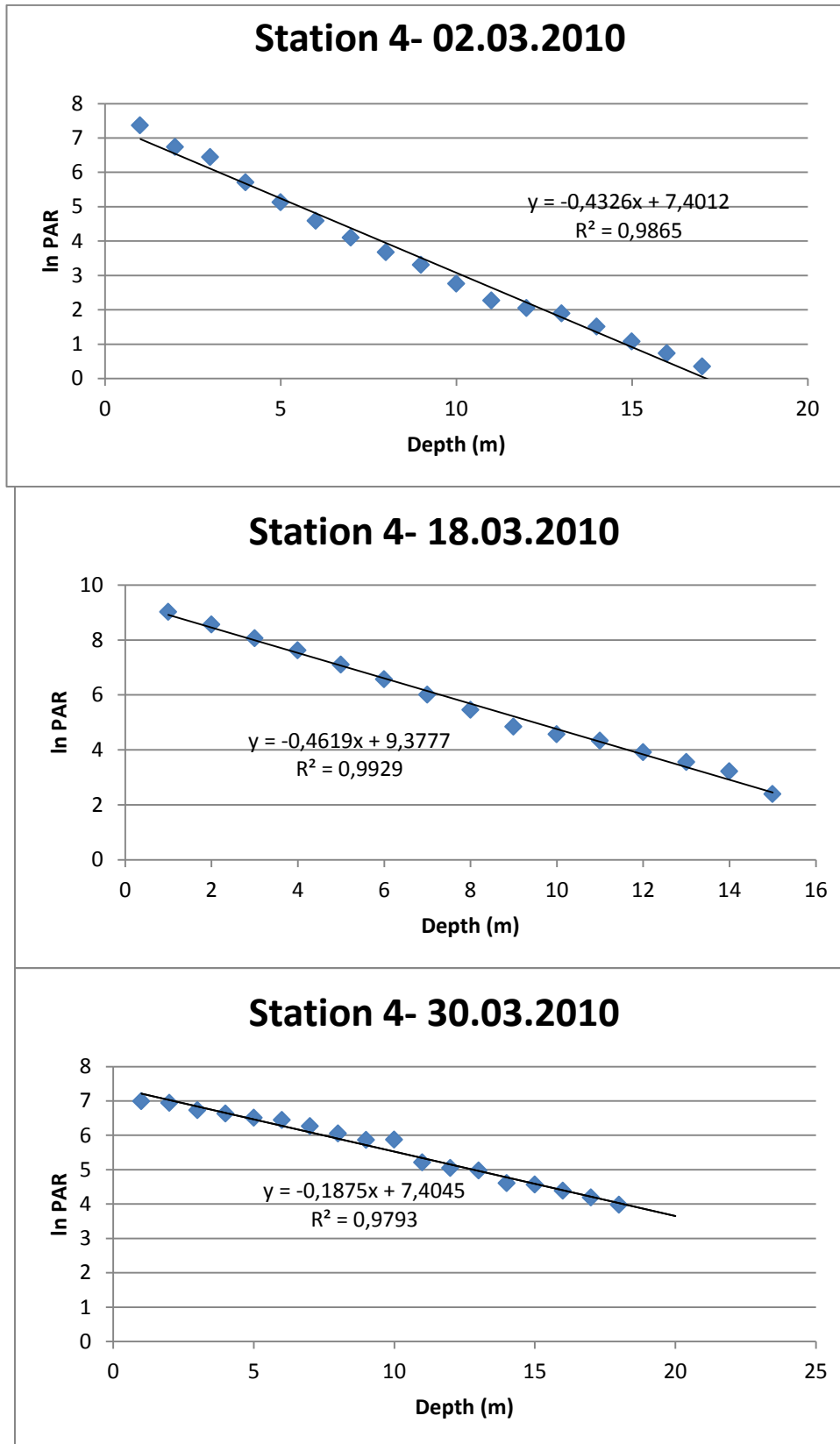


Figure A-43: Station 4 In PAR values versus Depth, For March, 2010

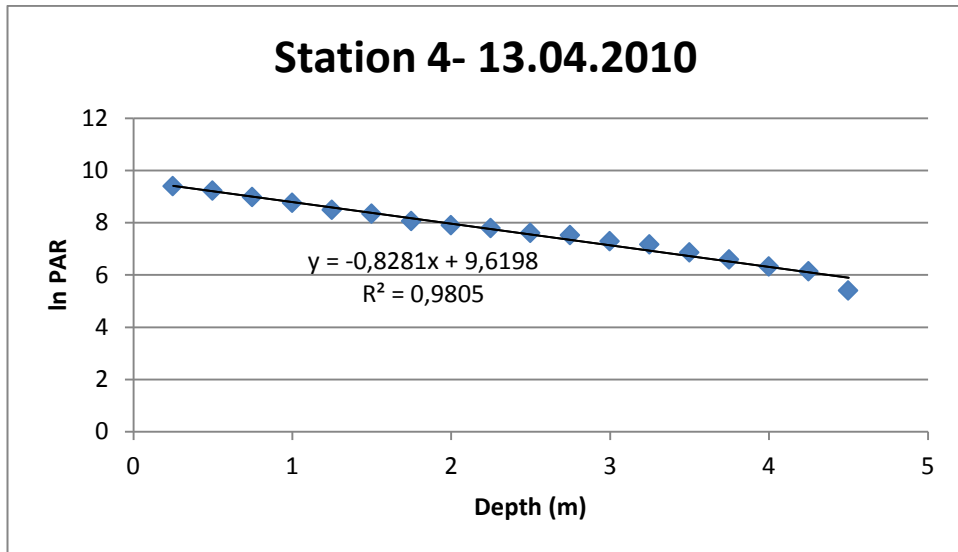


Figure A-44: Station 4 In PAR values versus Depth, For April, 2010

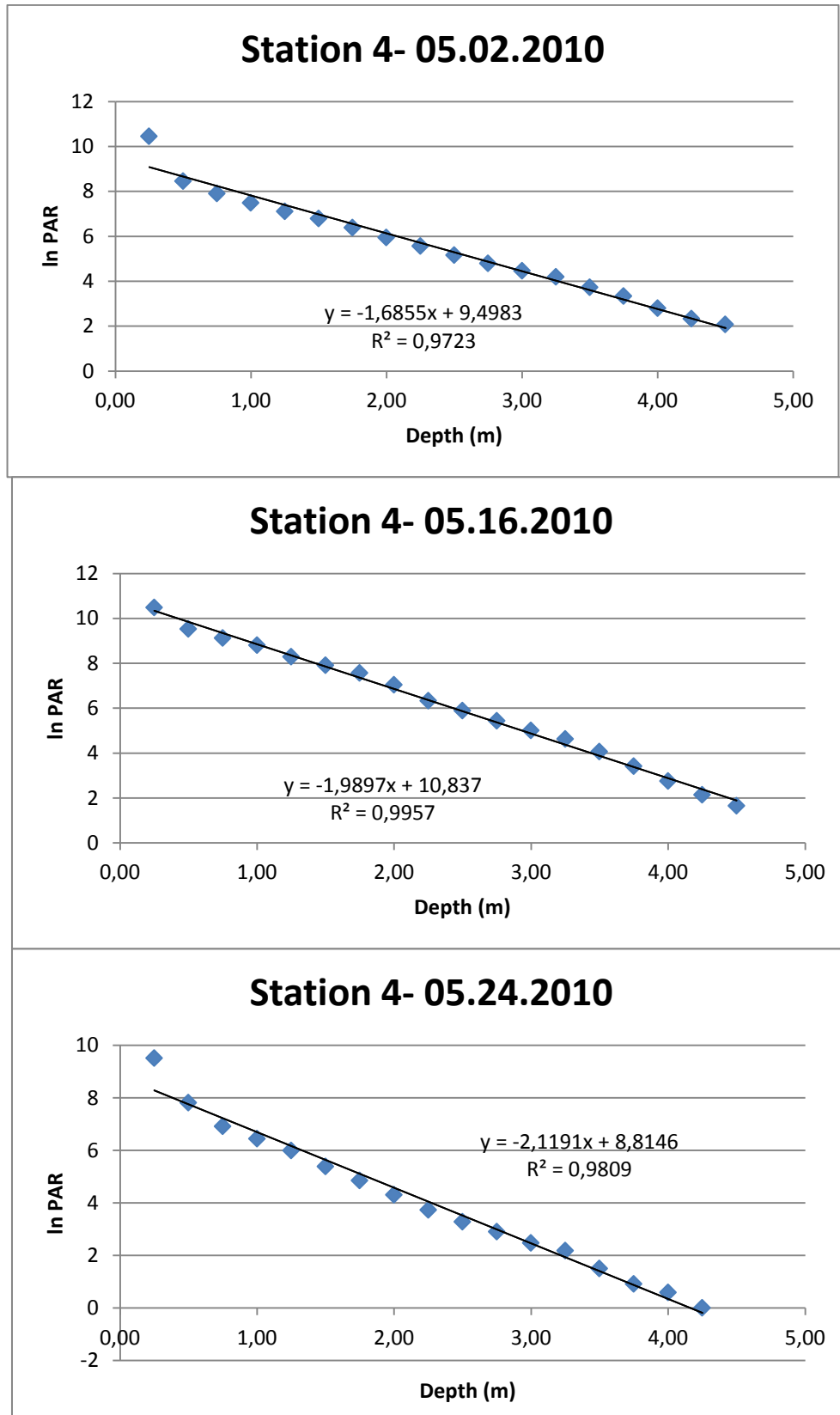


Figure A-45: Station 4 In PAR values versus Depth, For May, 2010



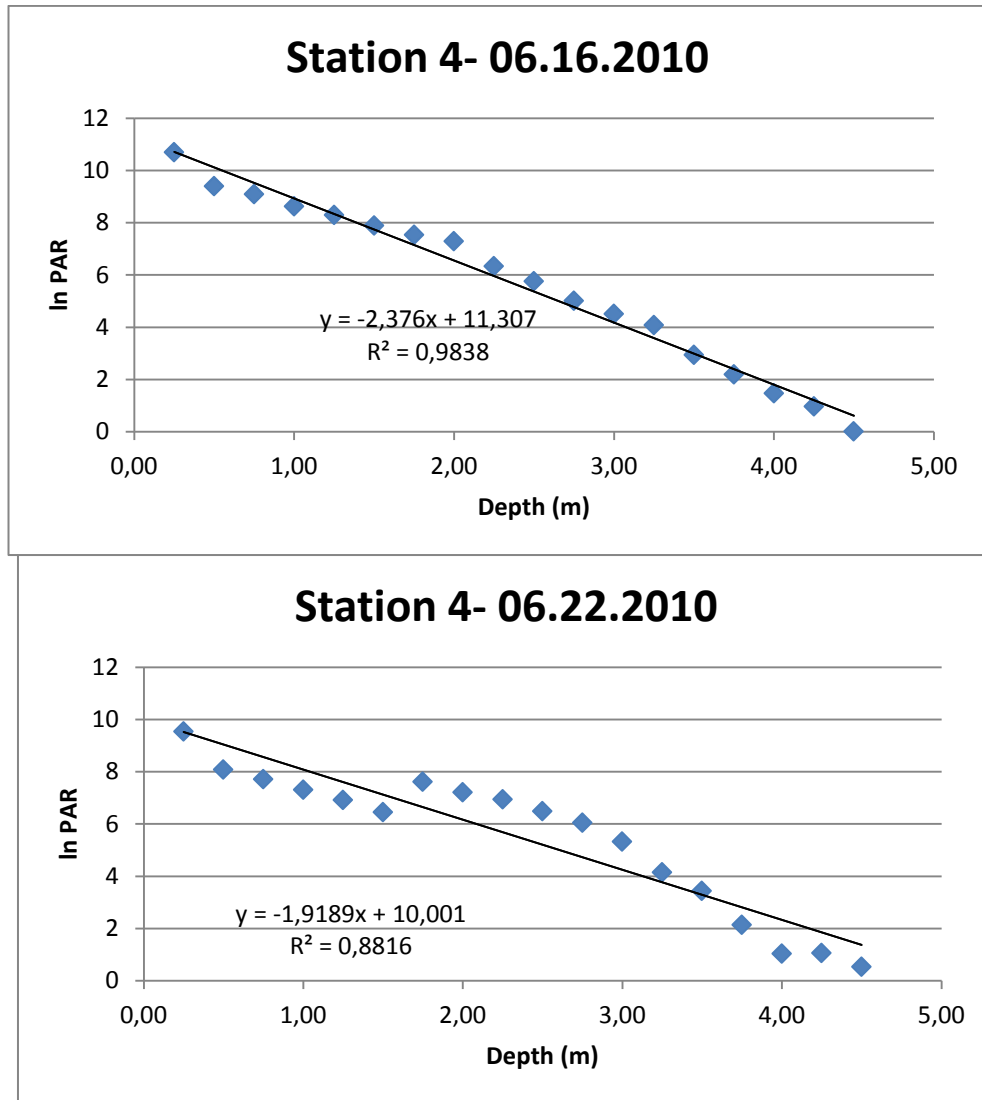


Figure A-46: Station 4 In PAR values versus Depth, For June, 2010

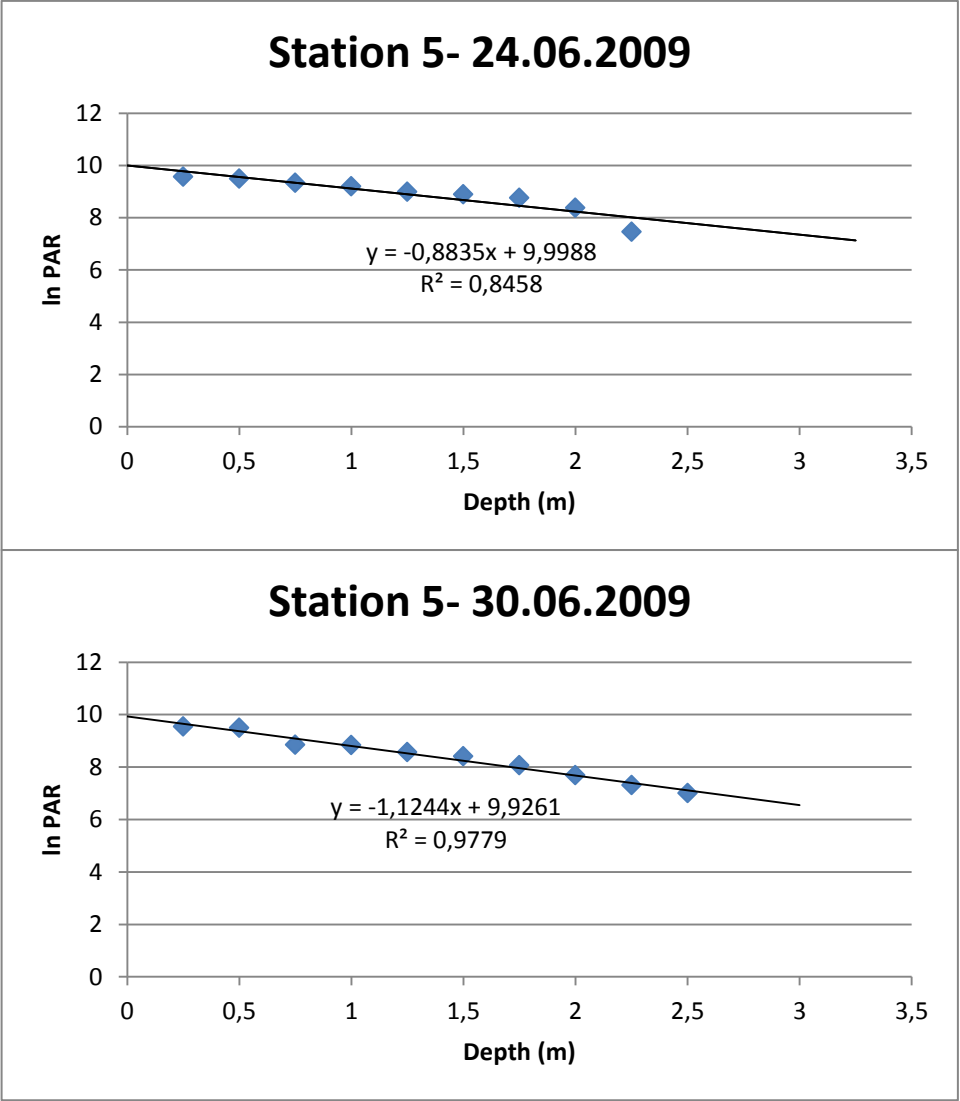


Figure A-47: Station 5 In PAR values versus Depth, For June, 2009

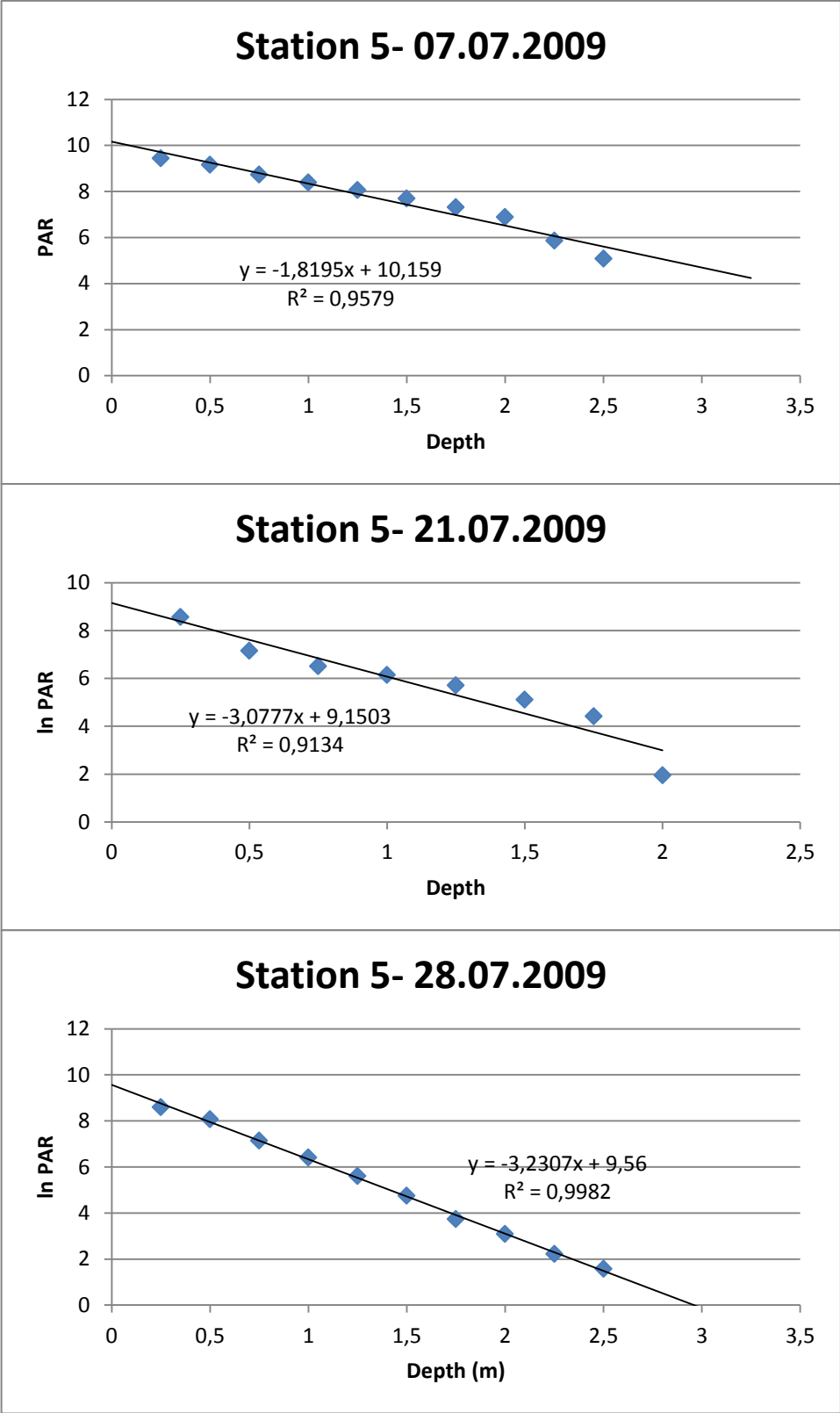


Figure A-48: Station 5 In PAR values versus Depth, For July, 2009

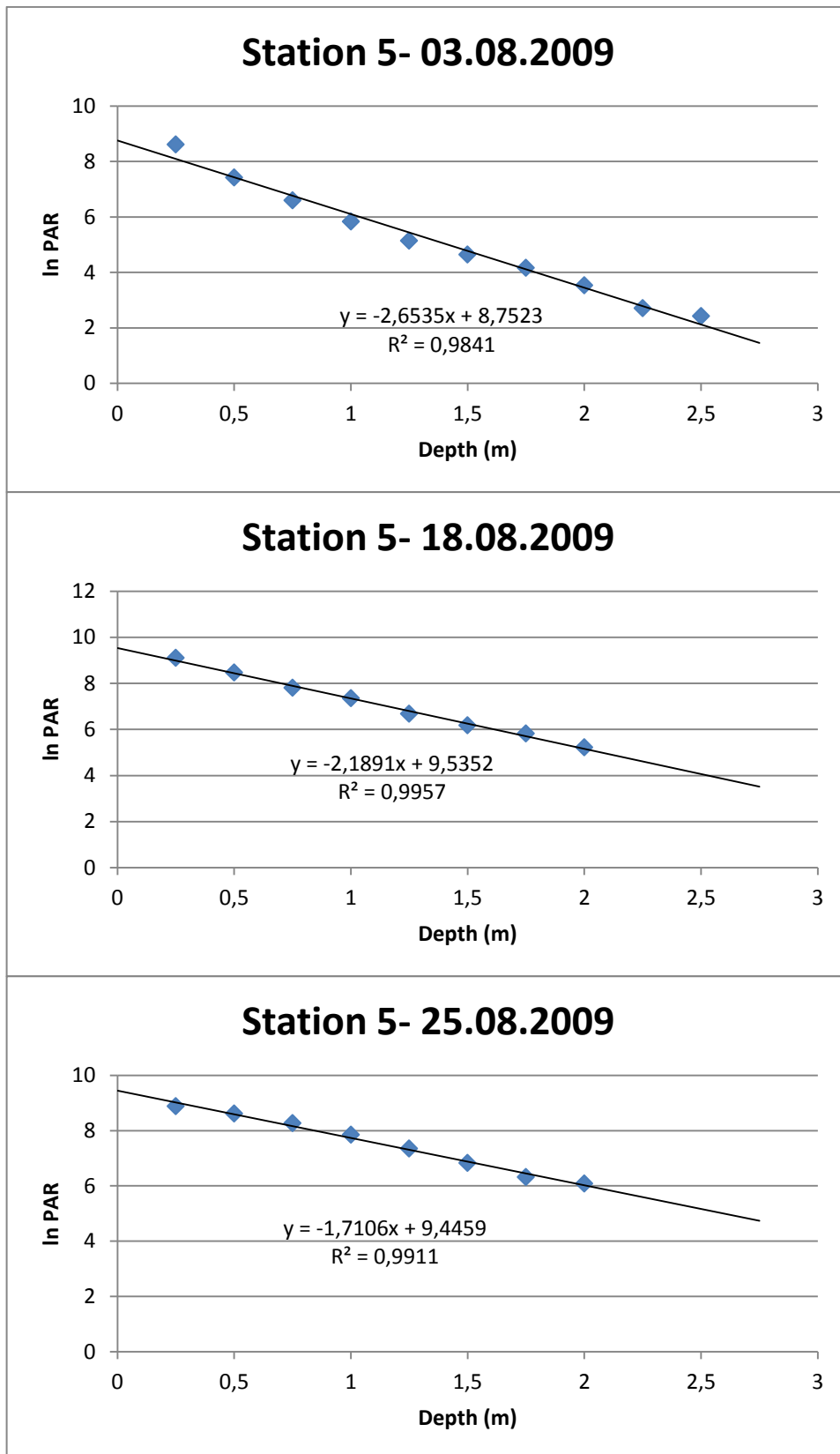


Figure A-49: Station 5 In PAR values versus Depth, For August, 2009

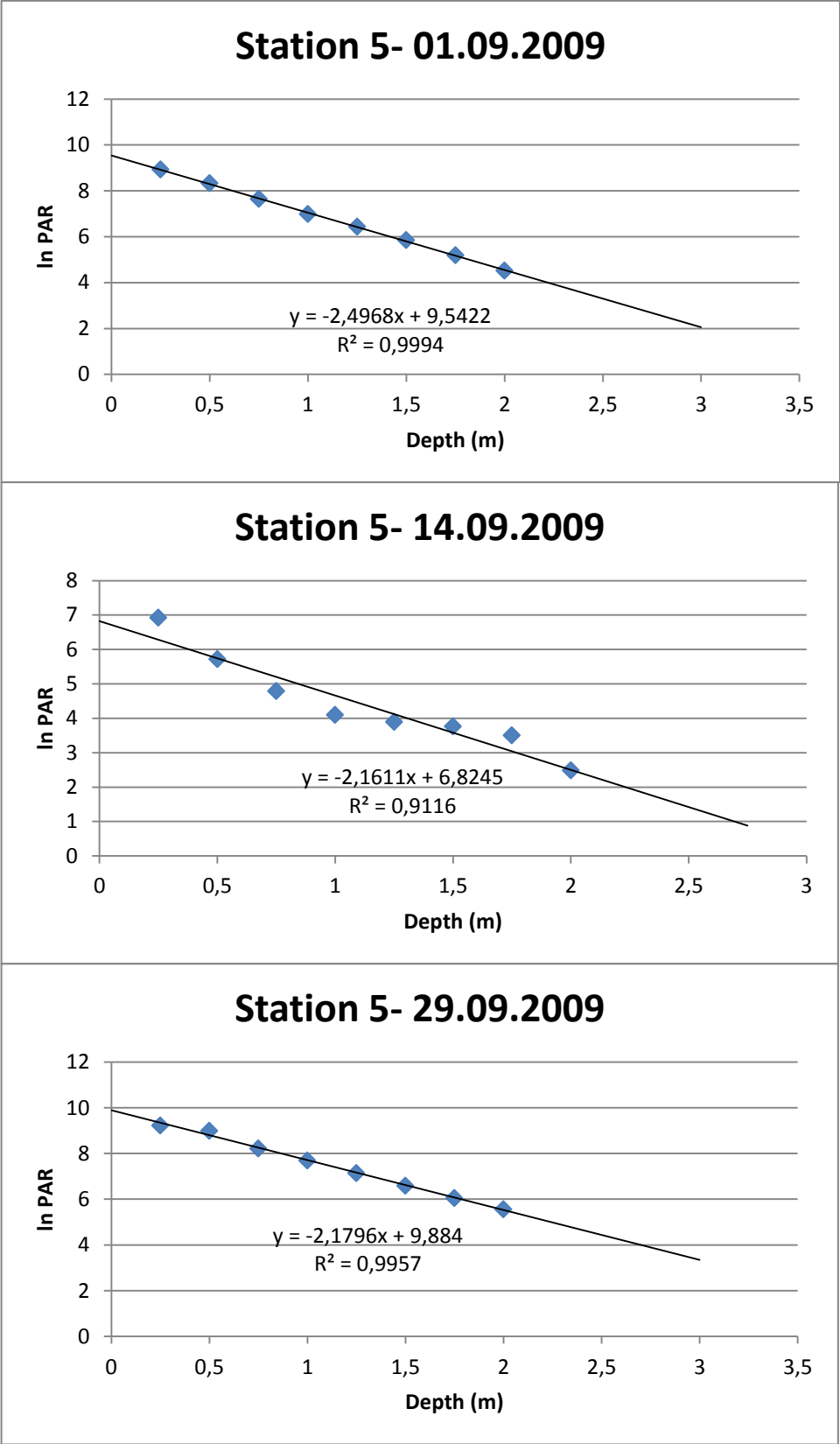


Figure A-50: Station 5 In PAR values versus Depth, For September, 2009

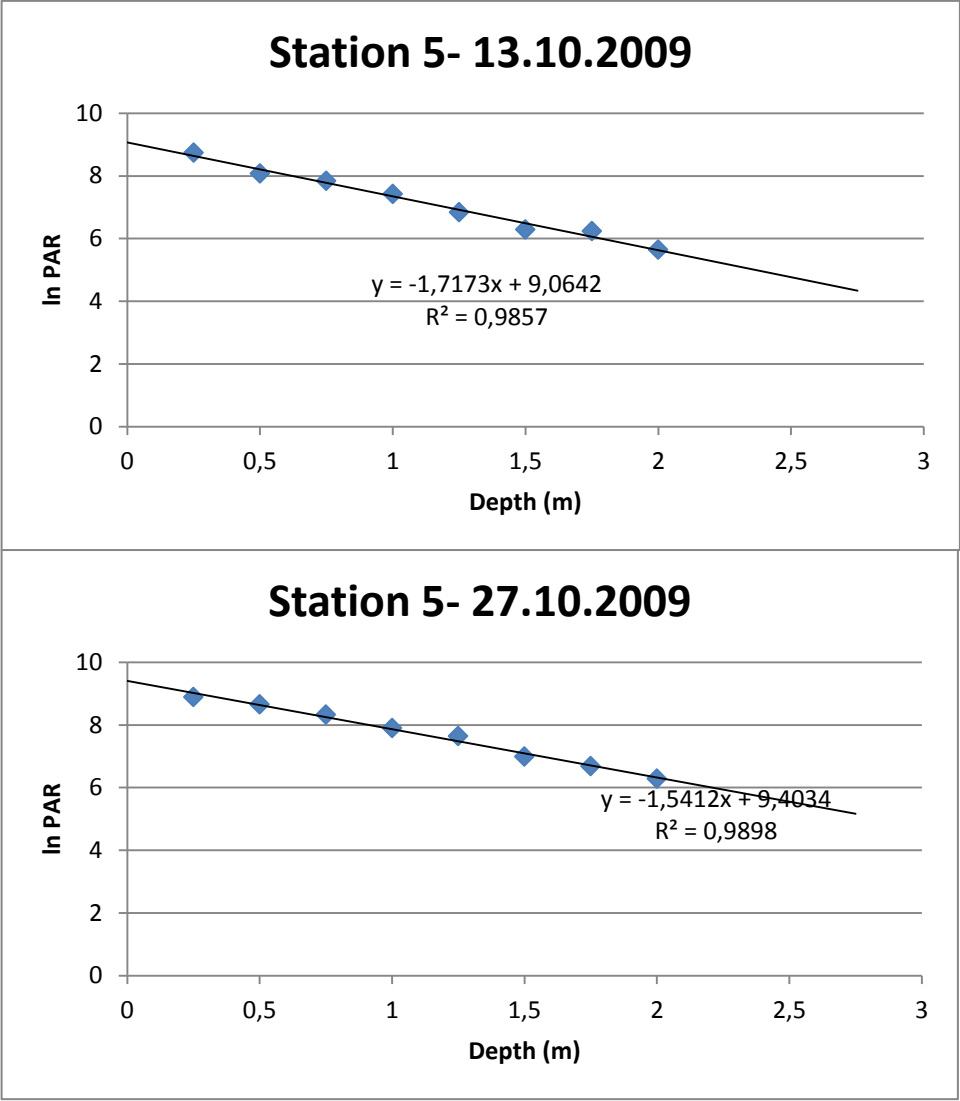


Figure A-51: Station 5 In PAR values versus Depth, For October, 2009

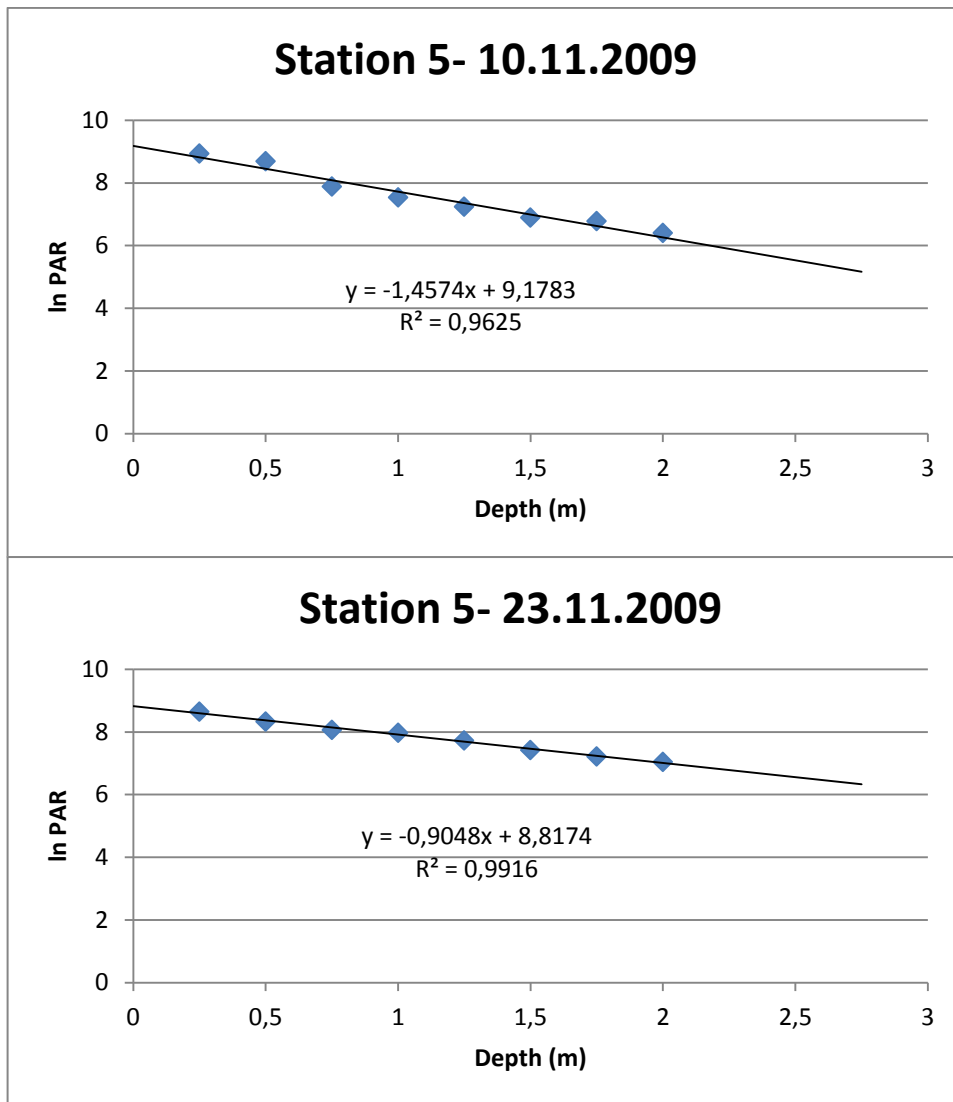


Figure A-52: Station 5 In PAR values versus Depth, For November, 2009

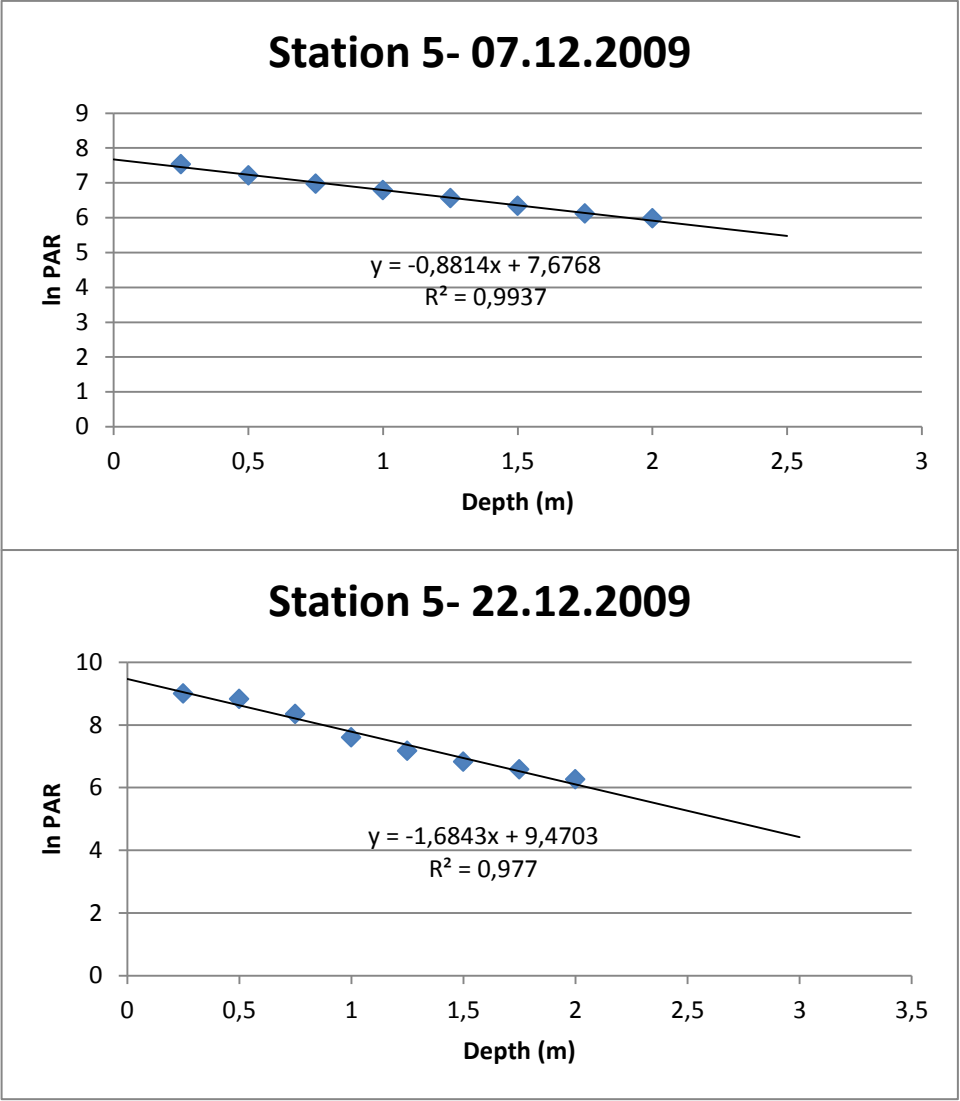


Figure A-53: Station 5 In PAR values versus Depth, For December, 2009



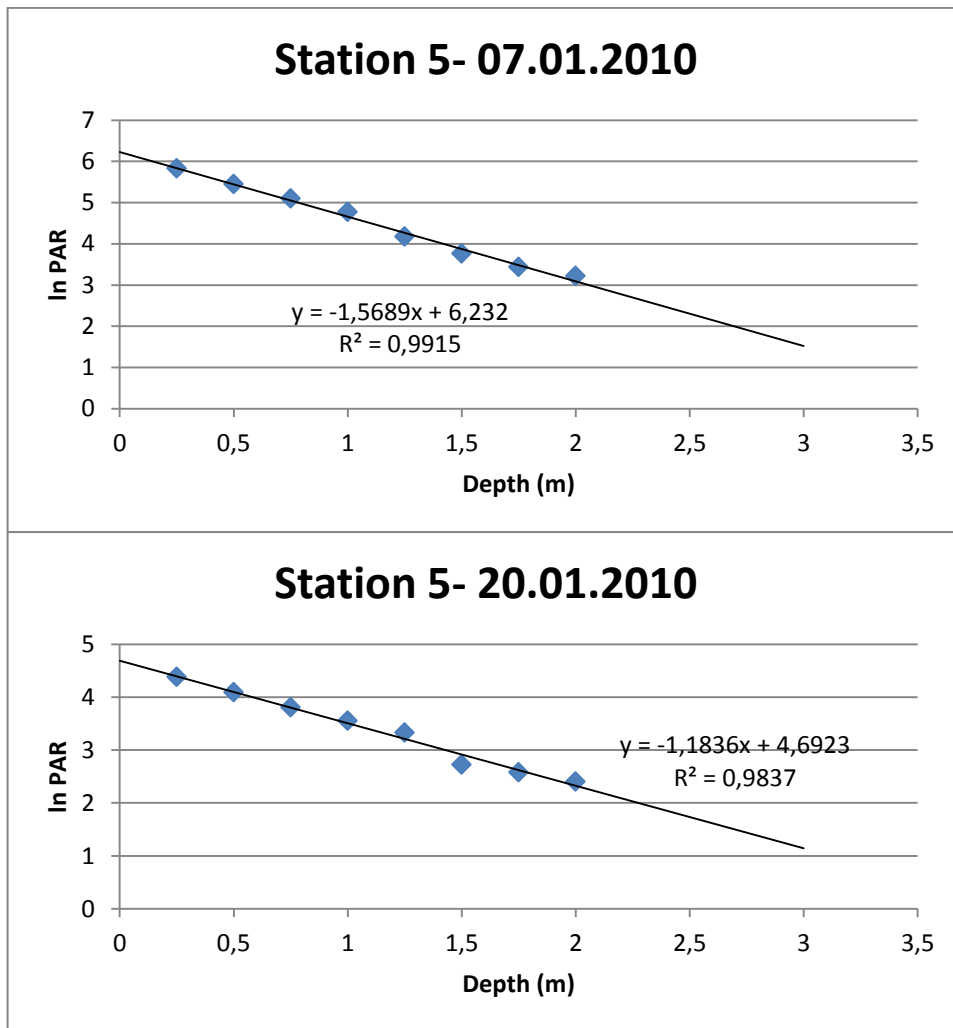


Figure A-54: Station 5 In PAR values versus Depth, For January, 2010

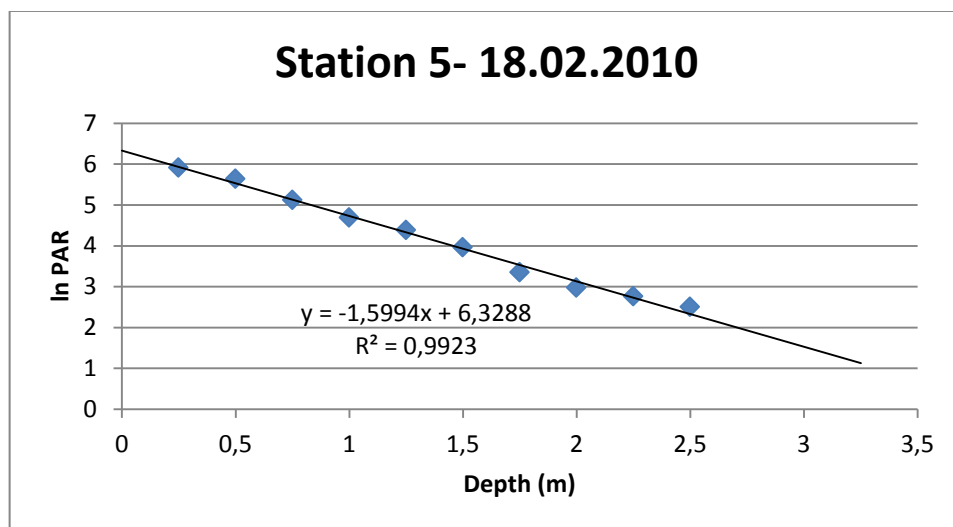


Figure A-55: Station 5 In PAR values versus Depth, For February, 2010

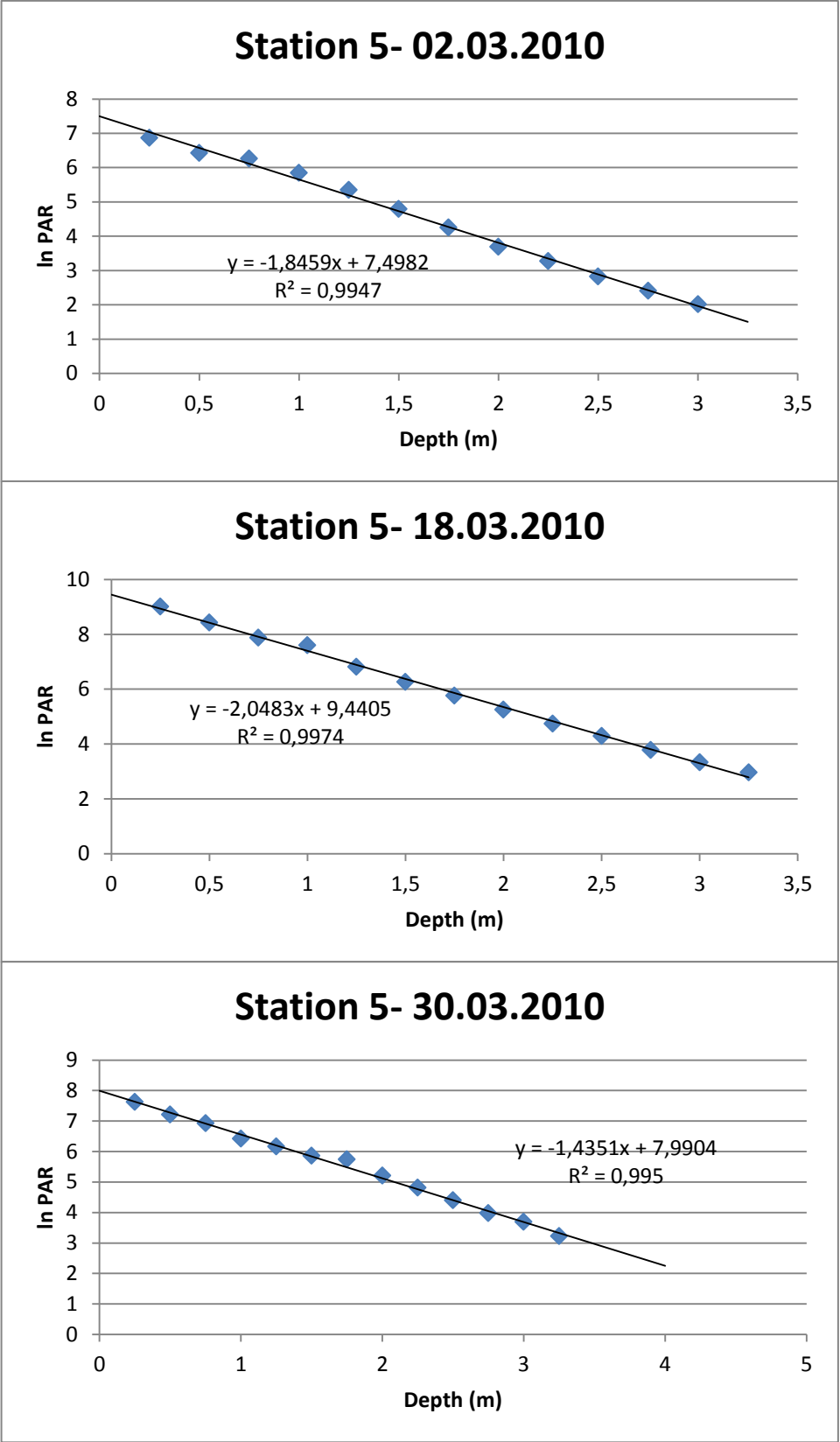


Figure A-56: Station 5 In PAR values versus Depth, For March, 2010

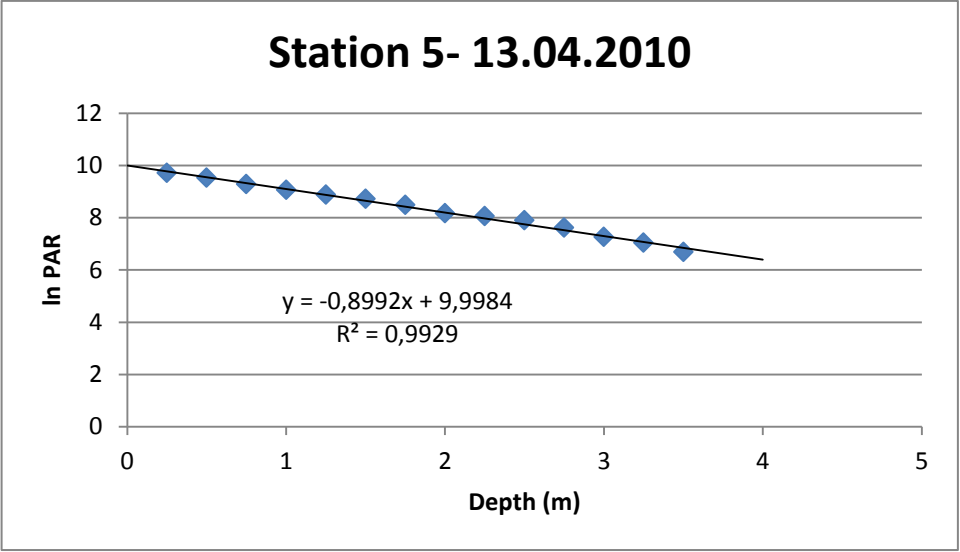


Figure A-57: Station 5 ln PAR values versus Depth, For April, 2010

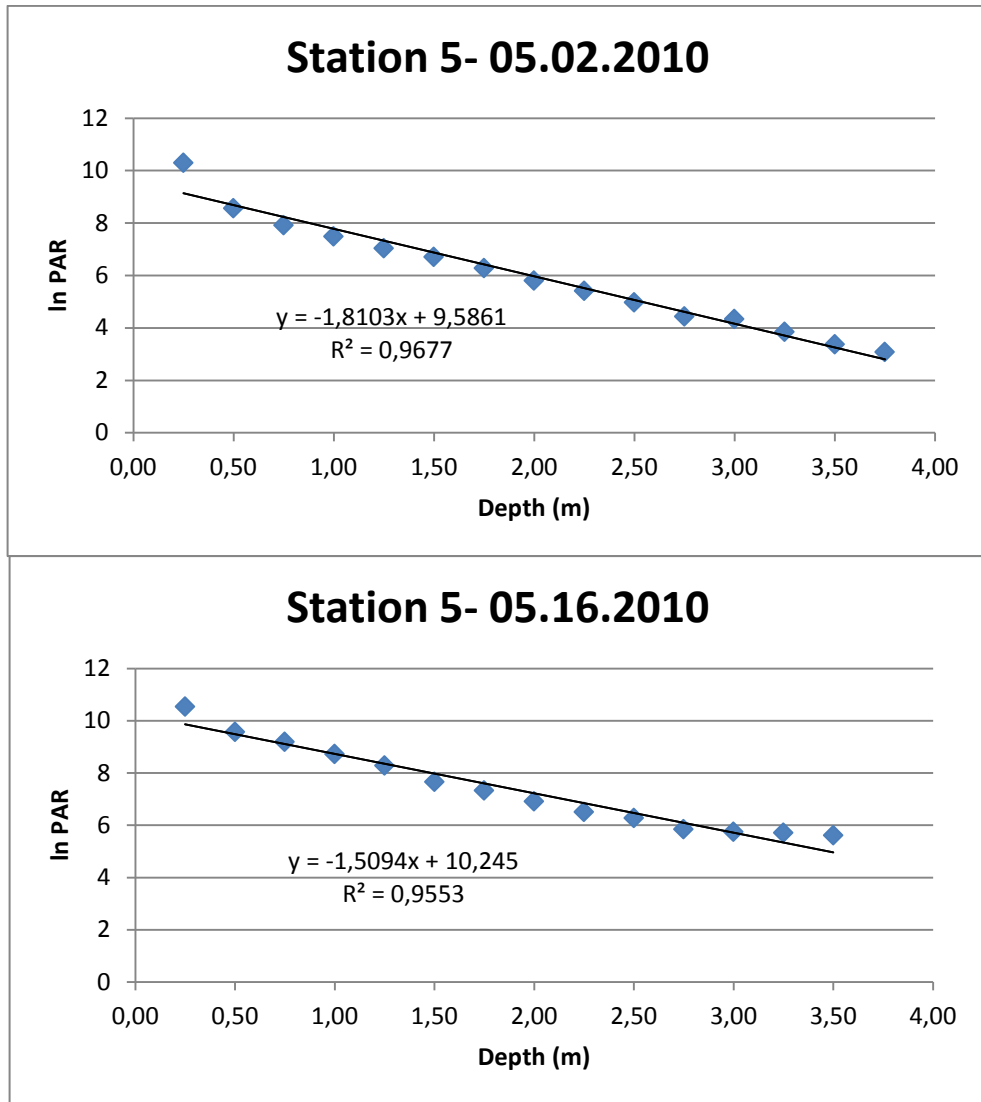


Figure A-58: Station 5 In PAR values versus Depth, For May, 2010

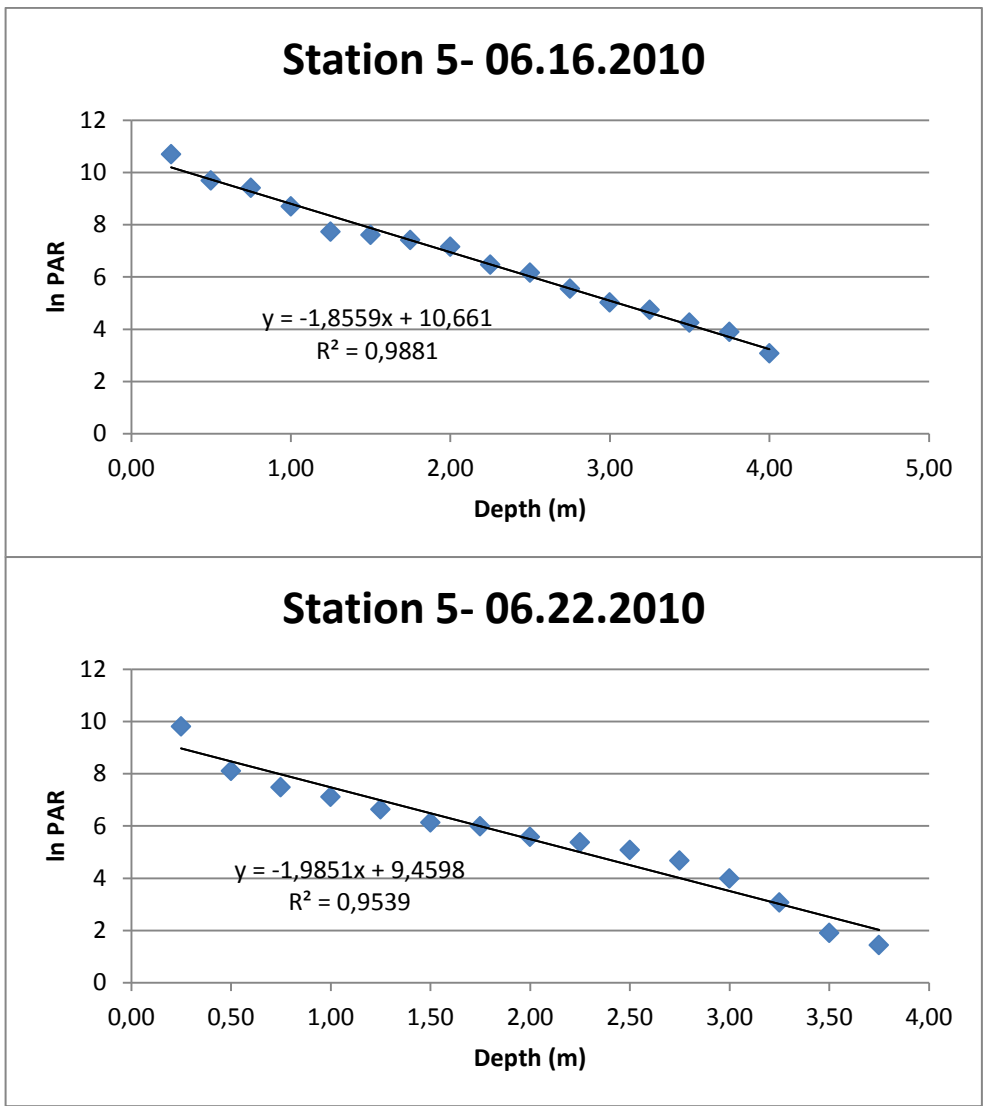


Figure A-59: Station 5 In PAR values versus Depth, For June, 2010